Investigation of NMDA Receptor Subunit Composition in the Developing Cat Visual System Following Brief Immersion in Darkness

By

Elise Marie Aronitz

Submitted in partial fulfillment of the requirements
for the degree of Master of Science

at

Dalhousie University
Halifax, Nova Scotia
July 2020

To my Mom and Dad.

I love you guys so much, thank you for teaching me to follow my dreams.

Table of Contents

List of Tables

List of Figures

Abstract

During early postnatal development, the critical period is a time during which the visual system exhibits robust plasticity, and neural circuitry can be easily modified by changing levels of visually-driven activity. Although the exact mechanisms of critical period plasticity are unknown, the subunit composition of the N-methyl-D-aspartate (NMDA) receptor is a putative mechanism for experience-dependent plasticity. The composition of the receptor is thought to mediate plasticity by modifying the threshold of activity needed to induce long-term potentiation and long-term depression, thus altering the likelihood of synaptic strengthening and weakening. The current study aimed to provide further insight into the role of the NMDA receptor composition in experience-dependent plasticity. This study employed a novel multiplex immunolabeling method to quantify NMDA receptor subunits composition in tissue slices from cat dorsal lateral geniculate nucleus (LGN) and primary visual cortex (V1). The method used in this study preserved *in situ* protein distribution within both regions, and therefore, allowed for an investigation into layer-specific changes in receptor composition. In order to assess how activity levels alter the NMDA receptor composition, animals were exposed to a 10-day period of darkness to eliminate visually-driven activity. We found that dark exposure altered NMDA receptor subunit composition in both the LGN and V1, shifting the composition towards its neonatal isoform in a universal manner. We also observed a significant reduction in neuron soma size in both the LGN and V1, which indicates that darkness may stall development or revert the brain to a more immature state. Together these results indicate that the NMDA receptor subunit composition is a potential mechanism of darkness mediated plasticity because the change in receptor composition produced by darkness predicts that the modification threshold would favour synaptic strengthening.

List of Abbreviations and Symbols Used

Abbreviations:

AMPA	α-amino-3-hydroxy-5-methyl-4-isoxazolepropionic acid
ANOVA	One-way analysis of variance
BDNF	Brain-derived neurotrophic factor
$Ca2^{+}$	Calcium
CaMKII	Calcium/calmodulin-dependent protein kinase II
ChABC	Chondroitinase ABC
CSPG	Chondroitin sulfate proteoglycans
DAR FF	Donkey anti-rabbit fab fragment
DE	Dark Exposure
DNA	Deoxyribonucleic acid
ECM	Extracellular matrix
Fab	Fragment-antigen binding
GABA	Gamma-aminobutyric acid
GAD	Glutamic acid decarboxylase
GAG	Glycosaminoglycan
GAR	Goat anti-rabbit
HAT	Histone acetyltransferase
HDACs	Histone deacetylases
iGluRs	Ionotropic glutamate receptors
LGN	Lateral Geniculate Nucleus
LTD	Long-term depression
LTP	Long-term potentiation
Lynx 1	Ly6/neurotoxin1
MAG	Myelin-associated glycoprotein
MD	Monocular deprivation
$Mg2^{+}$	Magnesium
nAChR	Nicotinic acetylcholine receptor

NF	Neurofilament
NF-H	Neurofilament -heavy
NF-L	Neurofilament - light
NF-M	Neurofilament - medium
NgR	Nogo Receptor
NMDA	N-methyl-D-aspartate
NR2A	NR2A subunit of the NMDA receptor
NR2B	NR2B subunit of the NMDA receptor
NT 435/455	NeuroTrace 435/455
OD	Ocular dominance
OMgp	Oligodendrocyte-myelin glycoprotein
OTX2	Orthodenticle homeobox 2
PBS	Phosphate-buffered saline
PirB	Paired immunoglobulin-like receptor B complex
PNN	Perineuronal nets
PV+	Parvalbumin positive
Rb-R2A	Rabbit polyclonal primary antibody against NMDAR2A
Rb-R2B	Rabbit polyclonal primary antibody against NMDAR2B
RbAR	Rabbit anti-rat
RGC	Retinal ganglion cells
RO	Reverse occlusion
SC	Superior colliculus
tPA	Tissue plasminogen activator
TTX	Tetrodotoxin
V1	Primary Visual Cortex

Symbols:

▼ – C436 P37 Normal

⬣ – C466 P40 Normal

◆ – C468 P40 Normal

▲ – C463 P40 Dark exposure

■ – C464 P40 Dark Exposure

● – C465 P40 Dark Exposure

Acknowledgements

First and foremost, I would like to thank Dr. Kevin Duffy for his guidance, mentorship, and encouragement throughout these past two years. I am grateful for the role he played in sparking my initial interest in visual neuroscience, which originated from the class he taught me. As well, Dr. Duffy introduced me to Dr. Donald Mitchell, who provided me with my first formal research opportunity in visual neuroscience, expanding my interest in the visual system. Further, I owe my thanks to both Dr. Mitchell and Dr. Nathan Crowder for being on my committee and providing aid and constructive feedback throughout my time at Dalhousie University.

I am very grateful to my friends who have provided support and encouragement throughout this process. I would like to give a special thanks to Julie Morrissey, Nicole Michaud, Elena Vorvis, Colin McCormick, Jared Shapiro, Elizabeth Myles, Jessica Johnson, Naomi Van Leeuwen, Colin Creaser, and Braden Kamermans for going above and beyond in helping me academically and personally. I am truly thankful for the inspiration, encouragement, and support my friends have provided.

I would especially like to thank my parents, Rose and Jim, for providing me with countless opportunities that allowed me to get to where I am today. Their constant love and encouragement motivated me to pursue my goals. I would like to thank my older brothers, Christopher and Stephan, for being my role models, inspiring me to pursue a degree in science, and teaching me to fight for what I want. As well, I would like to thank my younger sister, Nicole, for providing me with the opportunity to be a mentor and role model. I am unbelievably grateful to my family for the role they played in my education, and I own them immeasurable thanks.

Finally, I would like to thank Mike, who never faltered to support me in every way possible. I appreciate the countless number of times he has allowed me to talk non-stop about my research, and all the times he acted as the world's best sounding board for my ideas. He has been my biggest cheer squad and my best support system, and I am forever grateful for him.

CHAPTER 1 – INTRODUCTION

Colloquially, plasticity refers to the physical adaptability of material, i.e. how easily a material can be moulded or altered by force. When applying this definition to the field of neuroscience, neural plasticity refers to the brain's ability to adapt and modify its connections, function, and structure in response to external or internal stimuli. These plastic processes allow for the brain to adjust to a changing environment, and therefore permits an organism to successfully cope with the challenges brought on by environmental change (Bernhardi et al., 2017; Berlucchi and Buchtel, 2009; Cramer et al., 2011).

During early postnatal development, neural plasticity is essential to allow for neural circuitry to develop appropriately. There is a period during early development in which the brain exhibits an enhanced capacity for plasticity. This period is termed the 'critical period,' and is essential for the acquisition of many crucial functions, such as language, emotional processing, sleep, and development of senses, for example, vision (Lenneberg, 1967; Gross et al., 2002; Miyamoto et al., 2003; Wiesel, 1982; Hooks and Chen, 2007). During the critical period, changing levels or patterns of activity can readily form or modify circuits. Thus, the critical period likely plays a vital role in the formation of neuronal architecture necessary for a stable and operational mature brain. Although it is necessary for development of a functional nervous system, this period of enhanced plasticity is transient. As the animal ages, the critical period comes to a 'close' and plasticity within the brain diminishes considerably. Following closure of the critical period, connections are less susceptible to modifications as a result of experience. Consequently, the neural circuits that were formed and refined during the critical period

become stable and difficult to rewire (Hubel and Wiesel, 1970; Olson and Freeman, 1980; Levelt and Hübener, 2012).

Many functions within the brain develop in an experience-dependent manner, meaning external stimuli and experience influence development. For this reason, disturbances to experience during the critical period can prevent the formation of normal neural circuitry that is essential for proper functioning later in life, and thus can cause intractable deficits (Sengpiel, 2007; Hensch, 2004; Hooks and Chen, 2007). Due to low levels of plasticity following the closure of the critical period, failure to address these disturbances during the critical period can result in developmental deficits that are difficult, if not impossible, to undo. These disturbances are challenging to reverse following the closure of the critical period, as the brain exhibits low levels of plasticity, and therefore experience cannot efficiently alter circuitry. Consequently, it is difficult to rewire connections to compensate for developmental disruptions that were left untreated (Daw, 1998; Wu and Hunter, 2006). However, if these developmental deficits occur, it may be possible to reserve them by reinstating critical period-like plasticity following the closure of the critical period. Restoring high levels of plasticity would allow for abnormal circuits to be rewired in order to restore normal functioning. Understanding the molecular mechanisms associated with critical period plasticity may provide valuable information about potential strategies to reinstate high levels of plasticity long after the critical period closes. Knowledge about these mechanisms may provide insight into clinical interventions for individuals with intractable functional deficits caused by abnormal development.

The purpose of the current research project is to investigate the molecular mechanisms that mediate neural plasticity, specifically examining the mechanisms that facilitate visual system plasticity. As the visual system develops in an experience-dependent manner, and it is easy to manipulate visual experience, the visual system provides an ideal model to study neural plasticity. In particular, studies in this thesis will focus on the role of the N-methyl-D-aspartate (NMDA) glutamate receptor subunit composition in experience-dependent plasticity.

1.1 Animal Models in Vision Research

Within the field of visual neuroscience, the use of animal models has provided insight into the development and organization of the mammalian visual system. Using animals for research purposes has expanded our understanding of how experience influences visual development and has provided valuable information about how visual information is relayed and processed to produce behaviour. Early work using animal models focused on cats and non-human primates, however, more recent research increasingly uses rodents as well (Hubel and Wiesel, 1959, 1969; Hubel et al., 1977; Wiesel, 1982; Hooks and Chen, 2007).

The animal chosen to study experience-dependent plasticity for this research was the cat. While non-human primates would be the ideal model for studying plasticity within the visual system, as they share many visual traits with humans, there are financial and ethical issues associated with their use. In addition, the long gestation period with few offspring typical of non-human primates can significantly limit the speed at which this type of research can be conducted. As mentioned, rodents are also a popular animal

model, one that benefits from lower costs and less social stigma. However, rodents share few visual traits with primates, which makes them arguably less suited for research on the visual pathways. Despite the differences in visual system organization, rodents are still a fundamental model in plasticity research as they are an ideal animal model for gene-targeting technologies.

Compared to rodents, cats are better suited for the current research, as they share more visual traits with primates, such as the anatomy of their eye, and the organization of their visual pathway. Similar to primates, cats have a binocular visual system with forward-facing eyes, that allow for extensive overlap of the visual fields, stereoscopic vision, and vergence eye movements (Bough, 1970; Blake, 1979; Fox and Blake, 1971). Although cats and primates have differences in their colour vision and acuity, the similarities in their visual system make them a valuable model to study visual system development and plasticity (Jacobs, 1981; Hall and Mitchell, 1991).

1.2 Visual System, Plasticity, and Development

My research will focus on two primary components of the visual system, the dorsal lateral geniculate nucleus (LGN), and the primary visual cortex (V1). However, before reaching these regions, visual information in the retinal image must first be processed by neurons in the retina and then transmitted via retinal ganglion cell axons in the optic nerve, optic chiasm, and optic tract. The initial steps of visual processing occur at the retina, in which specialized cells convert light into neuronal signals. These impulses are transmitted by retinal ganglion cells (RGC) to the LGN, a visual relay station located in

the thalamus, or to the superior colliculus (SC), a midbrain structure responsible for transforming sensory input into movement behaviour.

At the optic chiasm, nasal retinal afferents decussate to synapse onto cells within the contralateral LGN, whereas temporal retinal afferents avoid decussation and synapse onto cells within the ipsilateral LGN (Reese, 2011). In frontal-eyed mammals, such as humans, non-human primates, and cats, semi-decussation is clearly present, and hemispheres process approximately equal amounts of ipsilateral and contralateral input. Unlike higher-order mammals, rodents do not display this semi-decussation of the optic nerves; instead, a much higher proportion of afferents decussate to synapse onto the contralateral LGN than avoid decussation to synapse onto the ipsilateral LGN. Therefore, V1 of rodents process far more contralateral information compared to ipsilateral information (Dräger and Olsen, 1980; Neveu and Jeffery, 2007).

Following decussation, visual information is either relayed to the LGN or the SC. In higher-order mammals, only about 10% of the RGC project to the SC, however, in rodents about 85-90% RGC project to the SC, which is another significant difference between visual system organization in rodents versus high-order mammals (Perry and Cowey, 1984; Ellis et al., 2016). Within the LGN of higher-order mammals, retinal afferents from each eye innervate eye-specific layers. The distinct lamination of the LGN can be visualized by staining tissue sections for Nissl substance, which are large granular bodies, found within neurons, that are composed of rough endoplasmic reticulum and ribosomes. Within humans and non-human primates, when visualizing the LGN with Nissl stain, it is possible to distinguish six distinct layers, each receiving eye-specific input. In cats, the LGN has three distinct layers named A, A1, and C. Layer A and A1

receive eye-specific inputs, with layer A receiving exclusively contralateral input and layer A1 receiving exclusively ipsilateral input. Unlike the A layers, layer C receives input from both eyes, however, the eye-specific segregation in this layer can not be visualized with Nissl stain alone (Guillery, 1970). Unlike binocular mammals, the LGN of rodents lacks distinct lamination; instead, retinal projections are organized into eye-specific domains. The LGN of rodents contain a small domain that receives exclusively contralateral input, as well as, a larger domain that receives both ipsilateral and contralateral input (Reese, 1988; Grieve, 2005; Zeater et al., 2015). In both rodents and binocular mammals, cells within the LGN project to V1. These projections from the LGN synapse onto cells within layer IV of V1. The cells within layer IV receiving information from the LGN then send projections to the more superficial layers of the cortex, layer II and III. These layers then send projections to layer V, as well as other cortical areas. Cells within layers II, III, and V all send projections to layer VI, which is the only layer to send projections back to the LGN (Daw, 2014).

During early V1 development in both cat and monkey, there is no distinction between eye-specific input (Rakic, 1977; Crair et al., 2001). However, as development continues, layer VI becomes segregated into approximately equal-width columns containing cells that respond preferentially to stimulation of one eye or the other, and that span the tangential aspect of V1 except in the monocular crescent. These columns are known as ocular dominance (OD) and seem to arise due to the geniculocortical afferents becoming segregated into alternating eye-specific columns within layer IV of V1. These OD columns are especially prominent in monkey V1 where they appear as distinct altering parallel stripes, in which the width of the columns are relatively equal (LeVay et

al., 1985). Unlike monkeys, the OD columns in cats have a less uniform pattern and more variance in column width (Anderson et al., 1988).

The ocular dominance of these columns is determined by the afferents from the monocular layers of the LGN that project to layer IV of V1. Cells situated within the layers above or below layer IV will have similar eye preference; therefore, this results in the formation of columns with eye preferences that run perpendicular to the cortical surface (Hubel and Wiesel, 1969). However, unlike binocular mammals, the visual system of rodents lacks the distinct columnar organization of cells that share functional properties; instead, V1 of rodents displays a 'salt-and-pepper' distribution of cells (Ohki and Reid, 2007). Although lacking distinct OD columns, V1 of rodents contain two functional segments, with one segment receiving inputs exclusively from the contralateral eye, and the other receiving binocular input (Zilles et al., 1984; Reid and Juraska, 1991).

In cats, the formation of OD columns occurs just after birth, prior to the onset of the critical period (Crair et al., 2001). The formation of OD columns appears to be mediated mechanisms that are different from those that mediate plasticity later in life. Thus, different processes appear to be responsible for the development of the visual system, with both experience-dependent and -independent mechanisms at work. Development of the visual system, and more broadly, the nervous system, can be divided into three distinct periods: the pre-critical period, the critical-period, and the post-critical period.

1.2.1 Pre-Critical Period Development

The initial stages of nervous system development follow a series of systematic steps that are mediated by intrinsic cues and are not dependent on externally-driven activity. As the nervous system is composed of approximately 100 billion neurons, with each cell having a unique location and function, its development must be strictly regulated to ensure proper functioning. The initial steps in neurodevelopment occur prenatally, which include the proliferation of cells that make up the brain, the differentiation of these cells into specific cell types, and the migration of these cells to their proper locations (Volpe, 2000). The cortex develops in an 'inside-out' manner, meaning the first wave of neurons born in the ventricular zone, migrate shorter distances and are located within deeper cortical layers, whereas younger neurons migrate further and are located in the upper cortical layers (Berry and Rogers, 1965; Rakic, 1974). These initial steps, which are vital for proper neural development and function, occur in the absence of external stimulation.

Prior to the critical period, experience-dependent plasticity within the visual system is low, and a large portion of visual development is independent of visually evoked activity, occurring either prenatally or postnatally before eye-opening. The development of the visual system begins with the prenatal production of RGCs, followed by the production of cells that compose the LGN, and then finally, the cells within V1 are formed. During the early stages of development within rhesus monkeys, RGC projections are guided via molecular cues to the optic chiasm and then to the LGN (Rakic, 1976, 1977). Within the LGN, the initial projections from the retina overlap with no clear eye-specific segregation. Nearing the end of the gestation period, the LGN becomes segregated, and the neurons composing V1 have been generated and positioned in their

final locations. At this time, the projections from the LGN to V1 are present, and the OD columns are beginning to form (Rakic, 1976, 1977). It appears that genetic cues are responsible for the early development of the visual system and are necessary for establishing columnar architecture. Research has shown that cats from the same litter have similar architecture within the visual cortex. Conversely, cats with different mothers, i.e. not genetically related, have a higher degree of variability in the architecture of V1 (Kaschube et al., 2002). These results support the theory that genetic cues are necessary for early visual system development (Kaschube et al., 2002).

Although visually-evoked activity does not drive pre-critical period development of V1, development at this stage requires spontaneous patterned retinal activity for eye-specific segregation of V1 and LGN. As blocking neural activity using TTX prevents segregation from occurring in the cat, it is clear that patterned retinal activity is necessary to ensure proper development prior to the critical period (Stryker and Harris, 1986; Shatz and Stryker, 1988). Once the initial steps of development are complete, external visual activity is required to refine the circuitry within the visual system.

1.2.2 Critical Period Development

Although the initial formation of visual system circuitry is largely gene-driven and occurs in the absence of experience-driven activity, as postnatal development continues into the critical period, visual stimulation becomes an essential factor mediating proper visual development by helping to establish precise and reliable neural circuits. In many animals, the onset of the critical period, during which the brain exhibits robust plasticity, does not align with eye-opening; instead, it appears to fall between eye-opening and puberty

(Daw, 2014). It has been proposed that the critical period can not 'open' until the visual system has developed adequate connections, and input to the system is reliable and precise (Knudsen, 2004). Once these conditions are met, and the critical period 'opens,' the visual system then requires visually-driven neural activity to ensure that appropriate connections and circuitry are formed and refined, which is essential for proper visual development.

As visual input heavily influences the development of the visual system during the critical period, abnormal visual experience during this period can result in improper visual development. Abnormal development can potentially lead to visual deficits, which can be reflected by anatomical and physiological changes in the visual system. The ground-breaking work conducted by David Hubel and Torsten Wiesel in the 1960s greatly influenced our understanding of how abnormal visual experience, specifically visual deprivation, alters the visual system. In a laboratory setting, monocular deprivation (MD), a method in which the eyelid is sutured shut, is typically used to produce abnormal visual experience. This form of unilateral deprivation is known to markedly alter the structure and functions of neurons within the visual system, causing changes to two of the main components of the visual pathway: the LGN and V1 (Wiesel and Hubel, 1963a, 1963b; Mwachaka et al., 2015a, 2015b).

Within the LGN, MD predominantly alters the layers receiving input from the deprived eye. In kittens, when compared to cells found in layers receiving input from the non-deprived eye, cells found in LGN layers receiving input from the deprived eye show a reduction in both soma size and dendritic field width (Friedlander et al., 1982; Guillery and Stelzner, 1970; Wiesel and Hubel, 1963a). Additionally, MD alters the cytoskeleton

of neurons within the layers of the LGN receiving input from the deprived eye, marked by a significant decrease in neurofilament (NF) levels, a constituent of the cytoskeleton that helps regulate neuron function and structure (Bickford et al., 1998; Duffy et al., 2018; Lasek, 1981).

Further along the visual pathway, within V1, the effect of MD can be observed in the organization of OD columns. Compared to animals with normal binocular vision, the cells within V1 of MD animals are excited primarily to stimulation of the non-deprived eye (Ganz et al., 1968; Blakemore and Van Sluyters, 1974). The dimensions of the OD columns reflect this difference in response, with columns receiving input from the deprived eye becoming smaller in size, and the columns receiving input from the non-deprived eye becoming larger and occupying more space within the cortex (Shatz and Stryker, 1978). The change in column size may be a result of a change in the morphology of geniculocortical afferents. Monocular deprivation decreases the complexity and arborization of these afferents, and thus, the projections from the deprived layers of the LGN take up less space within layer IV of V1 (Antonini and Stryker, 1993). Further, MD alters the cytoskeleton of neurons within the OD columns receiving input from the deprived eye, causing a reduction in NF expression (Duffy and Livingstone, 2005). The anatomical and physiological changes caused by MD are reflected behaviourally as well; MD from an early age results in reduced visual acuity in the deprived eye (Giffin and Mitchell, 1978; Mitchell, 1988).

Based on the severe alterations to the visual pathway caused by MD, it is clear that abnormal visual experience during the critical period of development can result in severe physiological, anatomical, and behavioural deficits. Proper visual input is needed

to mediate the refinement of visual system architecture that is essential for relaying and processing visual information. Although it may seem intuitive that this visually driven refinement is dependent on the absolute level of visual activity, it is instead the correlation of visual input into both eyes that appears to govern the activity-dependent development of the visual system (Guillery, 1972). Compared to early MD, early binocular deprivation produces a less severe physiological change within V1, which suggests that the absolute level of visual activity does not drive refinement (Wiesel and Hubel, 1965).

By measuring the severity of the MD induced changes, the visual system of rodents and cats begins to display a sensitivity to visual experience at approximately three to four weeks of age (Fagiolini et al., 1994; Gordon and Stryker, 1996; Hubel and Wiesel, 1970). In cats, the visual system is most susceptible to the effects of MD between four to six weeks of age. This age range, described as the peak of the critical period, is when the visual system exhibits the highest levels of plasticity and a short-term MD causes the majority of the cells within V1 to respond primarily to stimulation of the non-deprived eye (Hubel and Wiesel, 1970; Olson and Freeman, 1975, 1980). While the critical period typically begins at about three to four weeks of age, the ‘opening’ of the critical period also depends on the visual history of an animal. Research has shown that rearing cats in complete darkness from just after birth shifts the start and end of the critical period past the natural age (Cynader and Mitchell, 1980). This shift in the critical period further supports the idea that the critical period can not ‘open’ until input to the visual system is reliable, and adequate connections have formed.

1.2.3 Post-Critical Period Development

As development continues, and the critical period comes to a close, plasticity diminishes, and the visual system becomes less susceptible to experience-induced changes. With a decline in plasticity, abnormal visual experience elicits less severe physiological, anatomical, and behavioural changes. In cats, by approximately 12 weeks of age plasticity has declined significantly, as shown by a short period of MD causing only small changes to OD within V1 and having no effect on soma size within the LGN (Hubel and Wiesel, 1970; Olson and Freeman, 1980; Duffy et al., 2016). Plasticity within the visual system diminishes to negligible levels by approximately six months of age (Olson and Freeman, 1980). When using a short period of MD, it appears that the critical period ends around six months of age. However, previous research has shown that a three month MD starting at 8 months of age can produce a substantial shift in OD (Daw et al., 1992). Therefore, it seems that when more potent visual manipulations are used, such as long periods of MD, plasticity within the visual system extends to about one year of age.

1.3 Disruptions to Critical Period Development in Visual System of Humans

As previously stated, it is known that disruptions to visual input during early postnatal visual development result in anatomical, physiological, and behavioural changes. Although manipulating visual experience is useful in a laboratory setting to gain a better understanding of visual development and plasticity, visual disruptions in humans during critical period development can have detrimental and potentially intractable behavioural consequences. Disruptions during the critical period that result in an imbalanced

binocular visual input can cause improper visual development and potentially lead to the developmental disorder termed amblyopia.

1.3.1 Causes and Treatments of Amblyopia

Amblyopia typically manifests as a loss of monocular, or, less commonly, binocular visual acuity, as well as a severe decrease or even a loss of stereoacuity. The reduction in visual acuity indicative of amblyopia is not due to an optical error or retinal disease, but rather, is thought to be caused by improper processing of visual information caused by a loss, or rearrangement of connections within central the visual pathway (Von Noorden, 1967; Von Noorden and Campos, 2002; McKee et al., 2003; Daw, 2014). There are a variety of problems that can lead to imbalanced binocular input, thus altering development of neural connections that, in turn, lead to amblyopia (Barrett et al., 2004). Visuo-motor disruptions, such as strabismus, and sensory disruptions, such an anisometropia, or visual form deprivation, can cause amblyopia. Strabismus is a condition characterized by a misalignment of the eyes due to a muscular or neural deficit that causes an imbalance in binocular interactions, subsequently leading to suppression. Suppression caused by strabismus results in a loss of connections between the non-favoured eye and the cortex, which then leads to the development of amblyopia (Von Noorden and Campos, 2002). Anisometropia is characterized by a difference in refractive error between the two eyes, which causes unequal focusing, therefore leading to a blurred image on one retina. Individuals with anisometropia are inclined to favour the eye with the better retinal image. This preference can lead to the development of amblyopia (Daw, 2014; Weakley, 2001; Caputo et al., 2007). Additionally, visual deprivation, such as

cataracts, corneal opacities, or ptosis, can lead to stimulus-deprivation amblyopia. Generally, the effect of unilateral deprivation on vision is worse compared to strabismus or anisometropia, resulting in more significant degradation of the connections between the deprived eye and the visual cortex (Daw, 2014; Von Noorden and Campos, 2002).

Estimated to affect 2-2.5% of the general population, amblyopia is a prevalent developmental disorder of significant importance (Von Noorden and Campos, 2002). Amblyopia negatively affects one's quality of life by impacting education level, self-esteem, and employment prospects (Chua and Mitchell, 2004; Packwood et al., 1999; Sabri et al., 2006). In addition, individuals with amblyopia are at a higher risk of losing vision in the non-amblyopic eye compared to individuals with binocular vision (Tommila and Tarkkanen, 1981).

Clinically, in young pre-verbal children, amblyopia is usually diagnosed by examining fixation preferences, or by measuring visual acuity using a forced-choice preferential looking technique, such as the Teller acuity cards (Von Noorden and Campos, 2002; Dickey et al., 1991; McDonald et al., 1985). In verbal children and older individuals, amblyopia can be diagnosed by assessing optotype visual acuity using a LogMAR or Snellen chart (Morad et al., 1999; Holmes and Clarke, 2006).

Treatments for amblyopia typically involve forcing the individual to use the amblyopic eye by preventing visual input to the healthy eye (referred to as the fellow eye). Techniques such as an opaque patch or penalization that involves using optical or pharmaceutical interventions as a means to blur vision in the fellow eye can be used to deprive the fellow eye and thus force the use of the amblyopic eye (The Pediatric Eye Disease Investigator Group, 2003, 2009). Although patching therapy is the current gold

standard treatment for amblyopia, there are some difficulties associated with this intervention, the first such issue being age. The efficacy of patching therapy wanes as the individual ages, and by approximately seven years of age, this treatment is ineffective, resulting in little to no recovery of visual acuity in the amblyopic eye (Epelbaum et al., 1993; Daw, 1998). Compliance is a second significant issue associated with patching therapy, with this therapy having poor patient compliance, i.e. patients being resistant towards a strict patching regime. As there is a known correlation between recovery rate and compliance, low compliance can result in limited recovery (Loudon et al., 2002, 2003; Stewart et al., 2004). The two aforementioned issues associated with patching therapy highlight the need for more effective treatments of this disorder. By using animal models, we can gain a better understanding of the molecular mechanisms underlying amblyopia, potentially providing insight into a more effective treatment.

1.3.2 Animal Models of Amblyopia

The use of animal models in amblyopia research has enabled researchers to gain a deeper understanding of the molecular mechanisms associated with the disorder. As noted previously, unilateral deprivation is a common laboratory technique used to alter visual experience. Interestingly, the effects of MD on visual acuity mimic those seen in human amblyopes with deprivation amblyopia. Since MD can be used in a laboratory setting to mimic deprivation amblyopia, and the changes caused by MD are well documented, it can be said that amblyopia causes anatomical and physiological changes within the central visual pathway. Furthermore, animal models have aided researchers in developing and testing potential interventions that may be effective in promoting recovery of visual

acuity in the amblyopic eye, as well as reversing the anatomical changes associated with amblyopia.

Traditionally there are two paradigms for promoting recovery following MD: restoration of binocular visual input and occlusion of the fellow eye. The first paradigm is passive, in that following the removal of the MD, binocular vision is restored without any further manipulations. In this paradigm, acuity of the deprived eye shows some recovery, but never to normal levels (Mitchell, 1988; Olson and Freeman, 1978; Giffin and Mitchell, 1978; Mitchell et al., 1977). Moreover, there is a correlation between the age of implementation/length of deprivation and degree of recovery. Restoring binocular vision following MD results in some functional recovery within V1, however, an imbalance in responsiveness is still present, with cells favouring the non-deprived eye.

The second paradigm for promoting recovery following MD is known as reverse occlusion (RO). This paradigm mimics patching, in that the fellow eye is occluded to force the use of the deprived eye. Compared to restoring binocular vision, RO promotes better recovery of visual acuity in the deprived eye. However, recovery can occur at the expense of the fellow eye, as long periods of RO cause a reduction in fellow eye visual acuity. Additionally, the recovery induced by RO is not sustained once the RO is terminated and binocular vision is restored (Murphy and Mitchell, 1987). On a functional level, a short period of RO causes a near-complete reversal of OD within V1, with the deprived eye driving the majority of the cells (Blakemore and Van Sluyters, 1974; Movshon and Blakemore, 1974; Olson and Freeman, 1978). As well, there is a correlation between the amount of recovery and the age at which RO is initiated. In cats, RO occurring at approximately 12 weeks of age, i.e. when plasticity within the visual

system is declining, produces little recovery (Blakemore and Van Sluyters, 1974; Movshon, 1976). The limited recovery may be due to the inability for RO to recruit the mechanisms required for engaging what plasticity remains. As these traditional interventions are insufficient at promoting recovery following MD, novel treatments that can 'reboot' the brain to a more plastic state may result in better recovery of the deprived eye.

1.3.3 Novel Methods to Promote Recovery from MD

A handful of novel strategies that appear to reinstate high levels of plasticity have been successful in promoting recovery following MD in animal models. Maya-Vetencourt and colleagues were able to promote functional and behavioural recovery following MD in adult rats via chronic administration of the common antidepressant fluoxetine (Maya-Vetencourt et al., 2008). The results of their study suggest that fluoxetine may restore high levels of plasticity within the visual system. Although effective in rodents, this method was ineffective in human clinical trials (Huttunen et al., 2018; Sharif et al., 2019). Additionally, Morishita and colleagues found that increasing endogenous acetylcholine signalling, by inhibiting acetylcholinesterase (the enzyme that breaks down acetylcholine), promotes recovery following MD in mice (Morishita et al., 2010).

Regarding the visual system of cats, previous research has shown that a 10-day period of constant dark exposure is effective in reversing the visual deficits caused by amblyopic rearing (Duffy and Mitchell, 2013; Mitchell et al., 2016). Interestingly, five days of constant dark exposure, or ten days of dark exposure paired with intermittent light, were both ineffective at producing recovery following MD. The aforementioned 10-

day period of constant dark exposure appears to be necessary to restore plasticity within the visual system. This short period of darkness is effective in promoting recovery following a short seven-day MD initiated at postnatal day (P) 30. Furthermore, it was successful in promoting recovery following a six week MD starting at eye-opening, a situation that is more relevant to clinical applications (Duffy and Mitchell, 2013; Mitchell et al., 2016). Although effective, the timing of the dark exposure relative to the MD can alter the rate of recovery. When the 10-day period of darkness was initiated immediately following MD, the kittens appeared blind once removed from the dark. Nevertheless, visual acuity gradually improved, and within seven weeks, visual acuities in both eyes reached normal levels. In contrast, if darkness is imposed eight weeks after termination of the MD, following removal from the dark, the acuity of the deprived eye recovered to normal levels much more rapidly, taking approximately 7-10 days. It is important to note that delayed exposure to darkness promotes recovery in the deprived eye that does not come at the expense of the fellow eye, as visual acuity of the fellow eye does not decrease in this scenario (Duffy and Mitchell, 2013; Mitchell et al., 2016). On an anatomical level, following a one- or two-week MD, 10-days of darkness resulted in complete recovery of neuron soma size within the layers of the LGN receiving input from the deprived eye. However, darkness was ineffective in producing this full recovery in soma size following either a three- or six-week MD (Duffy et al., 2015, 2018). Unlike darkness, fellow eye monocular retinal inactivation with TTX produced a full recovery of neuron soma size following a six-week MD. Further, within the deprived layers of the LGN, fellow eye inactivation reversed the MD induced decrease in NF (Duffy et al., 2018). Additionally, binocular TTX injections occurring approximately eight weeks after

a seven-day MD resulted in complete recovery in deprived eye acuity (Fong et al., 2016). These results suggest that 10-days of dark exposure, or retinal inactivation, can modify the molecular mechanisms that are regulating plasticity to reinstate higher levels of plasticity within the visual system, and thus promote recovery following deprivation.

1.4 Molecular Mechanisms of Plasticity: Machinery Required for the Induction and Termination of the Critical Period

The anatomical and physiological changes caused by disruption to normal visual input appear to be produced by changes in input to the cortex, as blocking neural impulses within V1 using TTX prevented experience-dependent changes (Stryker and Harris, 1986). While it is evident that electrical activity regulates experience-dependent plasticity, the exact mechanisms in which activity mediates synaptic connections and critical period timing are not well understood.

Rodent models have been a valuable model for providing insight into the underlying molecular mechanisms of experience-dependent plasticity, as they allow the use of gene-targeting technologies. Despite the differences in rodents' visual characteristics, they experience MD-induced changes similar to those seen in primates and cats. Comparable to higher-order mammals, within rodents, MD during the critical period caused a shift in OD of neurons in V1 to favour the non-deprived eye (Fagiolini et al., 1994). Additionally, the geniculocortical afferents of the deprived eye stopped growing, and the deprived eye showed a reduction in visual acuity (Fagiolini et al., 1994; Gordon and Stryker, 1996; Antonini et al., 1999). Although V1 of rodents displays a 'salt-and-pepper' distribution of cells, as opposed to distinct ocular dominance columns, it is still possible to assess the physiological effects of MD. The ability to assess the

effects of MD in rodents has allowed us to gain a better understanding of the varied mechanisms that appear to mediate plasticity.

1.4.1 The Role of Inhibitory Circuitry in Critical Period Timing

An emerging belief is that visual system development is dependent on a balance between excitatory and inhibitory tone, and the equilibrium between these tones is required to activate the machinery and molecular cascades that mediate the induction and termination of the critical period (Hensch, 2004; Takesian and Hensch, 2013). Inhibitory circuitry is essential in reaching this equilibrium, and the use of gene-targeting technology has provided valuable information on the role of inhibitory circuitry in experience-dependent plasticity. Much of this research focuses on gamma-aminobutyric acid (GABA) and has revealed that GABAergic transmission and circuitry play an essential role in controlling experience-dependent plasticity and presumably contributes to the excitatory and inhibitory balance. Specifically, the development of GABAergic inhibition appears to control the onset of the critical period. Additionally, when GABAergic tone surpasses a threshold, it controls the closure of the critical period.

Hensch and colleagues demonstrated the role of GABAergic circuitry in experience-dependent plasticity in the 1990s, showing that mice lacking glutamic acid decarboxylase (GAB) 65, one of the two enzymes responsible for GABA synthesis, had less GABA transmission and did not show a shift in eye preference following a brief MD (Hensch et al., 1998). However, treating the animals with diazepam, a positive allosteric modulator of $GABA_A$ receptors, restored susceptibility to MD (Hensch et al., 1998). In support of the role of GABA transmission in plasticity, specifically, its importance in

mediating the onset of the critical period, diazepam treatment in wild-type mice before the natural onset of the critical period induced a precocious critical period. Additionally, in adult mice, diazepam treatment could not reinstate critical period-like plasticity; however, in mice lacking GAB65, diazepam treatment was able to induce robust plasticity before, during, and after the natural critical period (Fagiolini and Hensch, 2000).

Further supporting the role of GABAergic circuitry in experience-dependent plasticity, overexpression of the neurotrophin brain-derived neurotrophic factor (BDNF), a molecule that promotes the maturation of GABAergic neurons, can induce a premature critical period (Hanover et al., 1999; Huang et al., 1999). As neutrophins can promote the maturation of GABAergic neurons, they could play a role in mediating the onset of the critical period. Interestingly, dark rearing, which delays the onset of the critical period, decreases BDNF expression, which in turn delays the maturation of GABAergic circuitry (Chen et al., 2001; Castrén et al., 1992; Morales et al., 2002). This delay in maturation may be one factor responsible for the effects of darkness on experience-dependent plasticity, as increasing inhibition with overexpression of BDNF, or treatment with diazepam, prevents the darkness induced critical period delay (Gianfranceschi et al., 2003; Iwai et al., 2003). Altogether, these results suggest that even in the absence of visual input, the maturation of GABAergic circuitry plays a vital role in mediating the timing of the critical period. Interestingly, increasing inhibition later in life does not restore plasticity; instead, there is evidence to suggest that decreasing GABAergic inhibition following the closure of the critical period can restore high levels of plasticity (Maya-Vetencourt et al., 2008; Harauzov et al., 2010; Sale et al., 2007). Evidently, there

is an initial level of inhibition that is necessary to induce the onset of the critical period. However, once the level of inhibition passes a threshold, it may become responsible for limiting plasticity in a mature brain. Increasing inhibition could not restore robust plasticity in adult animals who have exited the critical period, but decreasing inhibition could. Thus, inhibition presumably helps limit plasticity in the mature brain.

One potential mechanism that may be responsible for the onset of the critical period and robust plasticity is the subunit composition of the $GABA_A$ receptor. The $GABA_A$ receptor is one of the two GABA receptors that regulate GABA transmission. The subunit composition of the $GABA_A$ receptor is developmentally regulated, which suggests it may play a role in experience-dependent plasticity (Fritschy et al., 1994; Huntsman et al., 1999; Chen et al., 2001). Prior to the onset of the critical period, GABAergic circuitry is immature, and the dominant subunit in the receptor is the immature α3 subunit (Chen et al., 2001). As development continues, expression of the α3 subunit decreases and the expression of α1 subunit increases, indicating that GABAergic circuitry is maturing and that new $GABA_A$ receptor subtypes are emerging (Chen et al., 2001). Around the peak of the critical period, there is a shift in relative subunit dominance, switching from a higher prevalence of the immature α3 subunit to a higher prevalence of the mature α1 subunit (Chen et al., 2001). The relationship between the shift of relative subunit dominance and the peak of the critical period suggests that the maturation of the $GABA_A$ receptors, from a molecular distinct immature form to a molecularly distinct mature form, may play an important role in mediating plasticity within the visual system.

Further supporting the notion that the maturation of inhibitory circuitry and $GABA_A$ receptors regulate plasticity, this switch in subunit dominance is dependent on visual experience. Dark rearing, a method known to extend critical period plasticity, alters the expression of both subunits, preventing the developmental decrease of subunit α3 expression and accelerating the developmental increase in subunit α1 expression (Chen et al., 2001). Interestingly, Fagiolini and colleagues showed that the presence of the $GABA_A$ receptor α1 subunit is needed to induce the critical period (Fagiolini et al., 2004). In young pre-critical period mice, mutations rendering the α1 subunit insensitive to diazepam prevented the premature onset of the critical period that would otherwise occur with diazepam treatment. However, these mice still entered the critical period at the appropriate age, as while insensitive to diazepam, α1 subunit-containing $GABA_A$ receptors were present (Fagiolini et al., 2004). Although the exact mechanisms through which the $GABA_A$ receptors mediate plasticity is unclear, these results suggest that the subunit expression relative to each other mediate the onset, and likely the termination, of the critical period. The developmental upregulation of the α1 subunit appears to be required to initiate the critical period. The shift in subunit dominance at the peak of the critical period indicates the emergence of molecularly distinct mature forms of the $GABA_A$ receptors that may be responsible for terminating the critical period through stabilizing the circuitry formed during the critical period.

Based on the results presented above, GABAergic circuitry is essential in regulating the critical period. Evidence suggests that one specific type of GABAergic fast-spiking interneuron, parvalbumin-positive (PV+) interneurons, play a crucial role in mediating experience-dependent plasticity. Parvalbumin is a calcium ion (Ca^{2+}) binding

protein, and more than half of the cortical interneurons express this protein (Kubota and Kawaguchi, 1994; Gonchar and Burkhalter, 1997). The maturation of these PV+ interneurons in the rodent V1 parallels the onset of the critical period (del Rio et al., 1994). As mentioned earlier, BDNF plays a role in the onset of the critical period, presumably due to its role in regulating the maturation of GABAergic neurons. Specifically, BDNF appears to mediate the maturation of PV+ interneurons, as overexpression of BDNF accelerates their maturation (Huang et al., 1999). One type of PV+ interneuron found in the cat V1 are basket cells, may potentially be extremely important in experience-dependent plasticity, as they have axonal arbors that can extend horizontally through OD columns (Buzás et al., 2001). In addition, basket cells may contribute to the excitatory-inhibitory equilibrium, as they synapse onto the soma of pyramidal cells with the synapses showing preferential enrichment of α1 subunit-containing $GABA_A$ receptors (Klausberger et al., 2002). The correlation between the maturation of these interneurons and their relationship with α1 subunit-containing $GABA_A$ receptors further supports the idea that PV+ cells, and inhibitory circuitry in general, play an essential role in the GABAergic inhibition that mediates the critical period.

Further research that explores the role of PV+ interneurons in plasticity, suggests that different molecules interact with these cells to aid in regulating plasticity within the visual system. One such molecule is orthodenticle homeobox 2 (OTX2). Visual experience promotes the transfer of OTX2 from the retina to V1, where it accumulates in PV+ interneurons. The accumulation of OTX2 within PV+ cells of V1 is activity-dependent, and dark rearing decreases its expression within V1 (Sugiyama et al., 2008).

OTX2 plays a role in experience-dependent plasticity by stimulating the maturation of GABAergic circuitry through increasing the number of PV+ cells, and thus, promoting the onset of the critical period. Infusions of OTX2 into V1 prior to the natural onset of the critical period sped up the maturation of PV+ interneurons, as shown by an increase in the number of PV+ cells (Sugiyama et al., 2008). These infusions also altered the timing of the critical period, accelerating both its opening and closing. As well, animals that received infusions of OTX2 displayed low levels of plasticity at the age of the natural critical period (Sugiyama et al., 2008). Furthermore, decreasing endogenous levels of OTX2 hinders the maturation of PV+ interneurons, which in turn prevents the opening of the critical period. However, under these circumstances, infusions of either OTX2 or a GABA agonist can rescue the critical period (Sugiyama et al., 2008).

OTX2 enters PV+ interneurons through interactions with chondroitin sulfate proteoglycans (CSPGs), which are extracellular matrix (ECM) structures that encase these interneurons. As the animal matures, these CSPGs condense into a lattice-like structure called perineuronal nets (PNN). (Sugiyama et al., 2009; Härtig et al., 1999; Crair et al., 2001). In the mature brain, a significant function of PNNs may be to maintain low levels of plasticity by facilitating the accumulation of OTX2 into PV+ interneurons. In adult rodents, preventing OTX2 synthesis or blocking it from entering PV+ interneurons restores high levels of plasticity, and allows for recovery from MD (Spatazza et al., 2013; Beurdeley et al., 2012). Cumulatively, this implies that OTX2 regulates the induction and closure of the critical period through interactions with PV+ interneurons, thereby, mediating the maturation of GABAergic circuitry. The initial accumulation of OTX2 into PV+ neurons triggers the onset of the critical period;

however, subsequent accumulation of OTX2 maintains low levels of plasticity later in life. Altogether, the maturation of PV+ interneurons, and more broadly inhibitory circuitry, plays a central role in regulating experience-dependent plasticity, specifically controlling the induction of the critical period. Further, inhibition tone surpassing a threshold likely initiates a cascade of events that will subsequently decrease plasticity and terminate the critical period.

1.4.2 The Role of the Extracellular Environment in Mediating Plasticity

There is evidence to suggest that the extracellular environment plays an important role in mediating experience-dependent plasticity. As activity-dependent refinement of neuronal circuitry plays a crucial role during development, the formation and removal of dendritic spines is a prominent process during refinement. The critical period is associated with high levels of spine motility, however, as plasticity declines, so does motility, and in the mature brain, dendritic spines are stable and immobile (Grutzendler et al., 2002). Therefore, extracellular molecules such as the four describe separately in the section the follow that control spine motility can be said to influence experience-dependent plasticity and development directly.

1.4.2.1 Tissue Plasminogen Activator

One molecule of interest is tissue plasminogen activator (tPA), an extracellular protease prominent in the mammalian brain that can promote neurite growth and increase spine motility. During the critical period, tPA catalyzes the conversion of plasminogen to plasmin, which degrades supportive extracellular molecules and increases spine flexibility, therefore allowing for connections to be rewired (Werb, 1997). Within the

context of the visual system, research has shown that tPA plays a vital role in critical period synaptic rearrangement and is necessary for MD induced changes in connections. A short period of MD in young mice increases tPA activity within V1; however, blocking tPA activity prevents the MD-induced shifts in OD. In addition, blocking tPA during RO prevents recovery from MD, but infusions of tPA can restore plasticity and promote recovery (Mataga et al., 2002, 2004; Müller and Griesinger, 1998).

Additionally, MD during the critical period results in an upregulation of spine motility. In the case where MD is not present, exogenous tPA treatment can be used to mimic this increase in spine motility (Oray et al., 2004). Further supporting the role of tPA in plasticity, tPA catalyzed proteolysis decreases with age, suggesting that tPA may be one of the molecules responsible for the activity-dependent refinement of connections (Daw, 2014). The reduction of tPA activity seen with age may help maintain spine stability, as there would be less plasmin induced degradation of supportive structures.

1.4.2.2 Lynx 1

The expression of some late-emerging proteins directly correlates with a decline in plasticity levels, suggesting that they may be responsible for helping to limit plasticity in the mature brain. As a result of the inversely proportional relationship, these proteins are often referred to as 'molecular brakes.' One example of a so-called molecular brake is Ly6/neurotoxin1 (Lynx1), an endogenous prototoxin that binds to the nicotinic acetylcholine receptor (nAChR), mitigating its function (Miwa et al., 1999). Within the LGN and PV+ GABAergic interneurons, expression of Lynx1 is developmentally regulated. Lynx1 expression increases following the critical period. However, mice lacking Lynx1 exhibit heightened plasticity past the natural end of the critical period. As

well, knocking out Lynx1 in adult mice promotes spontaneous recovery from an earlier MD after restoration of binocular vision (Morishita et al., 2010). Lynx1 presumably mediates plasticity through its interactions with the nAChR, therefore altering acetylcholine transmission. Blocking cholinergic signalling in young mice prevents MD induced changes in OD, suggesting that acetylcholine transmission is essential for experience-dependent plasticity (Bear and Singer, 1986). Further, both excitatory and inhibitory neurons express nAChRs, suggesting Lynx1 may regulate plasticity via altering the excitatory-inhibitory balance by modulating the function of both excitatory and inhibitory receptors (Morishita et al., 2010). Additionally, evidence suggests that Lynx1 inhibits plasticity by not only decreasing cholinergic signalling but also by hindering structural changes, as the presence of Lynx1 inhibits dendritic spine motility (Sajo et al., 2016). Together it appears that Lynx1 likely acts as a molecular brake by inhibiting acetylcholine transmission and preventing structural changes.

1.4.2.3 Chondroitin Sulfate Proteoglycans and Perineuronal Nets

Another example of molecular brakes is a family of extracellular proteins, CSPGs, which are major components of the ECM and are known to inhibit axonal sprouting and growth. Around the end of the critical period, CSPGs preferentially condense around the neuronal cell body and dendrites of PV+ interneurons to form net-like structures called PNNs. The organization of CSPGs into PNNs is complete after the end of the critical period and is indicative of a mature adult brain (Pizzorusso et al., 2002; Härtig et al., 1994, 1999; Köppe et al., 1997; Kind et al., 2013). In the visual cortex, the expression and organization of CSPGs is activity-dependent. Dark rearing, which is known to prolong plasticity, has been shown to reduce the expression of the CSPG aggrecan and delay the

formation of PNNs (Lander et al., 1997; Kind et al., 2013; Pizzorusso et al., 2002; Ye and Miao, 2013). As PNNs accumulate at the end of the critical period in an activity-dependent manner, and they preferentially encase PV+ interneurons, these components of the ECM appear to play a key role in mediating experience-dependent plasticity.

Research has shown that treating an adult rat with chondroitinase ABC (ChABC), an enzyme that digests the glycosaminoglycan (GAG) side chain of CSPGs, degrades PNNs and restores sensitivity to MD (Pizzorusso et al., 2002). Pairing this treatment with RO can promote structural and functional recovery from the effects of long-term MD in adult rats (Pizzorusso et al., 2006). Interestingly, while the degradation of CSPGs was effective in reactivating plasticity within V1 of adult rodents, this treatment was infective in promoting recovery following MD in cats (Vorobyov et al., 2013). Although ineffective in cats, degradation of CSPGs in V1 of rodents likely increases plasticity by enhancing spine motility, which suggests that PNNs stabilize connections refined during the critical period via limiting spine motility, and thus plasticity (de Vivo et al., 2013). CSPGs not only play an essential role in limiting plasticity within the mature brain but may also be responsible for mediating the onset of the critical period. Degradation of the GAG side-chain decreased the accumulation of OTX2 into PV+ cells, a protein that promotes the maturation of PV+ interneurons, and subsequently, the induction of the critical period.

The relationship between CSPGs and OTX2 indicates that these ECM proteins are necessary to promote the accumulation of OTX2 into PV+ cells, and therefore directly influence the onset of the critical period (Beurdeley et al., 2012). Once the critical period opens, these CSPGs can be degraded by tPA to allow for activity-dependent

modifications. The age-related decline of tPA activity presumably allows for CSPGs to become organized into PNNs, consequently allowing for the persistent accumulation of OTX2 into PV+ cells, which is necessary to maintain low levels of plasticity. Seemingly, multiple extracellular environment proteins work cohesively to regulate experience-dependent plasticity and allow for the visual system to develop properly.

1.4.2.4 Myelin

Another structural factor that has been implicated in mediating the closure of the critical period is myelin, the insulating layer around axons. Nogo-A/B, oligodendrocyte-myelin glycoprotein (OMgp), and myelin-associated glycoprotein (MAG), are proteins found in myelin that bind to the paired immunoglobulin-like receptor B complex (PirB) and the Nogo Receptor (NgR) to prevent axonal outgrowth (Atwal et al., 2008). These molecules likely limit plasticity within the visual system by interacting with NgR and PirB to limit axonal sprouting, a process that is essential for rewiring connections during the critical period. Disrupting NgR and PirB function can extend the critical period well past the natural age of cessation (McGee et al., 2005; Syken et al., 2006). Further, adult mice lacking the NgR receptor show enhanced dendritic spine turnover (Akbik et al., 2013). These results suggest that these myelin-associated proteins may play a role in stabilizing circuitry within the adult brain by preventing structural changes. As well, evidence suggests that Nogo, OMgp, MAG, PNNs, and CSPGs, work together to stabilize synapses within the mature brain, as CSPGs can interact with the NgR, and cells that are encased by PNNs tend to express this receptor (Dickendesher et al., 2012; Ye and Miao, 1994). These molecules may work as a cohesive unit by acting on NgR and PirB to

prevent rearrangement of the circuits that were refined during the critical period, and therefore, limiting plasticity in adulthood.

1.4.3 The Role of Neurofilaments in Regulating Activity-dependent Plasticity

As many components within the extracellular environment regulate plasticity, it seems likely that intracellular components responsible for maintaining structure and function may also help mediate plasticity. In mammals, the cytoskeleton is composed of three predominant forms of filaments: microfilaments, intermediate filaments, and microtubules. The family of intermediate filament proteins is of particular interest concerning plasticity, as they contribute to cell shape, stability, and function (Goldman et al., 2012). Within the nervous system, the expression of intermediate filaments is developmentally regulated, with nestin and vimentin being expressed predominately in the prenatal brain, and α-internexin and neurofilament (NF) being expressed in a postnatal mature brain (Lendahl et al., 1990; Kaplan et al., 1990; Fliegner et al., 1994). In the mature brain, NFs are a significant component of the neuronal cytoskeleton, where they help to regulate neuron stability, axon structure and growth (Hoffman et al., 1987). NFs are composed of three subunits, with each named corresponding to their molecular weight: neurofilament light (NF-L), neurofilament medium (NF-M), and neurofilament heavy (NF-M) (Morris and Lasek, 1982). Within the visual system, NF expression begins to increase following the peak of the critical period, and expression is at its highest during adulthood. Similarly, phosphorylation of NF increases with age, which increases the stability of the protein (Song et al., 2015). The relationship between NF expression and

age suggests that NF may be a molecular brake and could be responsible for maintaining low levels of plasticity during adulthood.

Further supporting the role of NF plasticity regulation, MD decreases NF expression within the layers of the LGN and cells within V1 receiving input from the deprived eye (Bickford et al., 1998; Duffy and Slusar, 2009; Duffy et al., 2018; Duffy and Livingstone, 2005). Dark rearing produces a universal decrease in NF expression within the LGN, suggesting that darkness delays the developmental increase of NF expression, and prevents NF expression that is characteristic of a mature brain (O'Leary et al., 2012). As well, a 10-day period of darkness starting at P30 decreases NF density in V1 (Duffy and Mitchell, 2013). Thus, it seems that changes in the structure of the cytoskeleton play a role in regulating plasticity, and upstream modifications possibly trigger these changes. However, it is unlikely that these changes in NF expression are the dominant mechanism for mediating experience-dependent plasticity.

1.4.4 The Role of Epigenetics in Regulating Activity-dependent Plasticity

Evidence suggests that epigenetic mechanisms are involved in regulating critical period plasticity (Fagiolini et al., 2009). Epigenetic modifications, such as deoxyribonucleic acid (DNA) methylation, can alter gene expression without altering the DNA sequence. In the case of DNA methylation, gene transcription is repressed by converting cytosine into 5-methylcytosine, which impedes the ability for transcription factors to access the DNA. Similar to this methylation, histone acetylation or deacetylation (the addition or removal of an acetyl group from histones), can increase or decrease activity, respectively. Histone acetyltransferase (HAT) and histone deacetylases (HDACs) control the acetylation and

deacetylation of histones, respectively. Within V1, histone acetylation is developmentally regulated, with higher levels of acetylation during the critical period and lower levels in adulthood. Further, critical period acetylation is dependent on experience, as a short period of dark exposure can decrease acetylation (Vierci et al., 2016). In the mature brain, upregulating acetylation via inhibition of HDACs can restore sensitivity to MD (Putignano et al., 2007). Thus, epigenetic mechanisms seem to play a role in mediating experience-dependent plasticity. Specifically, HDACs activity likely stabilizes neural circuitry and therefore is a mechanism preventing high levels of plasticity in adulthood.

1.5 The NMDA Receptor and Plasticity

As mentioned previously, it appears that a balance in excitatory and inhibitory tone is a fundamental component of visual development. As the importance of inhibitory circuitry and the role it plays in plasticity has been discussed already, the remainder of this thesis will focus on the role of the excitatory circuitry, specifically the NMDA receptor, in experience-dependent plasticity. The final section will cover the role the NMDA receptor plays in mediating plasticity, the link between the receptor and the sliding model of synaptic plasticity, and how the receptor may mediate the enhanced plasticity seen following dark exposure.

Within the central nervous system, glutamate, the primary excitatory neurotransmitter, facilitates excitatory neurotransmission. This type of transmission requires activation of ionotropic glutamate receptors (iGluRs), such as the NMDA receptor, kainite receptor, and α-amino-3-hydroxy-5-methyl-4-isoxazolepropionic acid (AMPA) receptors (Feldman and Knudsen, 1998). These receptors all belong to the same

family of iGluRs, and received their names from the selective agonists that were used to differentiate them (Foster and Fagg, 1984). Although all these receptors mediate excitatory neurotransmission, there are some distinct differences between the NMDA receptor and the other two that make NMDA of interest with respect to plasticity. First, unlike AMPA and kainite receptors, the NMDA receptor is permeable to Ca^{2+} ions. The second major difference is the voltage-dependence of the NMDA receptor, which arises due to the magnesium ion (Mg^{2+}) block that is present in the receptor pore. Ions can only flow through the receptor when the postsynaptic membrane becomes sufficiently depolarized through AMPA receptor-mediated depolarization. The depolarization causes the Mg^{2+} to become dislodged, clearing the pore and allowing for Ca^{2+} and Na^{+} migration (Mayer et al., 1984; Nowak et al., 1984). Thus, at baseline activity, individual excitatory inputs can not cause Ca^{2+} influx, because the neuron can not be sufficiently depolarized to dislodge the Mg^{2+}. The final unique property of the NMDA receptor is that it can only be activated when glutamate and glycine bind to it simultaneously (Johnson and Ascher, 1987; Kleckner and Dingledine, 1988).

Similar to other transmembrane glutamate receptors, the NMDA receptor assembles as a tetrameric complex of subunits (Rosenmund et al., 1998; Mano and Teichberg, 1998). However, unlike the AMPA and kainite receptors, which assembles as both homo- and heteromeric complexes, the NMDA receptor only assembles as a heteromeric complex. A functional NMDA receptor consists of two obligatory glycine binding NR1 subunits and two glutamate binding NR2 subunits. In some cases, a glycine binding NR3 subunit will replace one of the NR2 subunits, however, receptors containing

an NR3 subunit show a decrease in calcium permeability (Laube et al., 1998; Monyer et al., 1994; Perez-Otano et al., 2001).

1.5.1 The Role of the NMDA Receptor in Synaptic Potentiation

The NMDA receptor is an attractive candidate as a molecular mechanism of experience-dependent plasticity, as blocking the receptor during the critical period prevents the effects of MD (Bear et al., 1990; Daw et al., 1999; Kleinschmidt et al., 1987). Presumably, glutamatergic transmission, and subsequent activation of the NMDA receptor, is required for experience-dependent modifications and is therefore essential for refining the connections formed during the critical period. Evidence suggests that the NMDA receptor controls plasticity by altering synaptic efficacy through influencing the probability of long-term potentiation (LTP) or long-term depression (LTD). Both LTP and LTD are dependent on NMDA receptor activation/Ca^{2+} influx and are mechanisms of plasticity that follow the Hebbian rules of synaptic plasticity. The theory of Hebbian plasticity, first proposed by Donald Hebb in the 1940s, is a correlation-based theory of synaptic plasticity, that postulates that correlated activity of the pre- and post-synaptic cells determine the synaptic efficacy. Persistent and repetitive stimulation of postsynaptic cells by presynaptic cells produces an increase in synaptic efficacy. In contrast, low levels of synaptic activity produce a decrease in synaptic efficacy (Hebb, 1949). Long term potentiation, which was first characterized in the hippocampus, was the first experimental analogue of the activity-dependent synaptic modifications proposed by Hebb. A short high-frequency stimulation of presynaptic neurons can induce LTP. This type of stimulation results in a large influx of Ca^{2+} and a subsequent increase in synaptic strength

(Bliss and Lomo, 1973; Bliss and Collingridge, 1993). Conversely, long low-frequency stimulations can induce LTD, resulting in a smaller influx of Ca^{2+} and a subsequent decrease in synaptic strength (Dudek and Bear, 1992; Yang et al., 1999).

The induction of both LTP and LTD requires activation of the NMDA receptor, and the subsequent Ca^{2+} influx caused by the receptor activation causes a cascade of events that modify synaptic efficacy. A major modification that alters synaptic efficacy is the removal or inclusion of AMPA receptors into the postsynaptic membrane as a result of LTD or LTP, respectively. The change in the number of AMPA receptors can alter the strength of synaptic transmission, with more receptors making transmission stronger and fewer receptors making transmission weaker (Malenka and Bear, 2004). The role of the NMDA receptor in potentiation/depression is one of critical importance; for both to occur, the NMDA receptor must be activated. The activation of the NMDA receptor is dependent on the inherent voltage dependence of the receptor caused by the Mg^{2+} block (Coan et al., 1989). Furthermore, for the NMDA receptor to activate, depolarization that causes Mg^{2+} to become dislodged must co-occur with glutamate binding. In this manner, the NMDA receptor acts as a molecular coincidence detector, detecting the simultaneous activation of the pre- and post-synaptic neuron. In Hebbian style, low levels of simultaneous activation results in a weakening of the connection and high levels of simultaneous activation results in a strengthening of the connections. Further, preventing activation of the receptor inhibits the induction of both LTP and LTD (Collingridge et al., 1983; Pananceau and Gustafsson, 1997; Dudek and Bear, 1992). Evidence suggests that an increase in postsynaptic Ca^{2+} concentration is essential to induce both LTP and LTD. Moderate activation of the NMDA receptor, and modest Ca^{2+} influx are optimal for

inducing LTD, whereas, more robust activation of the NMDA receptor and more Ca^{2+} influx are necessary to induce LTP. Additionally, an increase in postsynaptic Ca^{2+} concentration is necessary for both LTP and LTD specific synaptic modifications (Lynch et al., 1983; Malenka et al., 1988; Mulkey and Malenka, 1992; Malenka, 1994). Interestingly, the kinetics of the receptor, and consequently, the amount of Ca^{2+} influx, appears to regulate whether LTP or LTD occurs, and therefore regulates synaptic strengthening or weakening. As the receptor subunit composition of the NMDA receptor can alter the functional properties of the receptor, and therefore, the Ca^{2+} influx, the subunit composition may mediate plasticity.

1.5.2 NMDA Receptor Subunit Composition

Further supporting its role in experience-dependent plasticity, the NMDA receptor subunit composition alters the receptor kinetics and thus can alter the amount of Ca^{2+} influx. Within the postnatal cortex, there are two dominant NR2 isoforms: NR2A and NR2B. Evidence suggests that the amount of these isoforms can alter the functional properties of the receptor. As well, their expression within V1 is developmentally regulated and activity-dependent, which suggests developmental differences in the expression of these isoforms may mediate plasticity by altering receptor function (Sheng et al., 1994; Monyer et al., 1994).

NMDA receptors containing NR2A and NR2B can assemble as either di-heteromers (NR1 and either NR2A or NR2B) or as tri-heteromers (NR1, NR2A, and NR2B) (Al-Hallaq et al., 2007). The different receptor compositions, di- or tri-heteromeric, cause differences in receptor kinetics, glutamate binding affinity, as well as

protein binding patterns, all of which may influence plasticity. Compared to di-heteromeric NR1/NR2A receptors, di-heteromeric NR1/NR2B receptors have slower kinetics, and thus a longer current duration. The kinetics of tri-heteromeric receptors are an intermediate case, falling in-between that of the di-heteromeric receptors (Flint et al., 1997; Monyer et al., 1992; Vicini et al., 1998). The prolonged receptor opening associated with the presence of NR2B subunits (i.e. slower kinetics) likely arises due to the higher glutamate binding affinity and slower dissociation rates seen in these receptors (Laurie and Seeburg, 1994). Further, as the receptors containing NR2B subunits remain open for longer, they allow for more Ca^{2+} influx, consequently influencing the induction of LTP versus LTD (Sobczyk et al., 2005).

The different NMDA configurations also vary in their protein interactions. Since the downstream effects caused by NMDA receptor activation influence LTP/LTD induction, the difference in protein interactions may determine the direction in which synaptic efficacy changes. One such protein that may directly influence the likelihood of LTP/LTD is calcium/calmodulin-dependent protein kinase II (CaMKII), an enzyme that is abundant at synapses (Peng et al., 2004). CaMKII is activated by a Ca^{2+}/calmodulin complex that forms from an interaction of calmodulin with the Ca^{2+} entering the cell. This kinase is involved in many signalling cascades and plays a vital role in the induction of LTP (Lisman et al., 2002). The composition of the NMDA receptor directly influences the binding affinity of CaMKII to the receptor. Activated CaMKII binds strongly to the N2RB subunits of the receptor, whereas it binds with much more weakly to NR2A subunits (Strack and Colbran, 1998; Gardoni et al., 1999; Leonard et al., 1999). When the active form of CaMKII binds to the NR2B subunits, CaMKII will remain active even

after the Ca^{2+}/calmodulin complex dissociates (Bayer et al., 2001). Evidence suggests that the association between CaMKII and NR2B subunits is necessary to induce LTP, as mutating the NR2B subunit to have reduced CaMKII binding affinity blocks the induction of LTP (Barria and Malinow, 2005). Interestingly, if the NR2A subunits are mutated to have high CaMKII binding affinity, LTP can be induced but not to the levels seen with NR2B subunits (Barria and Malinow, 2005). Thus, the induction of LTP seems to be dependent on the association between active CaMKII and NR2B subunits. The interaction of CaMKII and the NR2B subunit may allow for CaMKII to initiate various cascades, which will subsequently increase synaptic efficacy.

As mentioned, the NR2 subunit composition of the NMDA receptor is developmentally regulated. Within V1 of rodents, ferrets, and cats, there are development changes in NR2A/NR2B expression (Quinlan et al., 1999a; Roberts and Ramoa, 1999; Chen et al., 2000). In all three species, receptors containing the immature NR2B subunit are predominant in early postnatal life. As development continues, there is a progressive increase in receptors containing the mature NR2A subunit, increasing the expression of NR2A relative to NR2B expression. The gradual inclusion of the NR2A subunit is associated with a gradual shortening of the NMDA receptor current (Flint et al., 1997; Roberts and Ramoa, 1999). Interestingly, as NR2A expression increases during early development and into the critical period, the expression of NR2B remains the same (Chen et al., 2000). However, compared to expression during the critical period, both subunits show a decrease during adulthood. The progressive increase and subsequent decrease in NR2A expression follows a time course that parallels the critical period and visual development (Roberts and Ramoa, 1999; Chen et al., 2000). This developmental increase

in NR2A expression is activity-dependent, as dark rearing can delay the progressive increase of this subunit, and consequently the shortening of the NMDA current (Quinlan et al., 1999a; Nase et al., 1999; Carmignoto and Vicini, 1992; Giannakopoulos et al., 2010). Further, dark rearing does not alter the expression of the NR1 subunit, implying that visual deprivation alters the NMDA receptor kinetics as opposed to the absolute number (Quinlan et al., 1999a). Together, this suggests that the altered NMDA receptor function may be causing the darkness-induced delay in critical period onset, as opposed to a decrease in the number of NMDA receptors.

The developmental switch in the NR2A/NR2B ratio plays a significant role in altering the functional properties of the NMDA receptors, consequently changing the likelihood of inducing LTP or LTD, and thus altering levels of plasticity. As described above, activity and development modulate the subunit ratio. As development progresses, the ratio increases (NR2A levels increase, NR2B levels remain relatively steady), which subsequently shortens the receptor current and therefore decreases Ca^{2+} influx (Flint et al., 1997). These changes in receptor properties make potentiation more difficult to induce, but depression is easier to induce. Further, dark rearing delays the developmental increase of the NR2A/NR2B ratio and increases the receptor current (Quinlan et al., 1999a, 1999b; Philpot et al., 2001). As well, in rats, a short period of binocular deprivation around the peak of the critical period decreases the NR2A/NR2B ratio and increases the receptor current (Quinlan et al., 1999a; Philpot et al., 2001; Chen and Bear, 2007). As the ratio of the NMDA receptor subunits appears to mediate the likelihood of LTP or LTD, the composition of the receptor is a putative molecular mechanism of plasticity.

1.5.3 The BCM sliding Model of Synaptic Plasticity

While the Hebbian model of plasticity can be used to explain many aspects of the development of neural circuitry, since it is a positive feedback process, stronger connections become stronger. Therefore, the Hebbian model of plasticity fails to explain how cells avoid synaptic instability and saturation of synaptic strength. However, the BCM sliding model of synaptic plasticity, which builds off Hebbian plasticity, was able to avoid saturation by adding a threshold between LTP and LTD. When the postsynaptic firing rate is higher than the threshold, the correlated pre and postsynaptic activity can elicit LTP, and consequently, synaptic strengthening. When the postsynaptic firing rate is lower than the threshold, the correlated activity can elicit LTD, and therefore synaptic weakening. Furthermore, the threshold between LTP and LTD is not fixed but rather changes depending on the previous activity of the neuron (Cooper and Bear, 2012). If the postsynaptic neuron experiences a period of increased activity, then the threshold will increase; thus, LTD will be easier to induce, whereas the induction of LTP will be more difficult to induce. Conversely, a period of decreased activity will cause the threshold to decrease, favouring LTP over LTD; thus, LTP will be easier to induce (Figure 1) (Bienenstock et al., 1982). The ability for prior experience to alter the degree, and likelihood, of plasticity in response to activity, as seen in the BCM model, is called metaplasticity, as it is the plasticity of synaptic plasticity (Abraham and Bear, 1996).

Kirkwood et al. (1996) provided experimental evidence of metaplasticity by depriving rats of light, therefore decreasing activity, and attempting to induce both LTP and LTD in the brain slices of these animals. In both the dark reared and light reared rats, LTP could be induced using high-frequency stimulation, and LTD could be elicited using

low-frequency stimulation. However, Kirkwood and colleagues showed that the LTP/LTD threshold was different between the dark reared and light-exposed animals. The threshold was lower in the dark reared animals; thus, LTP is easier to elicit, and LTD is harder to elicit. Exposing the dark reared rats to a few days of light can reverse these effects. This shift in threshold was also confirmed experimentally in mice (Philpot et al., 2003). While research has provided experimental evidence of metaplasticity, an important caveat of these experiments is that since stimulation frequency was altered, this provides information about the presynaptic threshold as opposed to the postsynaptic threshold, which would be measured by the postsynaptic firing rate (Figure 2). The threshold measured in these experiments is important to note, as the BCM model makes assumptions about the postsynaptic threshold.

Interestingly, as the subunit composition of NMDA alters the kinetics of the receptors, which subsequently alters the threshold of activity needed to induce LTP versus LTD, the NMDA receptor may be the molecular basis of the BCM model (Figure 1) (Quinlan et al., 1999a, 1999b; Philpot et al., 2001, 2003, 2007). A low ratio, and therefore more NR2B relative to NR2A, shifts the LTP/LTD threshold so that lower stimulation can induce LTP. In this case, the receptor has slower kinetics, higher Ca^{2+} influx, and increased CaMKII binding, all of which increase the likelihood of LTP. Thus, moderate stimulation, as opposed to high-frequency stimulation, is sufficient to induce potentiation. Conversely, more NR2A relative to NR2B, and therefore a higher ratio, shifts the threshold so that stronger stimulation is required to induce LTP, but moderate stimulation can induce LTD. In this case, the receptor has faster kinetics, lower Ca^{2+}

influx, and minimal CaKMII binding, all of which decrease the likelihood of LTP induction (Flint et al., 1997; Philpot et al., 2001).

As the NR2A/NR2B ratio appears to directly alter plasticity through LTP and LTD, presumably, the developmental increase of this ratio within V1 may be responsible for low levels of plasticity in a mature brain. Increasing the LTP/LTD threshold increases the stimulation required to produce both LTP and LTD, making both potentiation and depression harder to induce, and thus decreasing plasticity within V1. On the contrary, manipulations to visual input that delays the developmental increase of the NR2A/NR2B ratio, such as dark rearing, being raised in the dark, (Quinlan et al., 1999a, 1999b; Philpot et al., 2001), or dark exposure, being exposed to a short period of darkness (Quinlan et al., 1999a; Chen and Bear, 2007), decreases the ratio, therefore decreases the stimulation required to produce both LTP and LTD, thus increasing plasticity. This sliding model of plasticity may account for the delayed critical period caused by dark rearing, as well as the increase in plasticity produced by a short period of dark exposure. In both cases, the NR2A/NR2B ratio would be lower compared to light-reared controls, and therefore, a lower frequency compared to the light-reared animals would be needed to induce both LTP and LTD, consequently increasing plasticity. As mentioned above, evidence supports this theory as dark rearing shifts the LTP/LTD threshold so that lower stimulation frequencies are able to produce potentiation and depression (Kirkwood et al., 1996; Philpot et al., 2003). These results give the impression that within the visual cortex, sensory experience alters the NR2A/NR2B ratio, which subsequently alters the threshold for inducing plasticity. Based on the evidence presented above, it seems likely that the NMDA receptor subunit composition is indeed the molecular basis of the BCM model

and is potentially one of the main excitatory molecular mechanisms of experience-dependent plasticity within the visual system.

1.6 The Current Study

The current study aimed to gain a better understanding of the role that the NMDA receptor subunit composition plays in experience-dependent plasticity. Although previous research has already demonstrated that dark exposure can alter the NMDA receptor composition (Quinlan et al., 1999a; Philpot et al., 2001; Chen and Bear, 2007), my research examined the NMDA receptor subunit composition in a higher-order mammal, the cat, in order to expand our scope of knowledge beyond what is already known in rodents. Additionally, my research examined how dark exposure alters receptor composition within both V1 and the LGN, and to my knowledge, no prior research has examined the change in receptor composition within the LGN. Finally, my research investigated how dark exposure alters receptor composition across the layers of the LGN and V1, which has not been examined previously.

In order to assess how visually driven activity alters NMDA receptor subunit composition within V1 and LGN, kittens were exposed to a short 10-day period of darkness, an intervention that eliminates visually-driven neural activity and is thought to increase plasticity. Young kittens were either light reared until P37/P40 or exposed to darkness for from P30-P40. The NR2A/NR2B ratio was examined within both the LGN and V1. As the LGN receives feedback from layer IV of V1, and MD induced changes are first observed within V1, this suggests that modifications within the LGN are reflective of modifications occurring in V1 (Trachtenberg et al., 2000). Since changes

within the LGN are thought to be indicative of changes occurring in higher level visual structures, examining the LGN will provided a deeper understanding how darkness alters the NMDA receptor composition within the visual system.

In order to investigate if a short period of dark exposure was sufficient in altering the NMDA receptor subunit composition within the cat visual system and if the potential change is layer or region-specific, a novel methodology for subunit visualization was developed. The new methodology employed multiplex immunolabeling to quantify the subunit ratio in thin slices from the cat visual system. This method preserves the *in situ* protein distribution, allowing us to investigate layer-specific receptor changes. Our methodology mimics a western blot; however, opposed to assessing expression in homogenized tissue, expression was assessed in sliced tissue on a cell-by-cell basis (Figure 3).

We found that a 10-day period of dark exposure is sufficient in shifting the NMDA receptor subunit composition towards the immature form. Animals exposed to darkness showed a decrease in NR2A/NR2B ratio within V1 and LGN that was universal and not layer-specific, which to the best of my knowledge, has never been shown before. As well, we observed a universal reduction in neuron soma size within V1 and LGN of cells expressing these subunits, indicating a short period of darkness may delay the developmental increase of cell size, or revert it to a younger state. The method developed for this research allows for the assessment of subunit composition on a layer-specific level, enabling superior spatial resolution compared to the more common and highly used western blot technique. In addition, the findings from this study further support the role

of the NMDA receptor subunit composition as the molecular basis of the BCM model and provide further evidence that experience alters the subunit ratio.

Overall, the results of this study provide insight into the molecular mechanisms of experience-dependent plasticity. From these results, we can infer that the NMDA receptor subunit composition may be responsible for the darkness mediated enhancement of plasticity by altering the threshold for neural plasticity in the manner described by the BCM model. Although previous research has already shown that a short period of darkness can alter the NMDA receptor subunit composition (Quinlan et al., 1999a; Chen and Bear, 2007), my research probed deeper into the exact mechanisms of the NMDA receptor-dependent sliding model of synaptic plasticity. By examining the NMDA receptor composition in both the LGN and V1, as well as, exploring layer-specific changes in the ratio, we were able to show that the shift in LTP/LTD threshold, which may be an excitatory mechanism responsible for the darkness mediated increase in plasticity, is not driven by a specific component or layer within the visual system.

CHAPTERS 2 – EXPERIMENTAL DESIGN

2.1 Cat Colony and Housing

Six kittens (4 males, 2 females, from 3 litters) were used to conduct this experiment. Kittens were born and raised in a closed breeding colony at Dalhousie University. Before any visual manipulations, the kittens were housed with their mother in a colony room on a 12:12 light/dark cycle. The colony rooms and litter boxes were cleaned daily. The kittens had ad libitum access to water/dry chow, and wet food was provided every afternoon.

2.2 Ethics Approval

All animal procedures followed protocols that were approved by the Dalhousie University Committee on Laboratory Animals and abided by the guidelines of the Canadian Council on Animal Care.

2.3 Design

This project consisted of two experimental groups: normal and dark exposure. Kittens in the normal condition were raised under normal rearing conditions without any visual intervention until postnatal day 37 (n=1) or postnatal day (P) 40 (n=2). Kittens in the dark-exposure (DE) group were reared normally until P30, then they were placed in complete darkness for ten days (n=3). Tissue from the P37 normal control was collected from a previous study and was kept in antigen preservative (50% ethylene glycol, 1% polyvinylpyrrolidone in phosphate-buffered saline (PBS)).

2.4 Experimental procedures

2.4.1 Dark Exposure

Kittens in the DE condition were placed in a darkroom facility for ten days. The darkroom facility (Figure 4), located in the Department of Psychology and Neuroscience at Dalhousie University, was previously described in detail by Mitchell (2013). The facility consists of six rooms: one lit room containing a sink, three dark anterooms, and two core darkrooms. The doors that connect the rooms are back-to-back double doors to ensure no light enters the rooms. The kittens were housed in a large cage (1.5 x 0.7 x 0.9 m) with their mothers in the primary darkroom (Figure 4, C1), which can be accessed through anterooms A1 and A2. The cage contained a litter box, a cardboard box lined with blankets for nesting, a mat, and bowls containing dry food, water, and wet food. During the 10-day period of darkness, the kittens had ad libitum access to water and dry food and received a daily bowl of wet food. To help establish circadian rhythms, the primary darkroom, in which the kittens were housed, contained a radio that turned on and off automatically at 7 AM and 7 PM, respectively. The primary darkroom was also equipped with an infrared camera, allowing care staff to monitor the wellbeing of the animals throughout the 10-day period.

Every day during the ten days, at approximately the same time each day, the kittens were transferred in a cat carrier from the primary darkroom to the adjacent darkroom (Figure 4, C2). Once complete, the primary darkroom was illuminated in order to clean the cages, litter box, and room. More dry food was provided if needed, water was replaced, and the kittens were supplied with the daily amount of wet food. While the cleaning occurred, the mother was allowed to move about the illuminated primary

darkroom. Following the completion of these tasks, the lights were turned off, and the kittens were transferred back to their cages in the primary darkroom.

Prior to entering the darkroom, the technicians caring for the animals were required to remove cellular phones, watches, key chains, and any other possible source of light from their persons, in order to prevent any light exposure.

The 10-day period of darkness was chosen as previous research has shown that this length of time is effective in enhancing the capacity for plasticity within the visual cortex, as this period of darkness promotes recovery following MD (Duffy and Mitchell, 2013; Mitchell et al., 2016). As well, 10-days of darkness is an ideal length, as shorter periods of dark exposure appear to be ineffective in increasing plasticity, as a shorter length of time does not promote recovery in the deprived eye (Mitchell et al., 2016).

2.4.2 Histology

At P40, the DE animals were removed from the darkroom in an opaque box and brought to the surgery room to be euthanized. Similarly, at P37 or P40, the normal animals were brought to the surgery room to be euthanized. The animals were placed under gaseous anesthesia (3-5% isoflurane in oxygen) and administered a lethal intraperitoneal injection of sodium pentobarbital (Euthanyl; 150mg/kg). A transcardial perfusion was performed using approximately 150 mL of phosphate-buffered saline followed by an equal volume of 4% dissolved paraformaldehyde in PBS. Immediately following the perfusion, the brains of each animal were extracted, and the visual cortex and thalamus, the area of the brain containing the LGN, was dissected. Following dissection, the tissue was placed in a cryoprotectant solution (30% sucrose in PBS) to prevent any tissue damage that may

occur with freezing. Once the cryoprotection was complete, the tissue was cut coronally into 50 µm thick sections using a sliding microtome (Leica SM2000R; Germany).

In order to assess the ratio between the NMDA receptor NR2A and NR2B subunits in tissue slices of the LGN and V1, a novel method employing multiplex immunolabeling that preserves the *in situ* protein distribution was developed (Figure 5). The sections were immersed in PBS containing a rabbit polyclonal primary antibody against NMDAR2B (Rb-R2B, 1:1,000 dilution, ab65783; Abcam, Cambridge), and left in the antibody solution overnight on the shaker table. The next day the tissue was washed with PBS and then exposed to a PBS solution containing donkey anti-rabbit fragment-antigen binding (fab) fragment (DAR FF) conjugated to Alexa Fluor® 594 for one hour (1:200 dilution, Jackson ImmunoResearch, West Grove). Fab fragments are monovalent antibodies in which the fragment antigen-binding region has been isolated from the Fc portion of the antibody. They are useful in this context because they can block binding sites when double labelling with primary antibodies that have the same host species. In this case, they were used to block all the possible binding sites on the first rabbit primary antibody, allowing us to use a second rabbit primary antibody against NMDAR2A.

After the tissue was immersed in the fab fragment, it was washed with PBS, and then immersed in PBS containing a rabbit polyclonal primary antibody against NMDAR2A (Rb-R2A, 1:1,000 dilution, ab16646, Cambridge) and left overnight on the shaker table. The next day, tissue was rinsed with PBS and exposed to a PBS solution containing goat anti-rabbit conjugated (GAR) to Alexa Fluor® GAR 488 for one hour (1:500 dilution, Jackson ImmunoResearch, West Grove). Once all the labelling was

complete, the tissues were mounted on a glass slide, with four to six pieces per slide, and allowed to dry for one hour.

Once dry, the section was stained for Nissl substance by exposing the mounted tissue to a PBS solution containing NeuroTrace 435/455 (NT 435/455), a fluorescent Nissl stain, for seven minutes (1:200 dilution, ThermoFischer Scientific). Following this, the mounted tissues were rinsed with PBS, then stained with Sudan black for 10 minutes, which helps minimize background fluorescence. The tissue was then rinsed with PBS until excess Sudan black was washed off, and then allowed to dry for 20 minutes. Once dry, the tissue was coverslipped with prolong gold antifade mounting medium (P36930, ThermoFischer Scientific**).**

2.4.3 Quantification

Quantification of subunit ratio and neuronal soma size was performed blind to the rearing condition of each animal. Two sections of both the left and the right V1 and one section of the LGN were selected from each animal to be quantified.

Immediately after coverslipping, images of the tissue were taken using a BX-51 epifluorescence microscope (Olympus; Markham, Ontario, Canada) that was fitted with an Infinity3S-1UR microscopy camera (Lumenera Corporation, Ottawa, ON), and an X-Cite 120Q illumination system (EXFO; Mississauga, Ontario, Canada). The images were taken using a 60x oil-immersion objective and were captured with a computerized stereology software (NewCast; Visiopharm, Denmark). The exposure time (55 ms) and light level (lowest possible setting) remained consistent for the pictures taken of the NR2A and NR2B labelling. Keeping the exposure time and light level consistent was

done to ensure any differences in fluorescence intensity observed were due to differences in protein level and not artificial differences caused by light level.

The layers of the LGN and V1 were identified before capturing images. Within each layer, the points of image capture were randomly selected. Approximately ten images were taken from each hemisphere of V1 layer 2/3, and LGN layer A and A1. Approximately seven pictures were taken from layers 4, 5, and 6 within each hemisphere of the V1. At each location, images of NMDAR2A, NMDAR2B, and NeuroTrace fluorescence Nissl stain were captured using filter sets specific to each marker (respectively, FITC – 3540C, LED-mCherry-A-OMF-ZERO, and BV 480 – 2432 A; Semrock, Rochester, NY). These three filter cubes were chosen as they are ideal for the secondary antibodies/fluorescence NT used, and do not show high levels of bleed-through between channels (

Table 1).

Once imaging was complete, images were transferred to Adobe Photoshop for quantification (Adobe; San Jose, CA). In Photoshop, the images for the three markers were put into separate layers and using the paint tool, cells expressing the NR2B subunit with a clear unstained soma were marked to be quantified. This criterion was chosen as previous research has shown that the R2B subunit expression remains relatively uniform throughout early development, and dark rearing does not seem to alter its expression (Roberts and Ramoa, 1999; Chen et al., 2000). Once identified, cells were quantified by using the freehand selection tool to trace the outer perimeter of the cells on the Nissl images. Once the cells were outlined, the cell area and greyscale means, which are representative of the fluorescence intensities, were measured from the NR2A and NR2B images. The ratio for each cell was determined by dividing the greyscale values of NR2A by the greyscale values of NR2B.

Statistical analyses were performed to assess differences in NR2A/NR2B subunit ratio and neuron soma size between conditions. Non-layer specific differences in subunit ratio and soma size were assessed for the data collected from the cells within the RV1, LV1, LGN layers receiving input from the right eye, and LGN layers receiving input from the left eye. Unpaired two-tailed t-tests with Welch's correction were performed using Graph Pad Prism Software (Version 8.0.0 for Mac OS X, GraphPad Software, San Diego, California USA, www.graphpad.com) to compare differences between the measurements for the cells in the DE condition versus the cells in the normal condition. Percent decrease of the dark exposure animals relative to the normal animals was calculated for both NR2A/NR2B ratio and neuronal soma area (1).

Percent Decrease:

$$= \left(\frac{(\text{Normal Values} - \text{Dark Exposure values})}{(\text{Normal Values})}\right) \times 100\% \qquad (1)$$

In order to assess if there were significant differences between the conditions at a layer-specific level within the LGN and V1, factorial analysis of variances (ANOVA) were performed using IBM SPSS Statistics (Version 25.0 for Windows, IBM Corp, Armonk NY) comparing the effects of condition, V1/LGN layer, and hemisphere on receptor subunit composition. Alpha was set to 0.5 for all statistical analyses.

Prior to statistical analysis, using Graph Pad Prism Software outliers were identified and removed with the robust regression and outlier removal (ROUT) method with the false discovery rate (FDR) set to 0.2% (Motulsky and Brown, 2006). A strict FDR was chosen to ensure only the outliers were detected, as the data contains a large spread of values. No outliers were observed in the NR2A/NR2B ratio data; however, outliers were present in and removed from the soma area data.

Data visualizations were performed using Graph Pad Prism Software (Version 8.0.0 for Mac OS X, GraphPad Software, San Diego, California USA, www.graphpad.com).

2.4.4 Experimental Controls

Two control experiments were performed to ensure the use of fab fragments was an appropriate method. In the first control experiment, we assessed if the second primary antibody, rabbit polyclonal primary antibody against NMDAR2A, bound to the fab

fragments (Figure 6A). Following a similar protocol described above, a piece of RV1 tissue from a P40 normal animal was incubated in Rb-R2B (1:1000) overnight on the shaker table. It was then rinsed with PBS and incubated in DAR FF Alexa Fluor 594 for one hour. The tissue was rinsed again, then placed in a PBS solution containing Rabbit anti-rat conjugated to Alexa Fluor® 488 for one hour (1:500). This secondary antibody was used to mimic the binding of the Rb-R2A primary, as both antibodies were raised in rabbit. Following the one-hour incubation, the tissue was mounted, allowed to dry, stained with NT 435/455 and Sudan black, then coverslipped and imaged. Based on the images taken, it seems that the Rb-R2A primary antibody does not bind to the fab fragments, as there was very little to no signal in the 488 channel (Figure 6A).

The second control experiment assessed if the fab fragment did indeed block the binding sites on the first primary antibody, Rb-R2B, from the second secondary. To evaluate if the second secondary bound to the fab fragment, we assessed the labelling of the second secondary antibody, goat anti-rabbit conjugated to Alexa Fluor® 488, without the presence of the second primary antibody (Figure 6B). Similar to above, a piece of tissue from a P40 control RV1 was incubated overnight in Rb-R2B (1:1000). Following the incubation period, it was rinsed with PBS, incubated in DAR FF Alexa Fluor 594 for one hour (1:200), rinsed with PBS, then incubated in GAR Alexa Fluor 488 (1:500 dilution) for one hour. Following this, it was rinsed again, stained for NT 435/455 and Sudan black, coverslipped, and imaged. Based on the images taken, it seems that the GAR Alexa Fluor 488 secondary does not bind to the fab fragment or the GAR- R2B antibody (Figure 6B). These control experiments indicate that the fab fragment does

indeed block the binding sites on the GAR- R2B antibody, allowing us to use primary antibodies from the same host species.

CHAPTER 3 – RESULTS

3.1 General Considerations

Greyscale level and neuron soma size measurements were recorded from 3502 cells. For animals in the dark exposure group, measurements were taken from 1704 cells, with 1070 being from V1 and 634 being from the LGN. Within the normal animals, measurements were taken from 1798 cells, with 1186 being from V1, and 612 being from the LGN. Using unpaired two-way t-tests with Welch's correction, we assessed non-layer specific differences between the conditions within RV1, LV1, layers of the LGN receiving input from the left eye, and layers of the LGN receiving input from the right eye. A factorial ANOVA was used to assess layer specific differences in subunit ratio and cell size. No outliers were identified in the subunit ratio data; however, outliers were identified and removed from the V1 and LGN cell size data (Table 2).

3.2 The Effects of Dark Exposure on the NMDA Receptor Subunit Composition within V1

The first part of the study focused on examining how a short period of dark exposure altered NMDA receptor subunit composition in both the LGN and V1. Examination of the NR2A and NR2B stained tissue revealed a difference in subunit labelling between the two conditions within V1 (Figure 7A) and the LGN (Figure 8A). Based on observations of the tissue, it appeared that within both the LGN and V1, dark exposure decreases NR2A labelling and increases NR2B labelling. Examination of the NMDA receptor subunit composition revealed a significant difference in subunit ratio between the groups

within both hemispheres of V1 (Figure 7B) and layers of the LGN receiving input from the left or right eye (Figure 8B). As ROUT did not identify any outliers in the subunit ratio data, no outliers were removed from this data prior to analysis.

Within LV1 (Figure 7B, left pane), dark exposure ($M = 0.522$, $SD = 0.101$, $n = 514$) caused a significant reduction in receptor subunit ratio compared to the normal group ($M = 0.702$, $SD = 0.094$, $n = 546$), $t(1038) = 30.03$, $p < 0.001$, with dark exposure decreasing the ratio by 25.64%. Similarly, within RV1 (Figure 7B, right pane), dark exposure ($M = 0.566$, $SD = 0.072$, $n = 556$) significantly altered the receptor subunit composition by reducing the NR2A/NR2B ratio compared to normal ($M = 0.700$, $SD = 0.127$, $n = 640$), $t(1038) = 22.93$, $p < 0.001$ with dark exposure decreasing the ratio by 19.14%. Overall, within V1, dark exposure decreases the NR2A/NR2B ratio by 22.39%. This decrease in ratio suggests that the there is an increase in NR2B relative to NR2A in dark exposure animals compared to normal animals. The decrease in ratio likely shifts the LTP/LTD threshold so that LTP is favoured over LTD and can be induced more easily.

The relationship between NR2B greyscale values and NR2A greyscale values within normal animals (Figure 7C, purple) and dark exposure animals (Figure 7C, teal) was plotted for both hemispheres. Within these scatterplots, each data point represents the NR2B greyscale values (x-axis) and the NR2A greyscale values (y-axis) from a single cell. Looking at the distribution of the data on the scatterplots, as well as the mean greyscale values of each subunit per condition (shown by the horizontal and vertical dashed lines), it seems that within both hemispheres, dark exposure increases NR2B greyscale values (as seen by the rightward horizontal shift in the teal data points and mean) and decreases NR2A greyscale values (as seen by the downward shift in the teal

data points and mean) compared to normal animals. However, based on the size difference between the means, it appears that in both hemispheres, dark exposure has a more significant impact on NR2B greyscale values compared to NR2A greyscale values.

Within V1, the relationship between NR2B greyscale values and NR2A greyscale values in normal animals (Figure 7C left pane, purple) and dark exposure animals (Figure 7C left pane, teal) was assessed using a Pearson's correlation coefficient. In LV1, a positive correlation between the variables was seen in both the normal animals ($r = 0.859$, $n = 546$, $p < 0.001$, $R^2 = 0.738$) and the dark exposure animals ($r = 0.547$, $n = 514$, $p < 0.001$, $R^2 = 0.299$). Within LV1 of normal animals, 73.8% of the variance in NR2A greyscale values can be explained by the linear relationship between NR2B and NR2A. However, within LV1 of dark exposure animals, only 29.9% of the variance in NR2A greyscale values can be explained by the linear relationship of the two variables. Within RV1, the correlation between NR2B greyscale values and NR2A greyscale values was assessed in normal animals (Figure 7C right pane, purple) and dark exposure animals (Figure 7C right pane, teal). Similar to LV1, within RV1 a positive relationship between the variables was seen in both the normal animals ($r = 0.861$, $n = 640$, $p < 0.001$, $R^2 = 0.741$) and the dark exposure animals ($r = 0.802$, $n = 565$, $p < 0.001$, $R^2 = 0.643$). Within RV1 of normal animals, 74.1% of the variance in NR2A greyscale values can be explained by the linear relationship between NR2B and NR2A. However, within LV1 of dark exposure animals, only 64.3% of the variance in NR2A greyscale values can be explained by the linear relationship of the two variables. Overall, in both conditions and hemispheres, there is a positive relationship between NR2B greyscale values and NR2A greyscale values. Irrespective of how darkness alters greyscale value, the observed

relationship between the NR2B and NR2A greyscale values suggests that within both conditions, cells with higher NR2B greyscale values tend to have higher NR2A greyscale values.

3.3 The Effects of Dark Exposure on the NMDA Receptor Subunit Composition within the LGN

Within layers of the LGN receiving input from the left eye (Figure 8B, left pane), darkness ($M = 0.676$, $SD = 0.071$, $n = 317$) significantly reduced the subunit ratio compared to normal animals ($M = 0.819$, $SD = 0.107$, $n = 310$), $t(536.3) = 19.68$), $p < 0.001$, with dark exposure decreasing the ratio by 17.46%. A similar reduction was seen in LGN layers receiving input from the right eye (Figure 8B, right pane), $t(474.7) = 30.03$, $p < 0.001$, in that dark exposure ($M = 0.669$, $SD = 0.078$, $n = 317$) reduced the ratio compared to the normal animals ($M = 0.832$, $SD = 0.136$, $n = 302$) by 19.59%. On average, within the LGN, dark exposure decreases the NR2A/NR2B ratio by 18.53%. This decease in subunit ratio suggests that within the LGN dark exposure increases the expression of NR2B relative to NR2A in a similar manner to that seen in V1.

The relationship between NR2B greyscale values and NR2A greyscale values within normal animals (Figure 8C, purple) and dark exposure animals (Figure 8C, teal) was plotted for the LGN layers receiving input from the left and the right eye. Within these scatterplots, each data point represents the NR2B greyscale values (x-axis) and the NR2A greyscale values (y-axis) from a single cell. Looking at the distribution of the data on the scatterplots, as well as the mean greyscale values of each subunit per condition, it seems that within the LGN, dark exposure increases NR2B greyscale values (as seen by

the rightward horizontal shift in the teal data points and mean) but does not seem to alter NR2A greyscale values.

The relationship between NR2B greyscale values and NR2A greyscale values in the LGN of normal animals (Figure 8C left panel, purple) and the LGN of dark exposure animals (Figure 8C left panel, teal) was assessed using a Pearson's correlation coefficient. Within LGN receiving input from the left eye, a positive correlation between the variables was seen in both the normal animals ($r = 0.868$, $n = 310$, $p < 0.001$, $R^2 = 0.753$) and the dark exposure animals ($r = 0.899$, $n = 317$, $p < 0.001$, $R^2 = 0.808$). Within layers receiving input from the left eye, in normal animals, 75.3% of the variance in NR2A greyscale values can be explained by the linear relationship between NR2B and NR2A. However, in dark exposure animals, 80.8% of the variance in NR2A greyscale values can be explained by the linear relationship between NR2B and NR2A. Within layers of the LGN receiving input from the right eye, the correlation between NR2B greyscale values and NR2A greyscale values was assessed in normal animals (Figure 8C right pane, purple) and dark exposure animals (Figure 8C right pane, teal). A positive relationship between the variables was seen in both the normal animals ($r = 0.843$, $n = 302$, $p < 0.001$, $R^2 = 0.710$) and the dark exposure animals ($r = 0.917$, $n = 317$, $p < 0.001$, $R^2 = 0.841$). In layers receiving input from the right eye of normal animals, 71% of the variance in NR2A greyscale values can be explained by the linear relationship between NR2B and NR2A. Within dark exposure animals, 84.1% of the variance in NR2A greyscale values can be explained by the linear relationship of the two variables. Similar to the results from V1, there is a positive relationship between NR2B greyscale values and NR2A greyscale values.

Together, the results from the LGN and V1 suggest that a short period of dark exposure increases plasticity capacity within these regions by, at a minimum, altering the NMDA receptor subunit composition. The decrease in subunit ratio seen in both the LGN and V1 indicates that, compared to normal animals, the proportion of NR2B relative to NR2A increases in dark exposure animals. Based on Figure 7C, it seems that the decrease in ratio in the V1 is caused by dark exposure animals have higher NR2B values and lower NR2A values. However, based on Figure 8C, the decrease in subunit ratio within the LGN is caused solely by an increase in NR2B greyscale values. This change in the NR2A/NR2B ratio likely modulates the modification threshold of LTP/LTD, shifting this threshold to the left. The downward shift in the threshold allows for both potentiation and depression to be induced at lower frequencies, thus increasing plasticity (Figure 1 and Figure 2). However, the shift in threshold causes LTP to be favoured over LTD, and "normal" levels of neuronal activity can more easily induce LTP. As darkness preferentially induces LTP, it allows for synaptic strengthening. This increase in synaptic strengthening may be why a short period of darkness is able to promote recovery following MD.

3.4 Change in NMDA Receptor Subunit Composition Caused by Dark Exposure is Universal (Not Layer Specific)

3.4.1 Universal Change in Receptor Composition within V1

To further assess the darkness induced change in subunit ratio, a condition by hemisphere by layer (2x2x4) factorial ANOVA was conducted on the NMDA receptor subunit ratio mean values. The raw data for LV1 and RV1 is shown in Figure 9A and B, respectively.

The factorial ANOVA revealed a main effect of condition (F (1,32) = 50.298, p < 0.001,η_p^2 = 0.611), however, there was no main effect of hemisphere (F (1,32) = 1.032, p = 0.317), or layer (F (3,32) = 2.589, p = 0.070). Furthermore, no interaction was observed between condition and hemisphere (F (1,32) = 0.698, p = 0.410), condition and layer (F (3,32) = 0.248, p = 0.862), hemisphere and layer (F (3,32) = 0.291, p = 0.832), or condition, hemisphere, and layer (F (3,32) = 0.061, p = 0.980). These results indicate that within V1, when not considering layer or hemisphere, dark exposure (M = 0.548, SD = 0.071) significantly reduces the NMDA receptor subunit ratio compared to normal (M = 0.705, SD = 0.078). As no main effect of layer was observed, this indicates that each layer displays a similar receptor composition. Further, since there were no significant interactions observed, this suggests that dark exposure alters the receptor composition across all the layers of V1 in an equal manner. Therefore, 10-days of dark exposure at the peak of the critical period causes a reduction in receptor subunit ratio that is universal and not layer-specific (Figure 9C). The percent decrease between dark exposure and normal animals is outlined in Table 3.

Analyzing pairwise comparisons from the factorial ANOVA revealed that there is no significant difference between subunit ratios within LV1 (M = 0.703) and RV1 (M = 0.707) of normal animals, F (1,32) = 0.016, p = 0.899. A similar result was seen within LV1 (M = 0.527) and RV1 (M = 0.568) of dark exposure animals, F (1,32) = 1.713, p = 0.200. This indicates that within each condition, the subunit ratios did not differ between the two hemispheres.

3.4.2 Universal Change in Receptor Composition within the LGN

To assess how dark exposure alters receptor composition within the LGN, a similar condition by layer by eye-specific input (2x2x2) factorial ANOVA as was performed on V1 data was conducted on the NMDA receptor subunit ratio mean values for the LGN. The raw data for the layers receiving input from the left eye and right eye are shown in Figure 10A and B, respectively. Similar to the results presented above, this analysis revealed a main effect of condition (F (1,16) = 20.658, $p < 0.001$, $\eta_p^2 = 0.564$), and no main effect of layer (F (1,16) = 0.364, $p = 0.555$), or eye segregated input (F (1,16) = 0.037, $p = 0.849$). As well, no interaction was found between condition and layer (F (1,16) = 0.137, $p = 0.716$), condition and eye-specific input (F (1,16) = 0.125, $p = 0.728$), layer and eye-specific input (F (1,16) = 0.051, $p = 0.825$), or condition, eye-specific input, and layer (F (1,16) = 0.001, $p = 0.978$). These results indicate that overall within the LGN, dark exposure ($M = 0.675$, $SD = 0.043$) significantly reduces the NMDA receptor subunit ratio compared to normal animals ($M = 0.834$, $SD = 0.098$). Comparable to the results found in V1, within the LGN, dark exposure alters the receptor subunit composition similarly across layers A and A1 and consequently causes a universal, non-layer specific, reduction in receptor subunit ratio (Figure 10C). The percent decrease between dark exposure and normal animals is outlined in Table 4.

Pairwise comparisons from the factorial ANOVA revealed that there is no significant difference between subunit ratios within LGN layers receiving input from the left eye ($M = 0.825$) and right eye ($M = 0.844$) of normal animals, F (1,16) = 0.149, $p = 0.704$. A similar result was seen within LGN layers receiving input from the left eye ($M = 0.677$) and right ($M = 0.671$) of dark exposure animals, F (1,16) = 0.013, $p = 0.911$. This

indicates that within each condition, the subunit ratios did not differ depending on eye input.

3.5 Darkness Alters Soma Area in Cells Expressing NR2A and NR2B within V1 and LGN

The second part of the study focused on examining how a short period of dark exposure altered neuron soma size within V1 and the LGN. Examination of the Nissl-stained tissue revealed a reduction in cell size in dark exposure animals compared to normal animals. This reduction was seen in both V1 (Figure 11A) and the LGN (Figure 12A). Examination of cell size revealed a significant difference between the groups within both hemispheres of V1 (Figure 11B and C) and layers of the LGN receiving input from the left or right eye (Figure 12B and C). Unlike the analysis above, outliers were found and removed from this data set prior to any analysis (Table 2).

Within LV1 (Figure 11B), there was a significant reduction in soma area between the dark exposure group (M = 84.23 μm^2, SD = 18.42, n = 491) and the normal group (M = 103.2 μm^2, SD = 23.02, n = 537), $t(1009) = 14.63$, $p < 0.001$. Dark exposure reduced soma area by 18.38% relative to normal animals. Similarly, within RV1 (Figure 11C), there was a significant difference in soma area between the dark exposure group (M = 81.58 μm^2, SD = 15.99, n = 548) and the normal group (M = 109.9 μm^2, SD = 23.81, n = 633), $t(1113) = 24.29$, $p < 0.001$. Dark exposure reduced the soma area by 25.77% relative to normal animals. On average, within V1, dark exposure reduced the soma area by 22.08% relative to normal animals.

Similar to above, within the layers of the LGN receiving input from the left eye (Figure 12B), there was a significant difference in soma area between the dark exposure group (M = 151.7 μm^2, SD = 54.23, n = 314) and the normal group (M = 184.1 μm^2, SD = 69.57, n = 306), t(576.2) = 6.457, $p < 0.001$. Dark exposure reduced the soma area by 17.59% relative to normal animals. Within the layers of the LGN receiving input from the right eye (Figure 12C), a similar significant difference was observed in neuronal soma area between the dark exposure group (M = 144.2 μm^2, SD = 47.73, n = 315) and the normal group (M = 185.8 μm^2, SD = 73.65 , n = 301), t(510.5) = 8.278, $p < 0.001$, with dark exposure reducing soma area by 22.39% relative to the normal animals. On average, within the LGN, dark exposure reduced the soma area by 20% relative to normal animals.

3.6 Layer Specific Analysis of Soma Area within V1

Lastly, we analyzed whether darkness altered soma area in cells expressing NMDA receptors in a layer-specific manner. To assess this in V1, a condition by hemisphere by layer (2x2x4) factorial ANOVA was conducted on V1 soma area. The raw data for LV1 and RV1 are shown in Figure 13A and B, respectively. Although there was no main effect of hemisphere, there was a main effect of condition, F (1,32) = 118.052, $p < 0.001$, η_p^2= 0.787, and layer, F (3,32) = 9.143, $p < 0.001$, η_p^2 = 0.462. A Bonferroni post hoc analysis revealed that the neurons in layer 4 (M = 84.74 μm^2, SD = 17.22) of V1 were smaller compared to those in layer 2/3 (M = 99.59 μm^2, SD = 15.433, $p < 0.001$), layer 5 (M = 97.28 μm^2, SD = 12.97, p = 0.002), and layer 6 (M = 94.51 μm^2, SD = 15.34, p = 0.004) (Figure 13C). These results indicate that within V1, when not considering layer or hemisphere, dark exposure (M = 82.56 μm^2, SD = 7.78) significantly reduces cell size

compared to normal (M = 106.45 μm^2, SD = 11.06). Furthermore, when condition is not considered, cells within layer 4 of V1 are smaller than cells in the other layers. Since there was no interaction between layer and condition, dark exposure causes a universal, non-layer specific, reduction in cell size. The percent decrease between dark exposure and normal animals for each layer is outlined in Table 5.

Within V1, the factorial ANOVA assessing layer-specific changes in cell size revealed an interaction between condition and hemisphere, F (1,32) = 5.007, p = 0.032, η_p^2 = 0.135. Analyzing pairwise comparisons showed that in the normal condition, cells within RV1 (M = 110.50 μm^2, SD = 9.45) were significantly larger compared to cells within LV1 (M = 102.41 μm^2, SD = 11.43), F (1,32) = 6.766, p = 0.014, η_p^2 = 0.175. A similar result was not seen between the hemispheres in dark exposure animals, F (1,32) = 0.317, p = 0.577 (Figure 14). This simple effect is likely the cause of the significant interaction between condition and hemisphere. This difference in cell size between layers within the normal animals is likely due to human error. Possibly occurring because of imperfect layer identification.

3.7 Layer Specific Analysis of Soma Area within the LGN

To further assess how dark exposure impacts cell size within the LGN, a condition by eye input by layer (2x2x4) factorial ANOVA was conducted on LGN soma area. The raw data for the layers of the LGN receiving input from the left eye and right eye are shown in Figure 15A and B, respectively. Unlike the ANOVA run on V1, there was only a main effect of condition on cell size within the LGN (F (1,16) = 19.264, p < 0.001, η_p^2 = 0.546), with no main effects of layer (F (1,16) = 2.899, p = 0.108), or which eye the layer

is receiving input from (F (1,16) = 0.130, p = 0.723). As well, no significant interaction was observed. These results indicate that within the LGN, when not considering layer or eye input, dark exposure (M = 148.01 μm^2, SD = 23.76) significantly reduces cell size compared to normal (M = 187.76 μm^2, SD = 19.15) (Figure 15C). As there was no interaction between layer and condition, within the LGN, dark exposure reduces cell size in a universal non-layer specific manner. The percent decrease between dark exposure and normal animals for each layer is outlined in Table 6.

The pairwise comparisons from the factorial ANOVA revealed that, within normal animals, there is no significant difference between cell size within LGN layers receiving input from the left eye (M = 186.67 μm^2) and right eye (M = 188.86 μm^2), F (1,16) = 0.029, p = 0.866. A similar result was seen within LGN layers receiving input from the left eye (M = 152.37 μm^2) and right (M = 143.65 μm^2) of dark exposure animals, F (1,16) = 0.463, p = 0.506. This result indicates that within each condition, the cell size did not differ between the layers receiving input from the left eye and right eye.

CHAPTER 4 – DISCUSSION

Evidence suggests that changes in the NMDA receptor subunit composition alters the nature of plasticity within the visual cortex. These changes in receptor composition are the presumed mechanism of metaplasticity, the ability for prior visual experience to alter the probability and direction of plasticity in response to activity, as previous research has shown that a short period of dark exposure imposed around the critical period can alter the NMDA receptor composition in rodents (Quinlan et al., 1999a; Philpot et al., 2001; Chen and Bear, 2007). In order to gain a better understanding of the role of the NMDA receptor in experience-dependent plasticity, the current study examined how a 10-day period of dark exposure altered the NMDA receptor subunit composition within a higher-order mammal, the cat. Additionally, layer-specific changes were examined in the LGN and V1 to provide more information about the NMDA dependent mechanisms of darkness mediated plasticity. As previous literature has shown that soma area within the LGN is altered by visual experience, we examined layer-specific changes in soma area within the LGN and V1 (Wiesel and Hubel, 1963a; Duffy et al., 2016). The results revealed that in cats, a brief period of darkness around the peak of the critical period is sufficient to significantly alter the NMDA receptor subunit composition, decreasing the NR2A/NR2B ratio, and therefore shifting the receptor towards its immature isoform. The decrease in the NR2A/NR2B ratio was observed in both regions examined and was not layer-specific, with the reduction occurring throughout all layers of the LGN and V1. Similarly, a universal reduction in neuron soma area was observed in both brain regions.

The current study supports previous research conducted on rodents that showed that a brief period of dark exposure alters the NMDA receptor subunit composition within

V1 (Quinlan et al., 1999a; Philpot et al., 2001; Chen and Bear, 2007). However, this study provides further information about how dark exposure alters the NMDA receptor subunit composition within the visual system, demonstrating that the change in receptor composition is not isolated to V1, but also occurs in the LGN. Further, dark exposure alters the composition of the NMDA receptor universally and not in a layer-specific manner. These novel findings suggest that dark exposure alters all cells containing NMDA receptors within the visual system. Furthermore, as the change in receptor composition is universal, a specific component or layer within the visual system does not drive the NMDA receptor-mediated change in LTP/LTD threshold. It seems that a universal change in the NMDA receptor subunit composition is a crucial molecular mechanism in experience-dependent plasticity. The results and implications of the study are discussed in further detail below.

4.1 The Effects of Darkness on the NMDA Receptor Composition

Similar to the results shown in the current study, previous research has shown that a short period of dark exposure decreases the NR2A/NR2B ratio relative to age-matched light-reared animals (Quinlan et al., 1999; Philpot et al., 2001; Chen and Bear, 2007). In rats, Chen and Bear (2007) showed that dark exposure decreased the ratio by approximately 20% compared to light reared animals. In accordance with Chen and Bear (2007), we observed a similar reduction in cats due to dark exposure, with darkness decreasing the ratio by 22.39% within V1 of cats. The LGN showed a comparable reduction in the ratio, with darkness decreasing it by 18.53%. The results from the current study, along with those from Chen and Bear (2007), suggest that a short period of darkness is sufficient in

altering the NMDA receptor subunit composition, and multiple regions within the visual system experience the effects of darkness.

The change in receptor composition within both the LGN and V1 further supports previous literature suggesting that the composition of the NMDA receptor is the molecular basis of the BCM sliding threshold model (Quinlan et al., 1999a, 1999b; Philpot et al., 2001, 2003, 2007). As a period of decreased activity is thought to decrease the LTP/LTD threshold, one would assume that the model is not isolated to a particular brain region, and if any region experiences a period of low activity, then LTP should become favoured over LTD (Bienenstock et al., 1982; Kirkwood et al., 1996). Since the molecular mechanism of the sliding threshold is presumed to be modifications in the NMDA receptor, and the model should not be selective to structure, this suggests that darkness should alter the subunit composition across all of the components of the visual system. This universal change in the visual pathway is precisely what we observed in the current research. These results further support the idea that the NMDA receptor composition is the molecular basis responsible for the shift in LTP/LTD threshold.

4.1.1 The Effects of Darkness Across the Layers of the LGN and V1

The universal change in receptor composition seen throughout the layers of the LGN and V1 suggest that NR2A/NR2B expression regulates the threshold for synaptic plasticity on a global scale, i.e. one brain region, or layer, does not experience a more substantial shift in the threshold for synaptic plasticity than any other. While previous research has shown robust changes in the NMDA receptor subunit composition in layers three and four of V1, no previous research has directly compared the changes across the layers (Carmignoto

and Vicini, 1992; Quinlan et al., 1999b). As we observed a reduction across all the layers of V1, our findings support those of Fagiolini et al. (1994), who demonstrated that dark rearing alters the physiological response in cells across all the layers of V1 in rats. Fagiolini and colleagues suggested that the altered physiological response of the dark reared rats may be due to an increase in the NMDA receptor current duration. We observed a non-layer specific reduction in the NR2A/NR2B ratio within V1, which would suggest the receptor current duration is increased across all the layers of V1, thus supporting the theory proposed by Fagiolini and colleagues.

While we observed no significant difference in the ratio between the layers of V1, the average ratio did follow a trend in both the normal and dark exposure animals. Although the trend is not significant, it is still of interest. The NR2A/NR2B ratio was highest in layer V, while layer II/III showed the smallest ratios out of all the layers. Layer IV and VI, both of which receive input from the LGN, have intermediary ratios; lower ratios compared to layer V, but higher ratios compared to layer II/III (Hubel and Wiesel, 1972; Blasdel and Lund, 1983). While the exact reason for this pattern is unknown, the pattern of NMDA receptor composition may correlate with the likelihood of inducing potentiation in that layer, which may contribute to the function of each layer. Another potential reason for this pattern is that each layer undergoes an age-related increase in the subunit ratio, with layer V increasing the fastest, and layer II/III increasing the slowest. This layer-specific age-related increase in ratio consequently increases the LTP/LTD threshold, thus making it more challenging to induce potentiation but easier to induce depression. As previous research has shown that LTP persists later into life in layer II/III,

compared to layer IV, this supports the idea that each layer undergoes an age-related increase in NR2A/NR2B ratio at different times (Jiang et al., 2007).

4.1.2 Potential Source for the Reduction in Subunit Ratio Caused by Darkness

In the current study, we observed that dark exposure decreased the subunit ratio relative to normal. While we did not explicitly examine how dark exposure alters the levels of the subunit individually, as we only looked at the difference in ratio between the groups, we can make assumptions of how darkness alters the levels based on the greyscale measurements. As seen in the scatterplots in Figure 6 and Figure 7, it appears that, compared to the NR2A subunit, the NR2B subunit is affected more by a short period of dark exposure. This change in NR2B subunit greyscale value appears to be especially true within the LGN, as the mean greyscale value of the NR2A subunit is almost identical between the two conditions. Based on these results, it seems that the LGN and V1 respond differently to dark exposure. However, we cannot be certain because we did not look at the isolated subunit level, and therefore we were unable to run statistical analysis to assess if there is a significant difference in the subunit level between the groups or between the LGN and V1. While we cannot be sure if a change in one or both subunits drives the reduction in ratio caused by darkness, we can infer from the scatterplots that within V1, a change in both subunits is likely driving the reduction in ratio, whereas within the LGN, the reduction in the ratio is likely driven only by a change in NR2B levels.

From previous literature, there is conflicting evidence about whether activity regulates the expression of the subunits individually or jointly. Chen and Bear (2006)

showed that, in mice, dark rearing alters the expression of both subunits, but not at the same time. Mice dark-reared until four weeks of age showed a significant increase in NR2B levels, while there was no change in NR2A levels. However, after seven weeks of dark rearing, a significant reduction in NR2A levels was observed. Therefore, it appears that a reduction in NR2A levels follows the original increase in NR2B levels. The ability for darkness to alter the subunit levels across different time courses may reflect the change we observed in the NR2A and NR2B greyscale values. It may be possible that in cats, a 10-day period of darkness at the peak of the critical period initially triggers an increase in NR2B levels, consequently decreasing the NR2A/NR2B ratio, but is not long enough to observe the subsequent decrease in NR2A levels. It is therefore possible that exposing an animal to longer durations of darkness could cause a subsequent decrease in NR2A levels following the early increase in NR2B levels, similar to what has been observed in rodents.

The idea that a decrease in NR2A levels occurs second to the increase in NR2B levels may explain why we observed a more substantial difference in NR2A greyscale means in V1 compared to the LGN. As previous research has shown that modifications within the LGN appear to be a reflection of modifications within V1, it may be possible that 10-days of dark exposure is sufficient to cause the initial increase in NR2B and the subsequent reduction in NR2A within V1. However, it might not be long enough for the change in NR2A levels to be revealed in the LGN (Trachtenberg et al., 2000). Therefore, it may be necessary to expose animals to a longer period of darkness in order for the reduction in NR2A levels to be observed in the LGN. Based on this theory, the results

from the current study help support the notion that changes in V1 drive experience-dependent modifications within the LGN (Trachtenberg et al., 2000).

Further supporting the theory that NR2B levels are driving the initial decrease in NR2A/NR2B ratio, Chen and Bear (2006) showed that visually depriving rats for three days increases NR2B subunit levels without altering levels of the NR2A subunit. While the authors suggest that the reduction in NR2A/NR2B ratio caused by dark exposure is solely due to the increase in NR2B levels, it could be that three days of dark exposure is not long enough to alter NR2A levels. Based on the results from the current study, and the results from Chen and Bear, it seems that dark exposure initially increases NR2B levels, which is then followed by a subsequent decrease in NR2A levels.

In opposition to the theory presented above, previous research has shown that, compared to normal animals, dark rearing rats from one to six weeks of age results in a significant decrease in synaptoneurosomal NR2A levels at all ages, while levels of NR2B are unaffected (Quinlan et al., 1999a). Interestingly, while the increase was smaller compared to normal animals, NR2A protein levels still showed a developmental increase in the dark reared animals. In dark reared animals, the NR2A levels increased by approximately two-fold between one week and six weeks of age. In normal animals, NR2A levels increased by approximately three-fold during the same period. These results suggest that while there is still a developmental increase in NR2A, dark rearing causes a slower and less substantial increase (Quinlan et al., 1999a). Further, exposing dark reared rats to light rapidly increases NR2A levels without altering NR2B levels (Quinlan et al., 1999a, 1999b). Moreover, Quinlan et al. (1999a) showed that placing the dark reared rats

that have been previously exposed to light back into the dark for 72 hours decreases NR2A levels to those seen prior to light exposure.

While it is unclear if darkness alters the NR2A/NR2B ratio by altering both subunits, or only NR2A, it appears that darkness slows development, as seen by the delayed NR2A developmental increase, or reverts the visual system to a more immature state, as seen by the increase in NR2B levels. Based on the previous literature, it may be possible that the short period of darkness used in the current study is causing a decrease in subunit ratio by increasing NR2B levels while slowing, preventing, or halting the developmental increase in NR2A protein levels. This notion may explain why there is a bigger difference in NR2B greyscale values between the conditions compared to NR2A levels. Darkness may slow the developmental increase in NR2A values, but it may take longer than ten days for this delay to be reflected in NR2B levels.

Additionally, the dark exposure-induced changes in the NR2A/NR2B ratio causes the receptor to resemble a more immature isoform, and as a result, darkness may be reverting the brain to a more immature form. Although we did not directly analyze how darkness alters the protein levels of the two subunits, the concept of slowing development or reverting the brain to a more immature form is paralleled by the difference in cell size between the two conditions.

4.2 The Effects of a Short Period of Darkness on Cell Size

We analyzed how darkness alters the soma area of cells within the LGN and V1. Interestingly, we observed that in both the LGN and V1, compared to normal animals, dark exposed animals had smaller cells. Similar to the change in subunit composition, the

change in cell size is universal in both regions and not isolated to an individual layer. The reduction in LGN cell size caused by dark exposure supports the results from previous literature showing that long durations of dark rearing can decrease the cross-sectional area of cells within the LGN (Kalil, 1978). Interestingly, cell size within the LGN showed a layer-specific pattern in both conditions, with layer A cells being slightly smaller compared to layer A1. Although the difference in cell size between the layers was not significant, a similar pattern has been shown (Guillery, 1973; Lingley et al., 2018). Within V1, although darkness caused an equal reduction in cell size relative to normal across all the layers, we observed a main effect of layer, with layer IV having smaller cells compared to all the layers irrespective of condition. The smaller cell size seen in layer IV is consistent with the fact that this layer contains spiny stellate cells, which tend to be smaller than the cells in other layers (Gilbert, 1983).

While it is unclear how darkness increases plasticity, the decrease in cell size may provide some information. As mentioned above, a short period of dark exposure may revert the visual system to a more immature state. This reversion may allow the visual system to rewire new connections when the animal is re-exposed to light. Previous cell size data from the Duffy lab can support this idea that darkness is reverting the brain to a more immature state. In theory, if darkness reverts the brain to a more immature state, the size of the cells within the visual system should be smaller compared to when the animals went into the dark (P30). While we did not analyze the cell size at P30 prior to the animals going into the dark, previous research in the Duffy lab has examined cell size within the LGN at this age and younger ages (P25). The results from the current research showed that at P40, following a 10-day period of darkness, left eye LGN layers had an

average cell size of 151.7 μm^2 (± 54.23), and right eye LGN layers had an average cell size of 144.2 μm^2 (± 47.73). Duffy et al. (2014) found that at P25 (C184) cells within the LGN were 170 μm^2 (± 76) in the left eye layers and 171 μm^2 (± 76) in the right eye layers. Further, within the LGN of normal P30 animals, the LGN has an average cell size of approximately 200 μm^2 (Lingley et al., 2018; Figure 3D insert). As a 10-day period of dark exposure starting at P30 decreases cell size to the point that they are smaller than cells seen in P30 and P25 animals, it seems that in the context of cell size, darkness is reverting the brain to a more immature state.

The reduction in cell size caused by darkness may be a secondary effect of darkness, which may be facilitated by changes in proteins responsible for cell structure. Previous research has shown that within V1, 10-days of dark exposure reduces the density of NFs, which are an experience-dependent molecular brake important in maintaining the neuronal cytoskeleton (Duffy and Mitchell, 2013). Since NFs are vital in the cytoskeleton, the loss of NF protein caused by darkness may result in the cell undergoing structural changes. Taken together, these results suggest that in the case of cell size, darkness reverts the brain to a younger state, therefore reducing cell size. Additionally, the reduction in cell size may be caused by other darkness induced changes, i.e. a secondary effect.

4.3 Comparing Hebbian and Homeostatic Plasticity in Dark Exposure

Understanding which form of plasticity is responsible for the effects of darkness is essential in gaining a better understanding of the molecular mechanisms of darkness. Hebbian and homeostatic plasticity are the two major forms of plasticity, and, as

described in the introduction, the basis of Hebbian plasticity is that correlated activity at the synapse determines synaptic strength. Hebbian plasticity holds that high levels of correlated synaptic activity increase synaptic strength, whereas low levels of correlated activity cause a reduction in synaptic strength (Hebb, 1949). Therefore, Hebbian plasticity is a positive feedback process, with stronger synapses becoming stronger, and weaker synapses becoming weaker. Although Hebbian plasticity is unable to explain how cells avoid synaptic instability, the addition of a sliding threshold in the BCM model was able to introduce firing rate homeostasis to Hebbian plasticity. The other major form of plasticity that allows firing rate homeostasis is homeostatic plasticity. Unlike the BCM model, which allows for firing rate homeostasis by altering the LTP/LTD threshold based on previous activity levels, homeostatic plasticity maintains a constant level of activity following perturbation through compensatory responses that are mediated by synaptic changes. One mechanism through which this stability is achieved is synaptic scaling, in which NMDA and AMPA receptors are trafficked to the surface of the synapse (Turrigiano et al., 1998). In order to maintain a constant state of activity in response to a disturbance, neurons will increase or decrease the accumulation of these receptors thereby compensating for the decrease or increase in firing rate, respectively, caused by the disturbance (Turrigiano, 2008). Although both the BCM model and homeostatic plasticity allow for homeostasis of the neuronal firing rate, the mechanisms through which they do so are different. With homeostatic plasticity, activity levels directly alter synaptic strength by increasing or decreasing the number of receptors. Conversely, the BCM model states that activity alters the ability for potentiation to be induced in the future, therefore altering plasticity (Keck et al., 2017).

Our results support the idea that the sliding threshold model of synaptic plasticity is responsible for the darkness mediated increase in plasticity. As darkness reduces overall cellular activity, this would cause a decrease in activity between the pre- and post-synaptic neurons. Therefore, if Hebbian mechanisms are at play, on average, there should be a weakening of synaptic strength, which consequently means cells receive fewer resources, which would be reflected by a reduction in cell size. However, if homeostatic mechanisms are responsible for the effects of darkness, there will be a compensatory increase in glutamate receptors to maintain a constant level of activity, which would prevent the reduction in resources, and no reduction in cell size would occur. As mentioned, the reduction in cell size caused by darkness may be due to darkness induced changes in other proteins. Therefore, the decrease in cell size may be the perturbation that initiates the compensatory response associated with homeostatic plasticity. However, this is unlikely, as previous research has shown that dark rearing does not alter the absolute number of NMDA receptors, thus supporting the theory that the BCM model, as opposed to homeostatic plasticity, is responsible for the effects of darkness (Quinlan et al., 1999a).

4.4 Using the BCM Model to Explain the Effects of Monocular Deprivation and Darkness Mediated Recovery from Monocular Deprivation

Previous research has shown that a short period of darkness can promote recovery following a period of monocular deprivation, however, the exact mechanisms through which darkness acts are unknown (Duffy and Mitchell, 2013). Based on the results from the current study, it appears that the BCM model may provide some insight into the molecular mechanisms responsible for darkness mediated recovery from MD. However,

before explaining how darkness promotes recovery from MD, it is helpful to discuss how the BCM model accounts for the effects of MD.

4.4.1 The BCM Model and Monocular Deprivation

The BCM model proposes that the effects of MD are produced by spontaneous retinal activity from the deprived eye, and this spontaneous activity is necessary to produce the MD induced changes. This theory is confirmed by research showing that brief monocular inactivation with TTX, which eliminates all retinal activity, fails to produce the same depression of responses in the deprived eye that are seen with lid suture (Rittenhouse et al., 1999; Frenkel and Bear, 2004). Further, MD has no effect on average firing rates within the LGN, but it does increase the amount of de-correlated activity (Linden et al., 2009). Therefore, it seems the noise produced by the deprived-eye retina during MD will not reduce activity but rather produce poorly correlated activity between the connections of the LGN and V1. This poorly correlated activity will produce LTD at these synapses, and therefore weaken the connections of the deprived eye (Cooper and Bear, 2012). The notion that LTD is responsible for the effects of MD is supported by previous research, which shows that effects of MD are dependent on NMDA receptor activation, as blocking its activation prevents the MD induced shift in OD and the reduction of cell size within the LGN (Kleinschmidt et al., 1987; Bear and Colman, 1990; Bear et al., 1990). Further, research has shown that MD induces LTD within V1, and the induction of LTD is dependent on the NMDA receptor (Heynen et al., 2003; Yoon et al., 2009). Finally, the induction of LTD is necessary to produce MD induced changes (Yoon et al., 2009; Yang et al., 2011).

The BCM model assumes that after a short period of MD, there will be a reduction in the LTP/LTD threshold, allowing for the non-deprived eye to induce LTP more easily, which then strengthens its connections. Previous research conducted on mice supports this theory. When recording from one hemisphere of V1, MD of the contralateral eye produces a depression in response after only one day of deprivation, therefore, LTD is taking place almost immediately after eye closure. After five to seven days of MD, the responses from the contralateral eye are still depressed, but the responses from the ipsilateral eye are potentiated (Frenkel and Bear, 2004). However, the potentiation in the ipsilateral eye is not a passive consequence caused by the reduction in activity produced by MD. Since potentiation of the ipsilateral eye does not occur after three days of MD followed by binocular deprivation, or only binocular deprivation, it seems that delayed potentiation of the ipsilateral eye occurs as a result of the reduction in activity in the contralateral eye relative to the ipsilateral eye, and is dependent on the visual experience of the ipsilateral eye (Blais et al., 2008). Further, potentiation of the ipsilateral eye is dependent on the activation of the NMDA receptor, and since monocular deprivation decreases the NR2A/NR2B ratio, potentiation is easier to induce (Sawtell et al., 2003; Chen and Bear, 2007). However, the results from these studies conducted on rodents may not apply to higher-order primates, as V1 processes more contralateral information within rodents (Dräger and Olsen, 1980; Neveu and Jeffery, 2007). Thus, MD may produce more profound results in rodents compared to higher-order primates when measuring changes in V1, as higher-order primates have equal contralateral and ipsilateral input into V1. Future research should examine how MD alters the NR2A/NR2B ratio in the LGN and V1 of higher-order animals. Although these results

were from rodents, they suggest that the shift in LTP/LTD threshold caused by a change in the NMDA receptor subunit composition is responsible for MD induced changes.

4.4.2 The BCM Model and Darkness Mediated Recovery from Monocular Deprivation

With an understanding of how the BCM model applies to the effects of MD, it is now possible to discuss how the BCM model accounts for darkness mediated recovery from MD. As the current study has shown that darkness decreases the NMDA receptor subunit ratio, darkness likely promotes recovery from MD by decreasing the LTP/LTD threshold, thus making LTP easier to induce compared to LTD. When potentiation is easier to induce, this enables strengthening of the weak connections between the deprived eye and the cortex. Further, as darkness is thought to increase plasticity, the connections between the cortex and the non-deprived eye can be easily modified, allowing the connections of the deprived eye to be rewired.

Although the exact mechanisms through which darkness increases plasticity are not known, it is likely that multiple processes may mediate this increase. In the context of the NMDA receptor, the shift in subunit composition towards the neonatal isoforms, as seen in the current study, likely contributes in some manner to the increase in plasticity (Quinlan et al., 1999a). While the BCM model never explicitly states how darkness increases plasticity, the shift in subunit composition towards the immature isoform may contribute to an increase in plasticity by lowering the LTP/LTD threshold, which in turn

enables lower stimulation frequencies to induce both potentiation and depression (Figure 1).

Interestingly, previous research has shown that darkness mediated recovery from MD is dependent on the fellow eye, as occlusion of the fellow eye, even for as little as 24 hours, prevents visual recovery of the deprived eye (Mitchell et al., 2019). This dependence on the fellow eye for the recovery of the deprived eye can potentially be explained in the context of the BCM model and the NMDA receptor. The BCM model states that the deprived eye will recover following monocular deprivation if neural activity induced by stimulation of the deprived eye is correlated with activity of the non-deprived eye (Kind, 1999). Thus, occluding the fellow eye following darkness prevents correlated activity between the two eyes, and therefore, the deprived eye does not recover. However, this does not explain why recovery does not occur after the occlusion is reversed (Mitchell et al., 2019). A change in the NMDA receptor subunit composition that occurs with light exposure may be another potential explanation for why the fellow eye drives recovery in the deprived eye following dark exposure. Typically, a short period of light exposure following a period of dark exposure causes a rapid increase in NR2A levels to a level above those observed in normal animals (Quinlan et al., 1999b). This increase in NR2A levels consequently increases the NR2A/NR2B ratio, therefore shortening the NMDA receptor current. The increase in ratio shifts the LTP/LTD threshold upwards, increasing the likelihood of LTD while making LTP less likely. As the BCM model focuses on homosynaptic modifications, which is input-specific synaptic plasticity, this increase in NR2A may be specific to the cells receiving input from the fellow eye. The rapid increase in ratio raises the threshold, thus favouring LTD over LTP,

and therefore, based on input-specific synaptic plasticity, the connections between the fellow eye and V1 will undergo depression and weakening. This weakening of fellow eye connections may be to accommodate the strengthening of connections between the deprived eye and V1. If the fellow eye is occluded, there may be no rapid increase in NR2A, therefore no input-specific LTD, and hence no weakening of the connections between the fellow eye and V1. Without the input-specific LTD, the deprived eye would be unable to compete to form new connections with neurons with V1, and consequently, would not show visual recovery. The idea that changes in the NMDA receptor following removal from darkness occur in an input specific manner can be tested by examining both NR2A levels and the NR2A/NR2B ratio in the LGN following MD and removal from the dark. The LGN is the ideal structure to examine in this scenario as changes in the LGN are thought to reflect changes in V1. The current research has shown that experience can alter the NMDA receptor subunit composition within the LGN, and most importantly, the eye-specific segregation of this nucleus permits examination input-specific changes in the NMDA receptor subunit composition. Assessing the NMDA receptor subunit composition within the LGN following MD and dark exposure will provide insight into the molecular mechanisms of darkness mediated recovery.

4.5 The BCM Model and Excitatory/Inhibitory Balance

As described in the introduction of this work, an emerging belief is that the balance between excitatory and inhibitory tone is an important factor in regulating the development of the visual system. Additionally, maintaining equilibrium in excitatory and inhibitory tone is necessary to activate different molecular cascades that are essential

to the timing of the critical period (Hensch, 2004; Takesian and Hensch, 2013). Since this balance appears to be crucial to visual development, it is important to understand how the BCM model and the balance in excitatory and inhibitory tone interact, especially in the context of darkness mediated recovery from MD. While there is very little research on the role of the BCM model on inhibitory synapses, the fact that inhibitory synapses can undergo both LTP and LTD, makes it likely that the facets of the BCM model may apply to these synapses (Castillo et al., 2011). Similar to excitatory synapses, the threshold between LTP/LTD likely changes in inhibitory synapses due to previous activity. However, the shift is likely opposite of that seen at excitatory synapses. A decrease in activity causes a downward shift in the LTP/LTD threshold at excitatory synapses, favouring LTP over LTD. Conversely, a decrease in activity likely causes an upward shift in LTP/LTD threshold at inhibitory synapses, therefore LTD will be favoured over LTP. When activity increases, the LTP/LTD threshold will shift downward in inhibitory synapses, favouring LTP over LTD (Figure 16). Thus, in dark exposure, LTP will be favoured at excitatory synapses, but LTD will be favoured at inhibitory synapses.

In support of this theory, Xue et al. (2014) observed that, in normally reared mice, the levels of synaptic excitation and inhibition are similar. However, after deprivation, there is a reduction in inhibitory cell activity, as well as a loss of inhibitory synapses (Chen et al., 2011; van Versendaal et al., 2012; Barnes et al., 2015). The decrease in strength and number of inhibitory synapses parallels the effects LTD has on excitatory synapses. Therefore, it appears that a period of decreased activity shifts the LTP/LTD threshold to favour LTD in inhibitory synapses, altering the excitatory/inhibitory balance. As inhibitory cells synapse onto excitatory cells, the proposed theory suggests that

changing levels of activity shift the LTP/LTD threshold in the opposite direction for excitatory and inhibitory synapses on the same cell. Experimental evidence supports the theory that the threshold can shift in opposite directions at different types of synapses on the same cell, as LTD can be induced at inhibitory synapses of a cell, while at the same time LTP can be promoted at the excitatory synapses of the same cell (Chevaleyre and Castillo, 2004; Wang and Maffei, 2014). Based on the evidence presented above, it appears that dark exposure may alter the excitatory/inhibitory balance by altering the LTP/LTD threshold of both excitatory and inhibitory synapses.

4.6 The BCM Model and TTX Mediated Recovery from MD

While darkness can promote recovery from MD in a laboratory setting, it has proven problematic in a clinical setting as a potential therapy for amblyopia due to a lack of ease of implementation. Another potential intervention that may be more practical in a clinical setting is retinal inactivation with TTX. Similar to dark exposure, binocular retinal inactivation with TTX approximately eight weeks following a seven day period of MD can promote visual recovery in kittens (Fong et al., 2016). Additionally, TTX-based retinal inactivation is thought to be more potent than darkness. Unlike a 10-day period of dark exposure, a 10-day period of fellow eye retinal inactivation with TTX immediately following a six-week MD can promote full recovery in neuron soma size and NF labelling density (Duffy et al., 2015, 2018).

Binocular retinal inactivation with TTX and dark exposure likely work in a similar manner, both decreasing the NR2A/NR2B ratio, and therefore allowing LTP to be induced more easily. The ability to induce LTP more easily likely allows for the

strengthening of weak connections between the deprived eye and the cortex. As inactivation is thought to be more potent, it may cause a greater reduction in the NR2A/NR2B ratio. However, compared to both binocular inactivation and dark exposure, fellow eye inactivation appears to be better at promoting recovery following MD, as seen by the recovery in neuron soma size and NF labelling density following a long MD (Duffy et al., 2018). The capability of monocular inactivation to promote better recovery can be explained by the BCM model and input-specific synaptic plasticity. Previous research has shown that while brief monocular inactivation does not produce depression in the inactive eye, it promotes potentiation in the active eye, and increases correlated firing rates within the LGN of awake and active animals (Frenkel and Bear, 2004; Linden et al., 2009). Interestingly, in anesthetized mice, retinal inactivation decreases activity within the LGN (Linden et al., 2009). Therefore, it appears that TTX can only promote recovery in awake animals. In the context of fellow eye inactivation, the active eye would be the initially deprived eye. Therefore, monocular TTX inactivation likely promotes recovery following MD by increasing potentiation in the deprived eye, allowing for the connections between this eye and the cortex to strengthen. The increase in correlated activity at the LGN protects the connections of the originally deprived eye from weakening, as an increase in correlated activity is thought to protect the synapses against depression (Blais et al., 2009).

Together, it seems that fellow eye inactivation is more effective in promoting recovery of the deprived eye compared to both dark exposure and binocular inactivation as it promotes eye-specific potentiation. This eye-specific potentiation allows for the connections between the cortex and the initially deprived eye to undergo LTP and

strengthen. Since the connections from the initially deprived eye are favourably undergoing LTP, and the synapses of the inactive eye do not undergo LTP as effortlessly, there is less competition for the deprived eye. With the reduction in competition, the connections from the deprived eye can reclaim cortical territory. Based on the results from this study and the research described above, it seems that the changes in the NMDA receptor subunit composition caused by retinal inactivation should be isolated to the regions in the visual system receiving input from the deprived eye. Specifically, the ratio should be decreased in these regions, shifting the LTP/LTD threshold to the right, therefore, making LTP easier to induce there. As well, since inactivation with TTX is thought to be more potent than darkness, both monocular and binocular retinal inactivation should cause a greater reduction in NR2A/NR2B ratio. In order to gain a better understanding of the molecular mechanism of TTX, future research should assess the difference in ratio between monocular retinal inactivation, binocular retinal inactivation, and dark exposure.

4.7 Retinal Inactivation as a Pharmaceutical Intervention for Amblyopia

The use of retinal inactivation is a promising pharmaceutical intervention for amblyopia, especially considering the current gold standard treatment (eye patching) has many difficulties associated with it (Loudon et al., 2002, 2003; Stewart et al., 2004). Unlike patching, compliance will not be an issue with retinal inactivation, as the intervention can not be removed. Also, in animals, inactivation appears to be effective in promoting recovery at older ages than is possible with reverse occlusion, an intervention used in animal research to mimic patching (Duffy et al., 2018). Although retinal inactivation

may be a more practical intervention, inactivation has other potential issues associated with its clinical use. One of the biggest concerns is the toxicity of TTX, as it is a potent neurotoxin. However, it would seem that much of the uncertainty and fear associated with the use of tetrodotoxin (TTX) in clinical applications arises not from the toxicity of TTX, but rather from the word 'toxin' contained its name and the negative connotations surrounding this. Certainly, TTX is a potent neurotoxin (mice LD50 ~8-300 μg/kg). However, it is 6-8 orders of magnitude less potent than botulinum toxin (mice LD50 ~0.00003 μg/kg), which is one of the most toxic substance on earth but is regularly used for cosmetic purposes, as it is the main ingredient of Botox (Schantz and Johnson, 1992; Chen et al., 2000; Münchau and Bhatia, 2000; Dhaked et al., 2010; Moczydlowski, 2013; Lago et al., 2015). While there may still be concerns associated with injecting a toxic substance into the eye, recent work in the Duffy lab has shown that intraocular injections of TTX does not cause damage to the optic nerve or the retinal ganglion cell layer of the injected eye. Additionally, the visual function of the inactive eye is not altered by the inactivation, as once reactive, the visual responses of the eye that was injected with TTX were similar to those seen prior to inactivation (DiCostanzo et al., 2020). As per the adage, "the dose makes the poison," although TTX may be toxic in large quantities when administered in small controlled doses, it appears that it does not cause damage to the visual system and allows for better recovery from MD. That being said, a better understanding of the dose and duration that will produce the most profound recovery in humans is needed in order to translate this treatment from cats to humans. As well, further research is required to determine the optimal age range to promote the best

recovery in humans. Although more work is needed on the use of TTX for treating human amblyopes, it has much potential as the next gold standard treatment.

Both darkness- and TTX-based interventions are promising candidates for novel treatments of amblyopia. Although there are still issues associated with their clinical use, both interventions are more potent than the current gold standard treatment, patching. Research that furthers our understanding of the molecular mechanisms of these interventions, such as an understanding of the role of the BCM model in monocular retinal inactivation, will be fundamental in optimizing these treatments for human use.

REFERENCES

Abraham WC, Bear MF (1996) Metaplasticity: the plasticity of synaptic plasticity. Trends Neurosci 19:126–130.

Akbik FV, Bhagat SM, Patel PR, Cafferty WBJ, Strittmatter SM (2013) Anatomical plasticity of adult brain is titrated by Nogo Receptor 1. Neuron 77:859–866.

Al-Hallaq RA, Conrads TP, Veenstra TD, Wenthold RJ (2007) NMDA di-heteromeric receptor populations and associated proteins in rat hippocampus. J Neurosci 27:8334–8343.

Anderson PA, Olavarria J, Van Sluyters RC (1988) The overall pattern of ocular dominance bands in cat visual cortex. J Neurosci Off J Soc Neurosci 8:2183–2200.

Antonini A, Fagiolini M, Stryker MP (1999) Anatomical correlates of functional plasticity in mouse visual cortex. J Neurosci 19:4388–4406.

Antonini A, Stryker MP (1993) Rapid remodeling of axonal arbors in the visual cortex. Science 260:1819–1821.

Atwal JK, Pinkston-Gosse J, Syken J, Stawicki S, Wu Y, Shatz C, Tessier-Lavigne M (2008) PirB is a functional receptor for myelin inhibitors of axonal regeneration. Science 322:967–970.

Barnes SJ, Sammons RP, Jacobsen RI, Mackie J, Keller GB, Keck T (2015) Subnetwork-specific homeostatic plasticity in mouse visual cortex in vivo. Neuron 86:1290–1303.

Barrett BT, Bradley A, McGraw PV (2004) Understanding the neural basis of amblyopia. The Neuroscientist 10:106–117.

Barria A, Malinow R (2005) NMDA receptor subunit composition controls synaptic plasticity by regulating binding to CaMKII. Neuron 48:289–301.

Bayer KU, Koninck PD, Leonard AS, Hell JW, Schulman H (2001) Interaction with the NMDA receptor locks CaMKII in an active conformation. Nature 411:801–805.

Bear MF (2003) Bidirectional synaptic plasticity: from theory to reality. Philos Trans R Soc B Biol Sci 358:649–655.

Bear MF, Colman H (1990) Binocular competition in the control of geniculate cell size depends upon visual cortical N-methyl-D-aspartate receptor activation. Proc Natl Acad Sci U S A 87:9246–9249.

Bear MF, Cooper LN, Ebner FF (1987) A physiological basis for a theory of synapse modification. Science 237:42–48.

Bear MF, Kleinschmidt A, Gu QA, Singer W (1990) Disruption of experience-dependent synaptic modifications in striate cortex by infusion of an NMDA receptor antagonist. J Neurosci 10:909–925.

Bear MF, Singer W (1986) Modulation of visual cortical plasticity by acetylcholine and noradrenaline. Nature 320:172–176.

Berlucchi G, Buchtel HA (2009) Neuronal plasticity: historical roots and evolution of meaning. Exp Brain Res 192:307–319.

Bernhardi R von, Bernhardi LE, Eugenín J (2017) What is neural plasticity? Adv Exp Med Biol 1015:1–15.

Berry M, Rogers AW (1965) The migration of neuroblasts in the developing cerebral cortex. J Anat 99:691–709.

Beurdeley M, Spatazza J, Lee HHC, Sugiyama S, Bernard C, Nardo AAD, Hensch TK, Prochiantz A (2012) Otx2 binding to perineuronal nets persistently regulates plasticity in the mature visual cortex. J Neurosci 32:9429–9437.

Bickford ME, Guido W, Godwin DW (1998) Neurofilament proteins in Y-cells of the cat lateral geniculate nucleus: normal expression and alteration with visual deprivation. J Neurosci 18:6549–6557.

Bienenstock EL, Cooper LN, Munro PW (1982) Theory for the development of neuron selectivity: orientation specificity and binocular interaction in visual cortex. J Neurosci Off J Soc Neurosci 2:32–48.

Blais BS, Cooper LN, Shouval HZ (2009) Effect of correlated lateral geniculate nucleus firing rates on predictions for monocular eye closure versus monocular retinal inactivation. Phys Rev E 80:061915.

Blais BS, Frenkel MY, Kuindersma SR, Muhammad R, Shouval HZ, Cooper LN, Bear MF (2008) Recovery from monocular deprivation using binocular deprivation. J Neurophysiol 100:2217–2224.

Blake R (1979) The visual system of the cat. Percept Psychophys 26:423–448.

Blakemore C, Van Sluyters RC (1974) Reversal of the physiological effects of monocular deprivation in kittens: further evidence for a sensitive period. J Physiol 237:195–216.

Blasdel GG, Lund JS (1983) Termination of afferent axons in macaque striate cortex. J Neurosci 3:1389–1413.

Bliss TV, Collingridge GL (1993) A synaptic model of memory: long-term potentiation in the hippocampus. Nature 361:31–39.

Bliss TV, Lomo T (1973) Long-lasting potentiation of synaptic transmission in the dentate area of the anaesthetized rabbit following stimulation of the perforant path. J Physiol 232:331–356.

Bough EW (1970) Stereoscopic vision in the macaque monkey: a behavioural demonstration. Nature 225:42–44.

Buzás P, Eysel UT, Adorján P, Kisvárday ZF (2001) Axonal topography of cortical basket cells in relation to orientation, direction, and ocular dominance maps. J Comp Neurol 437:259–285.

Caputo R, Frosini R, Libero CD, Campa L, Magro EF, Secci J (2007) Factors influencing severity of and recovery from anisometropic amblyopia. Strabismus 15:209–214.

Carmignoto G, Vicini S (1992) Activity-dependent decrease in NMDA receptor responses during development of the visual cortex. Science 258:1007–1011.

Castillo PE, Chiu CQ, Carroll RC (2011) Long-term synaptic plasticity at inhibitory synapses. Curr Opin Neurobiol 21:328–338.

Castrén E, Zafra F, Thoenen H, Lindholm D (1992) Light regulates expression of brain-derived neurotrophic factor mRNA in rat visual cortex. Proc Natl Acad Sci USA 89:9444–9448.

Chen JL, Lin WC, Cha JW, So PT, Kubota Y, Nedivi E (2011) Structural basis for the role of inhibition in facilitating adult brain plasticity. Nat Neurosci 14:587–594.

Chen L, Cooper NG, Mower GD (2000) Developmental changes in the expression of NMDA receptor subunits (NR1, NR2A, NR2B) in the cat visual cortex and the effects of dark rearing. Mol Brain Res 78:196–200.

Chen L, Yang C, Mower GD (2001) Developmental changes in the expression of GABA A receptor subunits (α 1, α 2, α 3) in the cat visual cortex and the effects of dark rearing. Mol Brain Res 88:135–143.

Chen WS, Bear MF (2007) Activity-dependent regulation of NR2B translation contributes to metaplasticity in mouse visual cortex. Neuropharmacology 52:200–214.

Chevaleyre V, Castillo PE (2004) Endocannabinoid-Mediated Metaplasticity in the Hippocampus. Neuron 43:871–881.

Chua B, Mitchell P (2004) Consequences of amblyopia on education, occupation, and long term vision loss. Br J Ophthalmol 88:1119–1121.

Coan EJ, Irving AJ, Collingridge GL (1989) Low-frequency activation of the NMDA receptor system can prevent the induction of LTP. Neurosci Lett 105:205–210.

Collingridge GL, Kehl SJ, McLennan H (1983) Excitatory amino acids in synaptic transmission in the Schaffer collateral-commissural pathway of the rat hippocampus. J Physiol 334:33–46.

Cooper LN, Bear MF (2012) The BCM theory of synapse modification at 30: interaction of theory with experiment. Nat Rev Neurosci 13:798–810.

Crair MC, Horton JC, Antonini A, Stryker MP (2001) Emergence of ocular dominance columns in cat visual cortex by 2 weeks of age. J Comp Neurol 430:235–249.

Cramer SC et al. (2011) Harnessing neuroplasticity for clinical applications. Brain 134:1591–1609.

Cynader M, Mitchell DE (1980) Prolonged sensitivity to monocular deprivation in dark-reared cats. J Neurophysiol 43:1026–1040.

Daw NW (1998) Critical periods and amblyopia. Arch Ophthalmol 116:502–505.

Daw NW (2014) Visual development, 3. ed. New York, NY: Springer.

Daw NW, Fox K, Sato H, Czepita D (1992) Critical period for monocular deprivation in the cat visual cortex. J Neurophysiol 67:197–202.

Daw NW, Gordon B, Fox KD, Flavin HJ, Kirsch JD, Beaver CJ, Ji Q, Reid SN, Czepita D (1999) Injection of MK-801 affects ocular dominance shifts more than visual activity. J Neurophysiol 81:204–215.

de Vivo L, Landi S, Panniello M, Baroncelli L, Chierzi S, Mariotti L, Spolidoro M, Pizzorusso T, Maffei L, Ratto GM (2013) Extracellular matrix inhibits structural and functional plasticity of dendritic spines in the adult visual cortex. Nat Commun 4:1484.

del Rio JA, Lecea L de, Ferrer I, Soriano E (1994) The development of parvalbumin-immunoreactivity in the neocortex of the mouse. Dev Brain Res 81:247–259.

Dhaked RK, Singh MK, Singh P, Gupta P (2010) Botulinum toxin: Bioweapon & magic drug. Indian J Med Res 132:489–503.

Dickendesher TL, Baldwin KT, Mironova YA, Koriyama Y, Raiker SJ, Askew KL, Wood A, Geoffroy CG, Zheng B, Liepmann CD, Katagiri Y, Benowitz LI, Geller HM, Giger RJ (2012) NgR1 and NgR3 are receptors for chondroitin sulfate proteoglycans. Nat Neurosci 15:703–712.

Dickey CF, Metz HS, Stewart SA, Scott WE (1991) The diagnosis of amblyopia in cross-fixation. J Pediatr Ophthalmol Strabismus 28:171–175.

DiCostanzo NR, Crowder NA, Kamermans BA, Duffy KR (2020) Retinal and optic nerve integrity following monocular inactivation for the treatment of amblyopia. Front Syst Neurosci 14:32.

Dräger UC, Olsen JF (1980) Origins of crossed and uncrossed retinal projections in pigmented and albino mice. J Comp Neurol 191:383–412.

Dudek SM, Bear MF (1992) Homosynaptic long-term depression in area CA1 of hippocampus and effects of N-methyl-D-aspartate receptor blockade. Proc Natl Acad Sci USA 89:4363–4367.

Duffy KR, Bukhamseen DH, Smithen MJ, Mitchell DE (2015) Binocular eyelid closure promotes anatomical but not behavioral recovery from monocular deprivation. Vision Res 114:151–160.

Duffy KR, Fong M-F, Mitchell DE, Bear MF (2018) Recovery from the anatomical effects of long-term monocular deprivation in cat lateral geniculate nucleus. J Comp Neurol 526:310–323.

Duffy KR, Holman KD, Mitchell DE (2014) Shrinkage of X cells in the lateral geniculate nucleus after monocular deprivation revealed by FoxP2 labeling. Vis Neurosci 31:253–261.

Duffy KR, Lingley AJ, Holman KD, Mitchell DE (2016) Susceptibility to monocular deprivation following immersion in darkness either late into or beyond the critical period. J Comp Neurol 524:2643–2653.

Duffy KR, Livingstone MS (2005) Loss of neurofilament labeling in the primary visual cortex of monocularly deprived monkeys. Cereb Cortex 15:1146–1154.

Duffy KR, Mitchell DE (2013) Darkness alters maturation of visual cortex and promotes fast recovery from monocular deprivation. Curr Biol 23:382–386.

Duffy KR, Slusar JE (2009) Monocular deprivation provokes alteration of the neuronal cytoskeleton in developing cat lateral geniculate nucleus. Vis Neurosci 26:319–328.

Ellis EM, Gauvain G, Sivyer B, Murphy GJ (2016) Shared and distinct retinal input to the mouse superior colliculus and dorsal lateral geniculate nucleus. J Neurophysiol 116:602–610.

Epelbaum M, Milleret C, Buisseret P, Duffer JL (1993) The sensitive period for strabismic amblyopia in humans. Ophthalmology 100:323–327.

Fagiolini M, Fritschy JM, Low K, Mohler H, Rudolph U, Hensch TK (2004) Specific GABAA circuits for visual cortical plasticity. Science 303:1681–1683.

Fagiolini M, Hensch TT (2000) Inhibitory threshold for critical-period activation in primary visual cortex. Nature 404:183–186.

Fagiolini M, Jensen CL, Champagne FA (2009) Epigenetic influences on brain development and plasticity. Curr Opin Neurobiol 19:207–212.

Fagiolini M, Pizzorusso T, Berardi N, Domenici L, Maffei L (1994) Functional postnatal development of the rat primary visual cortex and the role of visual experience: dark rearing and monocular deprivation. Vision Res 34:709–720.

Feldman DE, Knudsen EI (1998) Experience-dependent plasticity and the maturation of glutamatergic synapses. Neuron 20:1067–1071.

Fliegner KH, Kaplan MP, Wood TL, Pintar JE, Liem RKH (1994) Expression of the gene for the neuronal intermediate filament protein α-internexin coincides with the onset of neuronal differentiation in the developing rat nervous system. J Comp Neurol 342:161–173.

Flint AC, Maisch US, Weishaupt JH, Kriegstein AR, Monyer H (1997) R2A subunit expression shortens NMDA receptor synaptic currents in developing neocortex. J Neurosci 17:2469–2476.

Fong M, Mitchell DE, Duffy KR, Bear MF (2016) Rapid recovery from the effects of early monocular deprivation is enabled by temporary inactivation of the retinas. Proc Natl Acad Sci USA 113:14139.

Foster AC, Fagg GE (1984) Acidic amino acid binding sites in mammalian neuronal membranes: their characteristics and relationship to synaptic receptors. Brain Res 319:103.

Fox R, Blake RR (1971) Stereoscopic vision in the cat. Nature 233:55–56.

Frenkel MY, Bear MF (2004) How monocular deprivation shifts ocular dominance in visual cortex of young mice. Neuron 44:917–923.

Friedlander MJ, Stanford LR, Sherman SM (1982) Effects of monocular deprivation on the structure-function relationship of individual neurons in the cat's lateral geniculate nucleus. J Neurosci 2:321–330.

Fritschy JM, Paysan J, Enna A, Mohler H (1994) Switch in the expression of rat GABAA-receptor subtypes during postnatal development: an immunohistochemical study. J Neurosci Off J Soc Neurosci 14:5302–5324.

Ganz L, Fitch M, Satterberg JA (1968) The selective effect of visual deprivation on receptive field shape determined neurophysiologically. Exp Neurol 22:614–637.

Gardoni F, Schrama LH, Dalen JJ van, Gispen WH, Cattabeni F, Luca MD (1999) AlphaCaMKII binding to the C-terminal tail of NMDA receptor subunit NR2A and its modulation by autophosphorylation. FEBS Lett 456:394–398.

Gianfranceschi L, Siciliano R, Walls J, Morales B, Kirkwood A, Huang ZJ, Tonegawa S, Maffei L (2003) Visual cortex is rescued from the effects of dark rearing by overexpression of BDNF. Proc Natl Acad Sci USA 100:12486–12491.

Giannakopoulos M, Kouvelas ED, Mitsacos A (2010) Experience-dependent regulation of NMDA receptor subunit composition and phosphorylation in the retina and visual cortex. Invest Ophthalmol Vis Sci 51:1817–1822.

Giffin F, Mitchell DE (1978) The rate of recovery of vision after early monocular deprivation in kittens. J Physiol 274:511–537.

Gilbert CD (1983) Microcircuitry of the visual cortex. Annu Rev Neurosci 6:217–247.

Goldman RD, Cleland MM, Murthy SN, Mahammad S, Kuczmarski ER (2012) Inroads into the structure and function of intermediate filament networks. J Struct Biol 177:14–23.

Gonchar Y, Burkhalter A (1997) Three distinct families of GABAergic neurons in rat visual cortex. Cereb Cortex 7:347–358.

Gordon JA, Stryker MP (1996) Experience-dependent plasticity of binocular responses in the primary visual cortex of the mouse. J Neurosci 16:3274–3286.

Grieve KL (2005) Binocular visual responses in cells of the rat dLGN. J Physiol 566:119–124.

Gross C, Zhuang X, Stark K, Ramboz S, Oosting R, Kirby L, Santarelli L, Beck S, Hen R (2002) Serotonin1A receptor acts during development to establish normal anxiety-like behaviour in the adult. Nature 416:396–400.

Grutzendler J, Kasthuri N, Gan W-B (2002) Long-term dendritic spine stability in the adult cortex. Nature 420:812–816.

Guillery RW (1970) The laminar distribution of retinal fibers in the dorsal lateral geniculate nucleus of the cat: A new interpretation. J Comp Neurol 138:339–367.

Guillery RW (1972) Binocular competition in the control of geniculate cell growth. J Comp Neurol 144:117–129.

Guillery RW (1973) The effect of lid suture upon the growth of cells in the dorsal lateral geniculate nucleus of kittens. J Comp Neurol 148:417–422.

Guillery RW, Stelzner DJ (1970) The differential effects of unilateral lid closure upon the monocular and binocular segments of the dorsal lateral geniculate nucleus in the cat. J Comp Neurol 139:413–421.

Hall SE, Mitchell DE (1991) Grating acuity of cats measured with detection and discrimination tasks. Behav Brain Res 44:1–9.

Hanover JL, Huang ZJ, Tonegawa S, Stryker MP (1999) Brain-derived neurotrophic factor overexpression induces precocious critical period in mouse visual cortex. J Neurosci 19:RC40.

Harauzov A, Spolidoro M, DiCristo G, Pasquale RD, Cancedda L, Pizzorusso T, Viegi A, Berardi N, Maffei L (2010) Reducing intracortical inhibition in the adult visual cortex promotes ocular dominance plasticity. J Neurosci 30:361–371.

Härtig W, Brauer K, Bigl V, Brückner G (1994) Chondroitin sulfate proteoglycan-immunoreactivity of lectin-labeled perineuronal nets around parvalbumin-containing neurons. Brain Res 635:307–311.

Härtig W, Derouiche A, Welt K, Brauer K, Grosche J, Mäder M, Reichenbach A, Brückner G (1999) Cortical neurons immunoreactive for the potassium channel Kv3.1b subunit are predominantly surrounded by perineuronal nets presumed as a buffering system for cations. Brain Res 842:15–29.

Hebb DO (1949) The organization of behavior. Oxford, England: Wiley.

Hensch TK (2004) Critical period regulation. Annu Rev Neurosci 27:549–579.

Hensch TK, Fagiolini M, Mataga N, Stryker MP, Baekkeskov S, Kash SF (1998) Local GABA circuit control of experience-dependent plasticity in developing visual cortex. Science 282:1504–1508.

Heynen AJ, Liu CH, Bear MF, Yoon B-J, Chung HJ, Huganir RL (2003) Molecular mechanism for loss of visual cortical responsiveness following brief monocular deprivation. Nat Neurosci 6:854–862.

Hoffman PN, Cleveland DW, Griffin JW, Landes PW, Cowan NJ, Price DL (1987) Neurofilament gene expression: a major determinant of axonal caliber. Proc Natl Acad Sci USA 84:3472–3476.

Holmes JM, Clarke MP (2006) Amblyopia. Lancet 367:1343–1351.

Hooks BM, Chen C (2007) Critical periods in the visual system: changing views for a model of experience-dependent plasticity. Neuron 56:312–326.

Huang ZJ, Kirkwood A, Pizzorusso T, Porciatti V, Morales B, Bear MF, Maffei L, Tonegawa S (1999) BDNF regulates the maturation of inhibition and the critical period of plasticity in mouse visual cortex. Cell 98:739–755.

Hubel DH, Wiesel TN (1959) Receptive fields of single neurones in the cat's striate cortex. J Physiol 148:574–591.

Hubel DH, Wiesel TN (1969) Anatomical demonstration of columns in the monkey striate cortex. Nature 221:747–750.

Hubel DH, Wiesel TN (1970) The period of susceptibility to the physiological effects of unilateral eye closure in kittens. J Physiol 206:419–436.

Hubel DH, Wiesel TN (1972) Laminar and columnar distribution of geniculo-cortical fibers in the macaque monkey. J Comp Neurol 146:421–450.

Hubel DH, Wiesel TN, LeVay S (1977) Plasticity of ocular dominance columns in monkey striate cortex. Philos Trans R Soc B Biol Sci 278:377–409.

Huntsman MM, Muñoz A, Jones EG (1999) Temporal modulation of GABAA receptor subunit gene expression in developing monkey cerebral cortex. Neuroscience 91:1223–1245.

Huttunen HJ, Palva JM, Lindberg L, Palva S, Saarela V, Karvonen E, Latvala M-L, Liinamaa J, Booms S, Castrén E, Uusitalo H (2018) Effect of fluoxetine on adult amblyopia: a placebo-controlled study combining neuroplasticity-enhancing pharmacological intervention and perceptual training. bioRxiv:327650.

Iwai Y, Fagiolini M, Obata K, Hensch TK (2003) Rapid critical period induction by tonic inhibition in visual cortex. J Neurosci 23:6695–6702.

Jacobs GH (1981) Comparative color vision. New York, NY: Academic Press.

Jiang B, Treviño M, Kirkwood A (2007) Sequential development of long-term potentiation and depression in different layers of the mouse visual cortex. J Neurosci 27:9648–9652.

Johnson JW, Ascher P (1987) Glycine potentiates the NMDA response in cultured mouse brain neurons. Nature 325:529–531.

Kalil R (1978) Dark rearing in the cat: Effects on visuomotor behavior and cell growth in the dorsal lateral geniculate nucleus. J Comp Neurol 178:451–467.

Kaplan MP, Chin SS, Fliegner KH, Liem RK (1990) Alpha-internexin, a novel neuronal intermediate filament protein, precedes the low molecular weight neurofilament protein (NF-L) in the developing rat brain. J Neurosci 10:2735–2748.

Kaschube M, Wolf F, Geisel T, Löwel S (2002) Genetic influence on quantitative features of neocortical architecture. J Neurosci 22:7206–7217.

Keck T, Hübener M, Bonhoeffer T (2017) Interactions between synaptic homeostatic mechanisms: an attempt to reconcile BCM theory, synaptic scaling, and changing excitation/inhibition balance. Curr Opin Neurobiol 43:87–93.

Kind PC (1999) Cortical plasticity: Is it time for a change? Curr Biol 9:R640–R643.

Kind PC, Sengpiel F, Beaver CJ, Crocker-Buque A, Kelly GM, Matthews RT, Mitchell DE (2013) The development and activity-dependent expression of aggrecan in the cat visual cortex. Cereb Cortex 23:349–360.

Kirkwood A, Rioult MC, Bear MF (1996) Experience-dependent modification of synaptic plasticity in visual cortex. Nature 381:526–528.

Klausberger T, Roberts JD, Somogyi P (2002) Cell type- and input-specific differences in the number and subtypes of synaptic GABA(A) receptors in the hippocampus. J Neurosci 22:2513–2521.

Kleckner NW, Dingledine R (1988) Requirement for glycine in activation of NMDA-receptors expressed in Xenopus oocytes. Science 241:835–837.

Kleinschmidt A, Bear MF, Singer W (1987) Blockade of "NMDA" receptors disrupts experience-dependent plasticity of kitten striate cortex. Science 238:355–358.

Knudsen EI (2004) Sensitive periods in the development of the brain and behavior. J Cogn Neurosci 16:1412–1425.

Köppe G, Brückner G, Brauer K, Härtig W, Bigl V (1997) Developmental patterns of proteoglycan-containing extracellular matrix in perineuronal nets and neuropil of the postnatal rat brain. Cell Tissue Res 288:33–41.

Kubota Y, Kawaguchi Y (1994) Three classes of GABAergic interneurons in neocortex and neostriatum. Jpn J Physiol 44:145.

Lago J, Rodríguez LP, Blanco L, Vieites JM, Cabado AG (2015) Tetrodotoxin, an extremely potent marine neurotoxin: distribution, toxicity, origin and therapeutical uses. Mar Drugs 13:6384–6406.

Lander C, Kind P, Maleski M, Hockfield S (1997) A family of activity-dependent neuronal cell-surface chondroitin sulfate proteoglycans in cat visual cortex. J Neurosci 17:1928–1939.

Lasek RJ (1981) The dynamic ordering of neuronal cytoskeletons. Neurosci Res Program Bull 19:7–32.

Laube B, Kuhse J, Betz H (1998) Evidence for a tetrameric structure of recombinant NMDA receptors. J Neurosci 18:2954–2961.

Laurie DJ, Seeburg PH (1994) Ligand affinities at recombinant N-methyl-D-aspartate receptors depend on subunit composition. Eur J Pharmacol 268:335–345.

Lee HK, Kirkwood A (2019) Mechanisms of homeostatic synaptic plasticity in vivo. Front Cell Neurosci 13.

Lendahl U, Zimmerman LB, McKay RDG (1990) CNS stem cells express a new class of intermediate filament protein. Cell 60:585–595.

Lenneberg EH (1967) The biological foundations of language. Hosp Pract 2:59–67.

Leonard AS, Lim IA, Hemsworth DE, Horne MC, Hell JW (1999) Calcium/calmodulin-dependent protein kinase II is associated with the N-methyl-D-aspartate receptor. Proc Natl Acad Sci USA 96:3239–3244.

LeVay S, Connolly M, Houde J, Essen DV (1985) The complete pattern of ocular dominance stripes in the striate cortex and visual field of the macaque monkey. J Neurosci 5:486–501.

Levelt CN, Hübener M (2012) Critical-period plasticity in the visual cortex. Annu Rev Neurosci 35:309–330.

Linden ML, Heynen AJ, Haslinger RH, Bear MF (2009) Thalamic activity that drives visual cortical plasticity. Nat Neurosci 12:390–392.

Lingley AJ, Bowdridge JC, Farivar R, Duffy KR (2018) Mapping of neuron soma size as an effective approach to delineate differences between neural populations. J Neurosci Methods 304:126–135.

Lisman J, Schulman H, Cline H (2002) The molecular basis of CaMKII function in synaptic and behavioural memory. Nat Rev Neurosci 3:175–190.

Loudon SE, Polling JR, Simonsz HJ (2002) A preliminary report about the relation between visual acuity increase and compliance in patching therapy for amblyopia. Strabismus 10:79–82.

Loudon SE, Polling JR, Simonsz HJ (2003) Electronically measured compliance with occlusion therapy for amblyopia is related to visual acuity increase. Graefes Arch Clin Exp Ophthalmol 241:176–180.

Lynch G, Schottler F, Kelso S, Barrionuevo G, Larson J (1983) Intracellular injections of EGTA block induction of hippocampal long-term potentiation. Nature 305:719–721.

Malenka RC (1994) Synaptic plasticity in the hippocampus: LTP and LTD. Cell 78:535–538.

Malenka RC, Bear MF (2004) LTP and LTD: an embarrassment of riches. 44.

Malenka RC, Kauer JA, Zucker RS, Nicoll RA (1988) Postsynaptic calcium is sufficient for potentiation of hippocampal synaptic transmission. Science 242:81–84.

Mano I, Teichberg VI (1998) A tetrameric subunit stoichiometry for a glutamate receptor-channel complex. NeuroReport 9:327–331.

Mataga N, Mizuguchi Y, Hensch TK (2004) Experience-dependent pruning of dendritic spines in visual cortex by tissue plasminogen activator. Neuron 44:1031–1041.

Mataga N, Nagai N, Hensch TK (2002) Permissive proteolytic activity for visual cortical plasticity. Proc Natl Acad Sci 99:7717–7721.

Maya-Vetencourt JF, Sale A, Viegi A, Baroncelli L, Pasquale RD, O'Leary OF, Castrén E, Maffei L (2008) The antidepressant fluoxetine restores plasticity in the adult visual cortex. Science 320:385–388.

Mayer ML, Westbrook GL, Guthrie PB (1984) Voltage-dependent block by Mg2+ of NMDA responses in spinal cord neurones. Nature 309:261–263.

McDonald MA, Dobson V, Sebris SL, Baitch L, Varner D, Teller DY (1985) The acuity card procedure: a rapid test of infant acuity. Invest Ophthalmol Vis Sci 26:1158–1162.

McGee AW, Yang Y, Fischer QS, Daw NW, Strittmatter SM (2005) Experience-driven plasticity of visual cortex limited by myelin and Nogo receptor. Science 309:2222–2226.

McKee SP, Levi DM, Movshon JA (2003) The pattern of visual deficits in amblyopia. J Vis 3:380–405.

Mitchell DE (1988) The extent of visual recovery from early monocular or binocular visual deprivation in kittens. J Physiol 395:639–660.

Mitchell DE (2013) A shot in the dark: the use of darkness to investigate visual development and as a therapy for amblyopia. Clin Exp Optom 96:363–372.

Mitchell DE, Aronitz E, Bobbie-Ansah P, Crowder N, Duffy KR (2019) Fast recovery of the amblyopic eye acuity of kittens following brief exposure to total darkness depends on the fellow eye. Neural Plast 2019:7624837.

Mitchell DE, Cynader M, Movshon JA (1977) Recovery from the effects of monocular deprivation in kittens. J Comp Neurol 176:53–63.

Mitchell DE, MacNeill K, Crowder NA, Holman K, Duffy KR (2016) Recovery of visual functions in amblyopic animals following brief exposure to total darkness. J Physiol 594:149–167.

Miwa JM, Ibañez-Tallon I, Crabtree GW, Sánchez R, Šali A, Role LW, Heintz N (1999) lynx1, an endogenous toxin-like modulator of nicotinic acetylcholine receptors in the mammalian CNS. Neuron 23:105–114.

Miyamoto H, Katagiri H, Hensch T (2003) Experience-dependent slow-wave sleep development. Nat Neurosci 6:553–554.

Moczydlowski EG (2013) The molecular mystique of tetrodotoxin. Toxicon 63:165–183.

Monyer H, Burnashev N, Laurie DJ, Sakmann B, Seeburg PH (1994) Developmental and regional expression in the rat brain and functional properties of four NMDA receptors. Neuron 12:529–540.

Monyer H, Sprengel R, Schoepfer R, Herb A, Higuchi M, Lomeli H, Burnashev N, Sakmann B, Seeburg PH (1992) Heteromeric NMDA receptors: molecular and functional distinction of subtypes. Science 256:1217–1221.

Morad Y, Werker E, Nemet P (1999) Visual acuity tests using chart, line, and single optotype in healthy and amblyopic children. J AAPOS 3:94–97.

Morales B, Choi SY, Kirkwood A (2002) Dark rearing alters the development of GABAergic transmission in visual cortex. J Neurosci 22:8084–8090.

Morishita H, Miwa JM, Heintz N, Hensch TK (2010) Lynx1, a cholinergic brake, limits plasticity in adult visual cortex. Science 330:1238–1240.

Morris JR, Lasek RJ (1982) Stable polymers of the axonal cytoskeleton: the axoplasmic ghost. J Cell Biol 92:192–198.

Motulsky HJ, Brown RE (2006) Detecting outliers when fitting data with nonlinear regression - a new method based on robust nonlinear regression and the false discovery rate. BMC Bioinformatics 7:123.

Movshon JA (1976) Reversal of the physiological effects of monocular deprivation in the kitten's visual cortex. J Physiol 261:125–174.

Movshon JA, Blakemore C (1974) Functional reinnervation in kitten visual cortex. Nature 251:504–505.

Mulkey RM, Malenka RC (1992) Mechanisms underlying induction of homosynaptic long-term depression in area CA1 of the hippocampus. Neuron 9:967–975.

Müller CM, Griesinger CB (1998) Tissue plasminogen activator mediates reverse occlusion plasticity in visual cortex. Nat Neurosci 1:47–53.

Münchau A, Bhatia KP (2000) Uses of botulinum toxin injection in medicine today. BMJ 320:161–165.

Murphy KM, Mitchell DE (1987) Reduced visual acuity in both eyes of monocularly deprived kittens following a short or long period of reverse occlusion. J Neurosci 7:1526–1536.

Mwachaka P, Saidi H, Odula P, Mandela P (2015a) Effects of monocular deprivation on the thickness of neural retina. J Morphol Sci 32:111–120.

Mwachaka P, Saidi H, Odula P, Mandela P (2015b) Effect of monocular deprivation on rabbit neural retinal cell densities. J Ophthalmic Vis Res 10:144–150.

Nase G, Weishaupt J, Stern P, Singer W, Monyer H (1999) Genetic and epigenetic regulation of NMDA receptor expression in the rat visual cortex. Eur J Neurosci 11:4320–4326.

Neveu MM, Jeffery G (2007) Chiasm formation in man is fundamentally different from that in the mouse. Eye 21:1264–1270.

Nowak L, Prochiantz A, Herbet A, Bregestovski P, Ascher P (1984) Magnesium gates glutamate-activated channels in mouse central neurones. Nature 307:462–465.

Ohki K, Reid RC (2007) Specificity and randomness in the visual cortex. Curr Opin Neurobiol 17:401–407.

O'Leary TP, Kutcher MR, Mitchell DE, Duffy KR (2012) Recovery of neurofilament following early monocular deprivation. Front Syst Neurosci 6:22.

Olson CR, Freeman RD (1975) Progressive changes in kitten striate cortex during monocular vision. J Neurophysiol 38:26–32.

Olson CR, Freeman RD (1978) Monocular deprivation and recovery during sensitive period in kittens. J Neurophysiol 41:65–74.

Olson CR, Freeman RD (1980) Profile of the sensitive period for monocular deprivation in kittens. Exp Brain Res 39:17.

Oray S, Majewska A, Sur M (2004) Dendritic spine dynamics are regulated by monocular deprivation and extracellular matrix degradation. Neuron 44:1021–1030.

Packwood EA, Cruz OA, Rychwalski PJ, Keech RV (1999) The psychosocial effects of amblyopia study. J AAPOS 3:15–17.

Pananceau M, Gustafsson B (1997) NMDA receptor dependence of the input specific NMDA receptor-independent LTP in the hippocampal CA1 region. Brain Res 752:255–260.

Peng J, Kim MJ, Cheng D, Duong DM, Gygi SP, Sheng M (2004) Semiquantitative proteomic analysis of rat forebrain postsynaptic density fractions by mass spectrometry. J Biol Chem 279:21003–21011.

Perez-Otano I, Schulteis CT, Contractor A, Lipton SA, Trimmer JS, Sucher NJ, Heinemann SF (2001) Assembly with the NR1 subunit is required for surface expression of NR3A-containing NMDA receptor. J Neurosci 21:1228–1237.

Perry VH, Cowey A (1984) Retinal ganglion cells that project to the superior colliculus and pretectum in the macaque monkey. Neuroscience 12:1125–1137.

Philpot BD, Cho KKA, Bear MF (2007) Obligatory role of NR2A for metaplasticity in visual cortex. Neuron 53:495–502.

Philpot BD, Espinosa JS, Bear MF (2003) Evidence for altered NMDA receptor function as a basis for metaplasticity in visual cortex. J Neurosci 23:5583–5588.

Philpot BD, Sekhar AK, Shouval HZ, Bear MF (2001) Visual Experience and deprivation bidirectionally modify the composition and function of NMDA receptors in visual cortex. Neuron 29:157–169.

Pizzorusso T, Medini P, Berardi N, Chierzi S, Fawcett JW, Maffei L (2002) Reactivation of ocular dominance plasticity in the adult visual cortex. Science 298:1248–1251.

Pizzorusso T, Medini P, Landi S, Baldini S, Berardi N, Maffei L (2006) Structural and functional recovery from early monocular deprivation in adult rats. Proc Natl Acad Sci USA 103:8517–8522.

Putignano E, Lonetti G, Cancedda L, Ratto G, Costa M, Maffei L, Pizzorusso T (2007) Developmental downregulation of histone posttranslational modifications regulates visual cortical plasticity. Neuron 53:747–759.

Quinlan EM, Olstein DH, Bear MF (1999a) Bidirectional, experience-dependent regulation of N-methyl-D-aspartate receptor subunit composition in the rat visual cortex during postnatal development. Proc Natl Acad Sci 96:12876–12880.

Quinlan EM, Philpot BD, Huganir RL, Bear MF (1999b) Rapid, experience-dependent expression of synaptic NMDA receptors in visual cortex in vivo. Nat Neurosci 2:352–357.

Rakic P (1974) Neurons in rhesus monkey visual cortex: systematic relation between time of origin and eventual disposition. Science 183:425–427.

Rakic P (1976) Prenatal genesis of connections subserving ocular dominance in the rhesus monkey. Nature 261:467–471.

Rakic P (1977) Prenatal development of the visual system in rhesus monkey. Philos Trans R Soc B Biol Sci 278:245–260.

Reese BE (1988) “Hidden lamination” in the dorsal lateral geniculate nucleus: the functional organization of this thalamic region in the rat. Brain Res 472:119–137.

Reese BE (2011) Development of the retina and optic pathway. Vision Res 51:613–632.

Reid SNM, Juraska JM (1991) The cytoarchitectonic boundaries of the monocular and binocular areas of the rat primary visual cortex. Brain Res 563:293–296.

Rittenhouse CD, Shouval HZ, Paradiso MA, Bear MF (1999) Monocular deprivation induces homosynaptic long-term depression in visual cortex. Nature 397:347–350.

Roberts EB, Ramoa AS (1999) Enhanced NR2A subunit expression and decreased NMDA receptor decay time at the onset of ocular dominance plasticity in the ferret. J Neurophysiol 81:2587–2591.

Rosenmund C, Stern-Bach Y, Stevens CF (1998) The tetrameric structure of a glutamate receptor channel. Science 280:1596–1599.

Sabri K, Knapp CM, Thompson JR, Gottlob I (2006) The VF-14 and psychological impact of amblyopia and strabismus. Invest Ophthalmol Vis Sci 47:4386–4392.

Sajo M, Ellis-Davies G, Morishita H (2016) Lynx1 limits dendritic spine turnover in the adult visual cortex. J Neurosci 36:9472–9478.

Sale A, Maya-Vetencourt JF, Medini P, Cenni MC, Baroncelli L, Pasquale RD, Maffei L (2007) Environmental enrichment in adulthood promotes amblyopia recovery through a reduction of intracortical inhibition. Nat Neurosci 10:679–681.

Sawtell NB, Frenkel MY, Philpot BD, Nakazawa K, Tonegawa S, Bear MF (2003) NMDA receptor-dependent ocular dominance plasticity in adult visual cortex. Neuron 38:977–985.

Schantz EJ, Johnson EA (1992) Properties and use of botulinum toxin and other microbial neurotoxins in medicine. Microbiol Rev 56:80–99.

Sengpiel F (2007) The critical period. Curr Biol 17:742.

Sharif MH, Talebnejad MR, Rastegar K, Khalili MR, Nowroozzadeh MH (2019) Oral fluoxetine in the management of amblyopic patients aged between 10 and 40 years old: a randomized clinical trial. Eye 33:1060–1067.

Shatz CJ, Stryker MP (1978) Ocular dominance in layer IV of the cat's visual cortex and the effects of monocular deprivation. J Physiol 281:267–283.

Shatz CJ, Stryker MP (1988) Prenatal tetrodotoxin infusion blocks segregation of retinogeniculate afferents. Science 242:87–89.

Sheng M, Cummings J, Roldan LA, Jan YN, Jan LY (1994) Changing subunit composition of heteromeric NMDA receptors during development of rat cortex. Nature 368:144–147.

Sobczyk A, Scheuss V, Svoboda K (2005) NMDA Receptor subunit-dependent [Ca2+] signaling in individual hippocampal dendritic spines. J Neurosci 25:6037–6046.

Song S, Mitchell DE, Crowder NA, Duffy KR (2015) Postnatal accumulation of intermediate filaments in the cat and human primary visual cortex. J Comp Neurol 523:2111–2126.

Spatazza J, Lee HHC, Nardo AAD, Tibaldi L, Joliot A, Hensch TK, Prochiantz A (2013) Choroid-plexus-derived Otx2 homeoprotein constrains adult cortical plasticity. Cell Rep 3:1815–1823.

Stewart CE, Moseley MJ, Stephens DA, Fielder AR (2004) Treatment dose-response in amblyopia therapy: the Monitored Occlusion Treatment of Amblyopia Study (MOTAS). Invest Ophthalmol Vis Sci 45:3048–3054.

Strack S, Colbran RJ (1998) Autophosphorylation-dependent targeting of calcium/ calmodulin-dependent protein kinase II by the NR2B subunit of the N-methyl- D-aspartate receptor. J Biol Chem 273:20689–20692.

Stryker MP, Harris WA (1986) Binocular impulse blockade prevents the formation of ocular dominance columns in cat visual cortex. J Neurosci 6:2117–2133.

Sugiyama S, Nardo AAD, Aizawa S, Matsuo I, Volovitch M, Prochiantz A, Hensch TK (2008) Experience-dependent transfer of Otx2 homeoprotein into the visual cortex activates postnatal plasticity. Cell 134:508–520.

Sugiyama S, Prochiantz A, Hensch TK (2009) From brain formation to plasticity: insights on Otx2 homeoprotein. Dev Growth Differ 51:369–377.

Syken J, GrandPre T, Kanold PO, Shatz CJ (2006) PirB restricts ocular-dominance plasticity in visual cortex. Science 313:1795–1800.

Takesian AE, Hensch TK (2013) Balancing plasticity/stability across brain development. Prog Brain Res 207:3–34.

The Pediatric Eye Disease Investigator Group (2003) A comparison of atropine and patching treatments for moderate amblyopia by patient age, cause of amblyopia, depth of amblyopia, and other factors. Ophthalmology 110:1632–1637.

The Pediatric Eye Disease Investigator Group (2009) Pharmacological plus optical penalization treatment for amblyopia: results of a randomized trial. Arch Ophthalmol 127:22–30.

Tommila V, Tarkkanen A (1981) Incidence of loss of vision in the healthy eye in amblyopia. Br J Ophthalmol 65:575–577.

Trachtenberg JT, Trepel C, Stryker MP (2000) Rapid extragranular plasticity in the absence of thalamocortical plasticity in the developing primary visual cortex. Science 287:2029–2032.

Turrigiano GG (2008) The self-tuning neuron: synaptic scaling of excitatory synapses. Cell 135:422–435.

Turrigiano GG, Leslie KR, Desai NS, Rutherford LC, Nelson SB (1998) Activity-dependent scaling of quantal amplitude in neocortical neurons. Nature 391:892–896.

van Versendaal D, Rajendran R, Saiepour MH, Klooster J, Smit-Rigter L, Sommeijer JP, De Zeeuw CI, Hofer SB, Heimel JA, Levelt CN (2012) Elimination of inhibitory synapses is a major component of adult ocular dominance plasticity. Neuron 74:374–383.

Vicini S, Wang JF, Li JH, Zhu WJ, Wang YH, Luo JH, Wolfe BB, Grayson DR (1998) Functional and pharmacological differences between recombinant N-methyl-D-aspartate receptors. J Neurophysiol 79:555.

Vierci G, Pannunzio B, Bornia N, Rossi FM (2016) H3 and H4 lysine acetylation correlates with developmental and experimentally induced adult experience-dependent plasticity in the mouse visual cortex. J Exp Neurosci 2016:49–64.

Volpe JJ (2000) Overview: normal and abnormal human brain development. Ment Retard Dev Disabil Res Rev 6:1–5.

Von Noorden GK (1967) Classification of amblyopia. Am J Ophthalmol 63:238–244.

Von Noorden GK, Campos EC (2002) Binocular vision and ocular motility, 6. ed. St. Louis, Mo: Mosby.

Vorobyov V, Kwok JCF, Fawcett JW, Sengpiel F (2013) Effects of digesting chondroitin sulfate proteoglycans on plasticity in cat primary visual cortex. J Neurosci 33:234–243.

Wang L, Maffei A (2014) Inhibitory plasticity dictates the sign of plasticity at excitatory synapses. J Neurosci Off J Soc Neurosci 34:1083–1093.

Weakley DR (2001) The association between nonstrabismic anisometropia, amblyopia, and subnormal binocularity. Ophthalmology 108:163–171.

Werb Z (1997) ECM and cell surface proteolysis: regulating cellular ecology. Cell 91:439–442.

Wiesel TN (1982) Postnatal development of the visual cortex and the influence of environment. Nature 299:583–591.

Wiesel TN, Hubel DH (1963a) Effects of visual deprivation on morphology and physiology of cells in the cats lateral geniculate body. J Neurophysiol 26:978–993.

Wiesel TN, Hubel DH (1963b) Single-cell responses in striate cortex of kittens deprived of vision in one eye. J Neurophysiol 26:1003–1017.

Wiesel TN, Hubel DH (1965) Comparison of the effects of unilateral and bilateral eye closure on cortical unit responses in kittens. J Neurophysiol 28:1029–1040.

Wu C, Hunter DG (2006) Amblyopia: diagnostic and therapeutic options. Am J Ophthalmol 141:175–184.

Xue M, Atallah BV, Scanziani M (2014) Equalizing excitation–inhibition ratios across visual cortical neurons. Nature 511:596–600.

Yang K, Xiong W, Yang G, Kojic L, Taghibiglou C, Wang YT, Cynader M (2011) The regulatory role of long-term depression in juvenile and adult mouse ocular dominance plasticity. Sci Rep 1:203.

Yang SN, Tang YG, Zucker RS (1999) Selective induction of LTP and LTD by postsynaptic [Ca2+]i elevation. J Neurophysiol 81:781–787.

Ye Q, Miao QL (1994) Matrix biology. Matrix Biol 32:352–363.

Ye Q, Miao QL (2013) Experience-dependent development of perineuronal nets and chondroitin sulfate proteoglycan receptors in mouse visual cortex. Matrix Biol J Int Soc Matrix Biol 32:352–363.

Yoon BJ, Smith GB, Heynen AJ, Neve RL, Bear MF (2009) Essential role for a long-term depression mechanism in ocular dominance plasticity. Proc Natl Acad Sci USA 106:9860–9865.

Zeater N, Cheong SK, Solomon SG, Dreher B, Martin PR (2015) Binocular visual responses in the primate lateral geniculate nucleus. Curr Biol 25:3190–3195.

Zilles K, Wree A, Schleicher A, Divac I (1984) The monocular and binocular subfields of the rat's primary visual cortex: A quantitative morphological approach. J Comp Neurol 226:391–402.

Table 1 Table of percent of signal contamination through for the filter cubes used.

Percentages indicate the extent to which the signal (i.e. fluorescence) is due to the fluorophore for each channel. The bolded percentages indicate the percent of signal for the fluorophore matched with its respective filter cube. The amount of background seen was minimized by using Sudan black and using the lowest light setting.

	Filter Cube		
Fluorophore	**LED - mCherry-A- OMF - ZERO**	**FITC - 3540C**	**BV480 - 2432A**
Alexa Fluor 594	**76.0%**	0.0%	0.0%
Alexa Fluor 488	3.0%	**56.0%**	2.9%
Neurotrace 435/455	0.3%	9.3%	**38.7%**
Background	20.7%	35.0%	58.4%

Table 2 Information about the number of outliers removed for cell size analysis.

Analysis was done on the LV1, RV1, layers of the LGN receiving input from the left eye (LE LGN Layers), and layers of the LGN receiving input from the left eye (RE LGN Layers).

	Condition	Data Points Analysed After Outlier Removal	Number of Outliers Removed
LV1	Normal	537	9
	Dark Exposure	491	23
RV1	Normal	633	7
	Dark Exposure	548	8
LE LGN Layers	Normal	306	4
	Dark Exposure	314	3
RE LGN Layers	Normal	301	1
	Dark Exposure	315	2

Table 3 Average ratio per layer and percent decrease between the normal animals and dark exposure animals for the layers of V1.

	Average Normal Ratio	Average Dark Exposure Ratio	Percent Decrease
Layer 2/3	0.659	0.515	21.846
Layer 4	0.677	0.543	19.801
Layer 5	0.756	0.584	22.662
Layer 6	0.728	0.547	24.853

Table 4 Average ratio per layer and percent decrease between the normal animals and dark exposure animals for the layers of the LGN.

	Average Normal Ratio	**Average Dark Exposure Ratio**	**Percent Decrease**
Layer A	0.852	0.678	20.380
Layer A1	0.818	0.670	18.034

Table 5 Average cell size across the layers of V1 for normal and dark exposure animals, and the percent decrease between the normal animals and dark exposure animals.

	Average Normal Cell Size (μm^2)	**Average Dark Exposure Cell Size (μm^2)**	**Percent Decrease**
Layer 2/3	112.867	86.305	23.533
Layer 4	98.234	71.239	27.480
Layer 5	107.461	87.100	18.947
Layer 6	107.259	85.600	20.193

Table 6 Average cell size across the layers of the LGN for normal and dark exposure animals, and the percent decrease between the normal animals and dark exposure animals

	Average Normal Cell Size (μm^2)	**Average Dark Exposure Cell Size (μm^2)**	**Percent Decrease**
Layer A	183.299	137.058	25.227
Layer A1	192.229	158.970	17.302

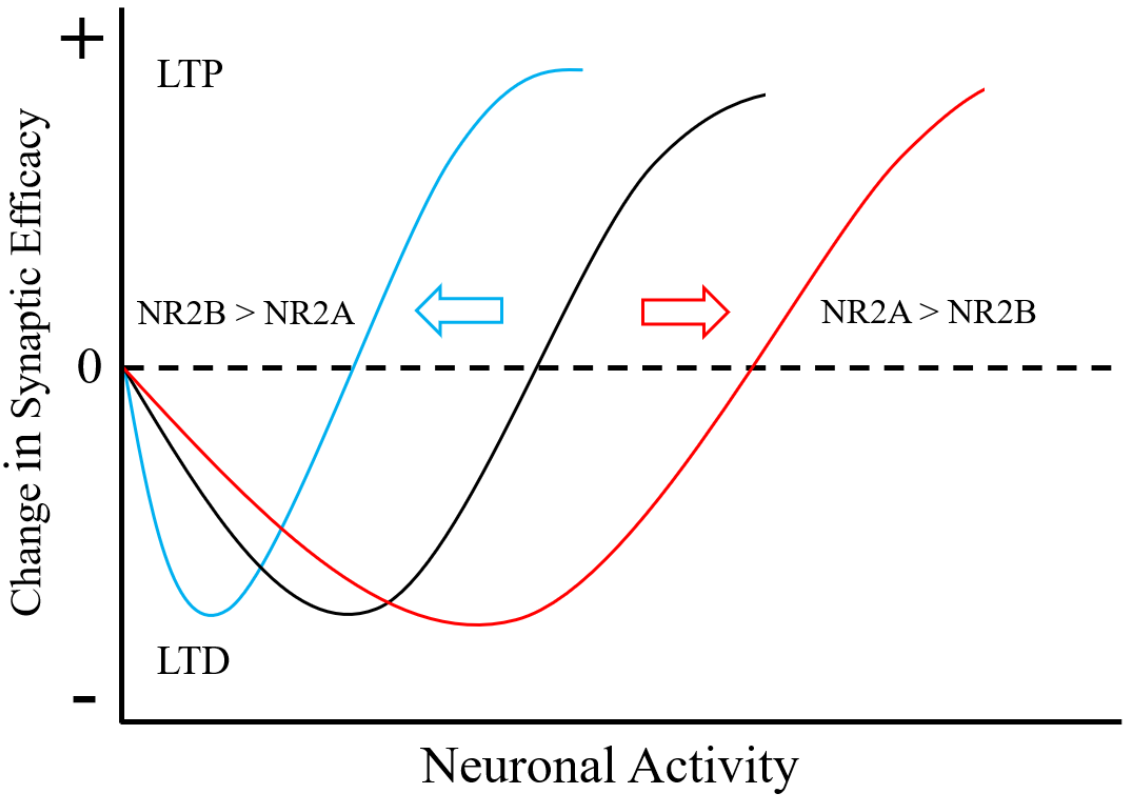

Figure 1 Illustration of how subunit composition of the NMDA receptor regulates the threshold for LTP/LTD.

The y-axis represents a change in excitatory synaptic efficacy that occurs due to differences in postsynaptic responses elicited by varying levels of stimulation (x-axis). When previous activity is high, the NR2A/NR2B ratio increases, thus the LTP/LTD threshold shifts higher and LTD is favoured over LTP (red curve). When previous activity is low, the NR2A/NR2B ratio decreases, thus the LTD/LTD threshold shifts lower, and LTP is favoured over LTD (blue curve). The blue curve represents the shift in LTP/LTD threshold that likely occurs during dark exposure due to the decrease in NR2A/NR2B ratio. The dashed line indicates the modification threshold that separates LTD from LTP. During dark exposure, LTP is favoured over LTD, and synaptic strengthening is more likely to occur (Modified from Bear et al., 1987; Bear, 2003; Lee and Kirkwood, 2019).

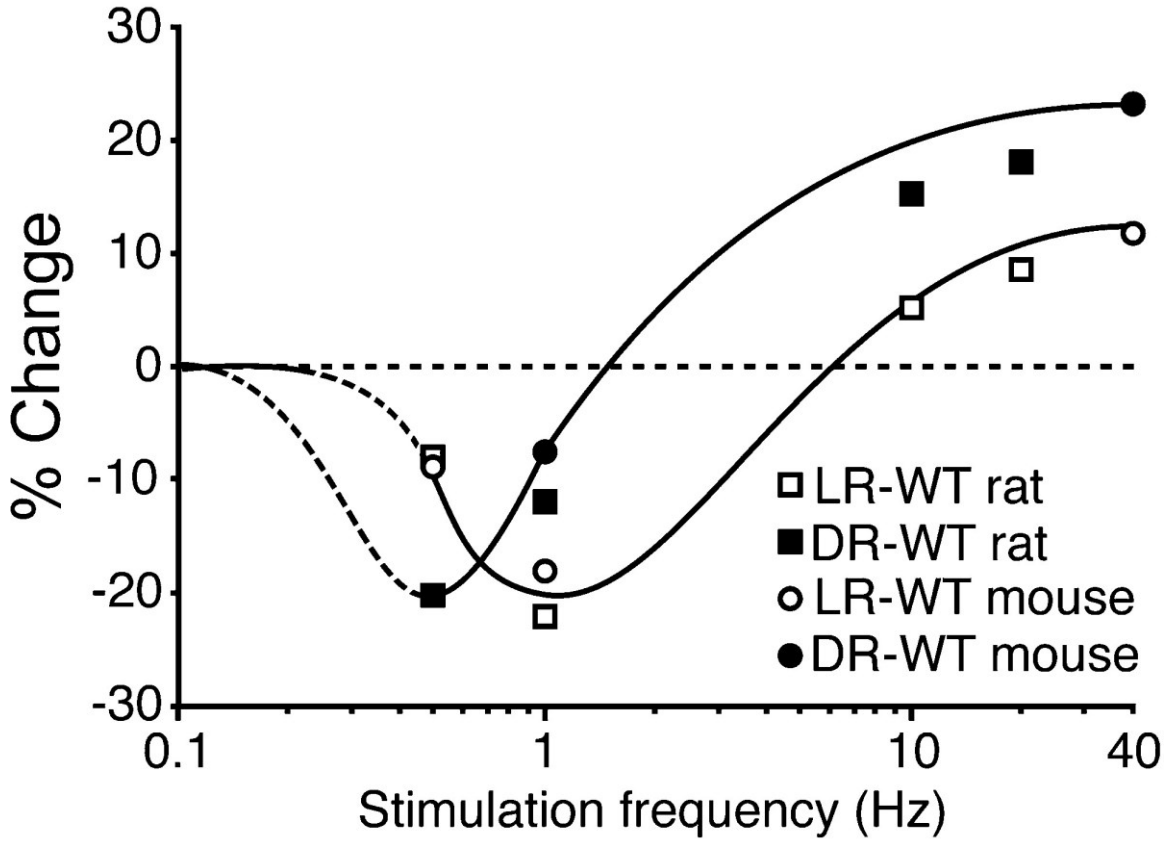

Figure 2 Experimental evidence of the BCM model shown in dark reared and light reared rats and mice.

The graph represents the stimulation frequency response functions that were derived from V1 of light reared and dark reared animals to provide experimental evidence of the BCM model. The x-axis represents the stimulation frequency used to induce the change in field potentiation amplitude (y-axis). The dashed lines of the curves have not been confirmed experimentally but were inferred from previous data. This figure represents the shift in the presynaptic LTP/LTD threshold as a result of dark rearing (Figure from Philpot et al., 2007).

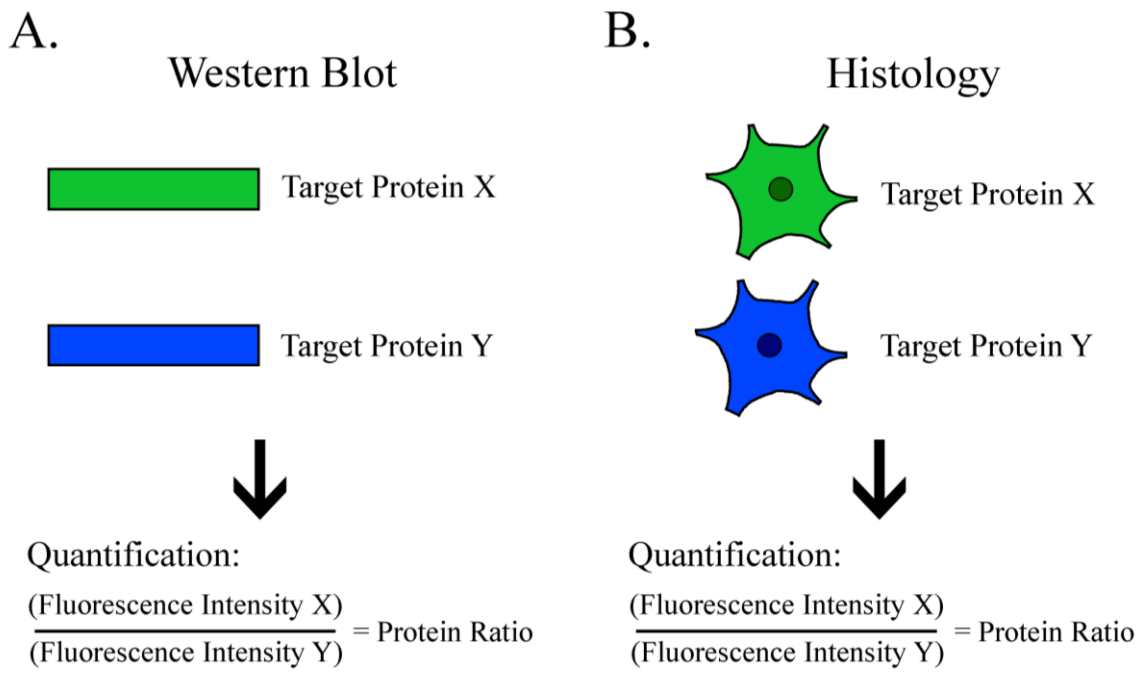

Figure 3 Visual comparison between a western blot (A) and a novel histological approach developed for this research (B).

In both cases, the ratio between the two proteins is measured based on fluorescence intensity. However, in the novel method, a protein ratio is assessed on a cell-by-cell basis, preserving *in situ* results lost with the western blot method.

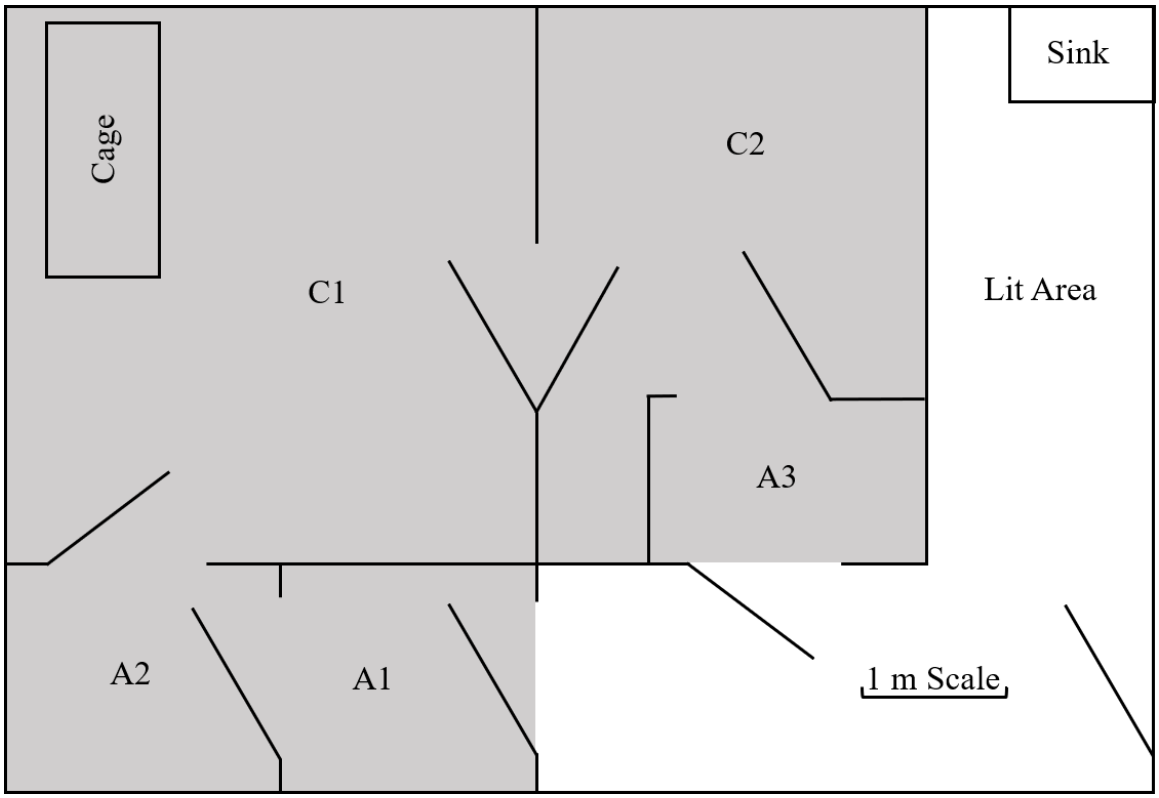

Figure 4 Schematic of darkroom facility.

The darkroom facility, shown to scale, consists of an illuminated area containing a sink, three anterooms (A1, A2, and A3), a primary darkroom (C1), and a secondary core darkroom (C2). In this study, the animals were kept within the primary darkroom (C1). When the room was cleaned, animals were transferred to the secondary core darkroom (C2) in cat carriers (Mitchell, 2013). Operation of this facility is designed to enable immersion in complete darkness for ten consecutive days.

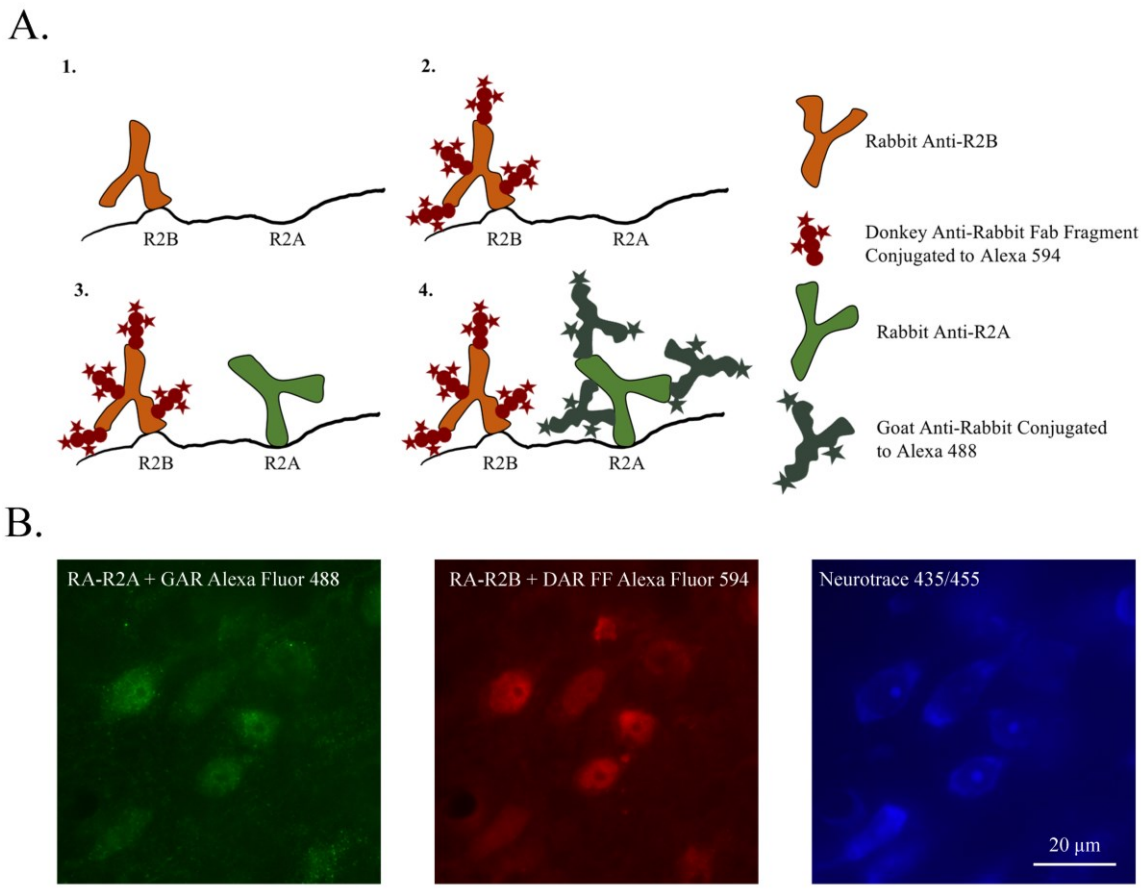

Figure 5 Schematic of multiplex immunolabeling procedure employed for our new approach to measuring the NMDA receptor subunit ratio.

(**A**) Tissue was first incubated in a rabbit Anti-R2B primary antibody (**A1**), followed by a donkey anti-rabbit Fab fragment conjugated to Alexa 594 (**A2**). After this, tissue was exposed to a rabbit Anti-R2A primary antibody (**A3**), and then goat anti-rabbit conjugated to Alexa 488 secondary antibody (**A4**). Following this, the tissue was labelled for Nissl substance with a fluorescence Nissl stain (Not illustrated). (**B**) Labelling of the NMDA receptor subunits and Nissl substance. This novel approach to multiplexing enables the isolation of proteins according to fluorescence wavelength.

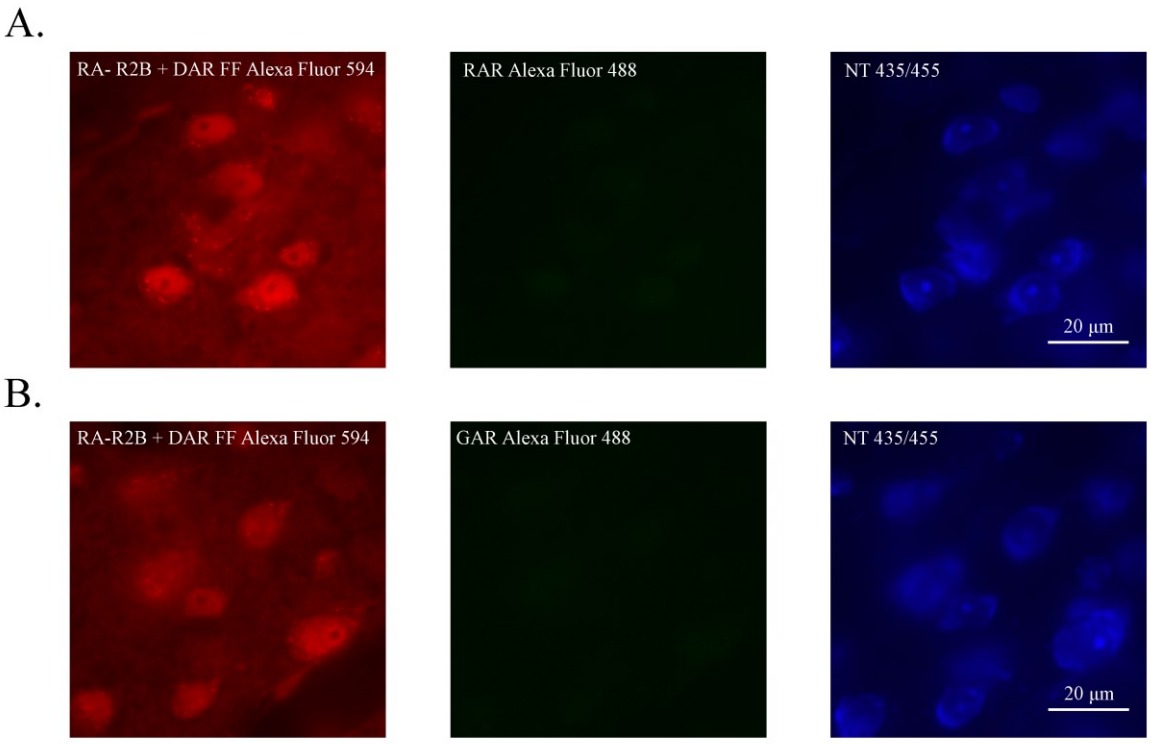

Figure 6 Schematic of experimental controls for the novel method employed in this study.

(**A**) To assess binding of the second primary antibody (rabbit-anti NMDAR2A (Rb-R2A)), to the fab fragments, labelling of a rabbit anti-rat (RbAR) conjugated to Alexa Fluor 488 secondary antibody was evaluated. This antibody was chosen as it was raised in rabbit, and presumably, its binding pattern should be similar to that of Rb-R2A. Minimal labelling is seen in the second panel, suggesting Rb-R2A primary antibody will not bind to the fab fragments. (**B**) In order to assess if the fab fragments blocked the binding sites on the first primary antibody, rabbit-anti NMDAR2B (Rb-R2B), and to see if the second secondary will bind to the fab fragments, the labelling of the secondary antibody was evaluated without the Rb-R2A antibody in solution. Minimal labelling is seen in the second panel, which indicates that the fab fragments blocked the binding sites on the Rb-R2B antibody, and the goat anti-rabbit conjugated to Alexa Fluor 488 will not bind to the fab fragments.

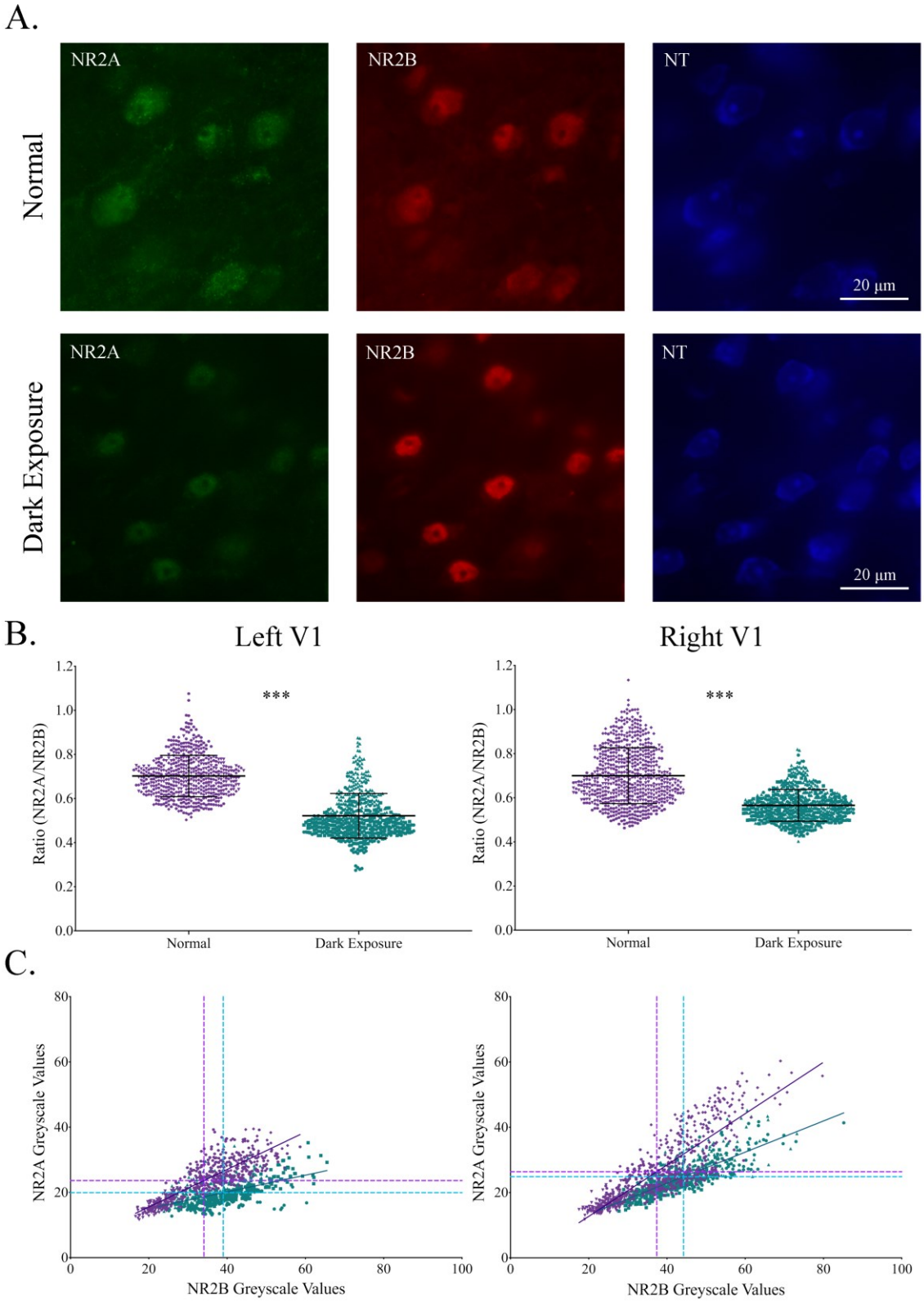
A.
NR2A
NR2B
NT
Normal
20 µm
NR2A
NR2B
NT
Dark Exposure
20 µm
B.
Left V1
Right V1
Ratio (NR2A/NR2B)
***
Normal
Dark Exposure
C.
NR2A Greyscale Values
NR2B Greyscale Values

Figure 7 The effects of a 10-day period of darkness that occurs at the peak of the critical period on the NMDA receptor NR2A/NR2B subunit ratio within V1 of kittens.

(**A**) Dark exposure-induced changes in the NMDA receptor subunits were revealed by multiplexing tissue with rabbit polyclonal primary antibodies against NMDAR2B and NMDAR2A. (**B**) Quantification of subunit expression revealed a significant difference in the NMDA receptor NR2A/NR2B ratio following dark exposure in both LV1 ($p < 0.001$) and RV1 ($p < 0.001$). Each data point represents the ratio from an individual cell. In **B** and **C**, purple data points indicate the normal animal data, and teal data points indicate the DE animal data. A specific symbol represents each animal. C436 P37 normal is represented by the upside-down triangle (▼), C466 P40 normal is represented by the hexagon (⬢), and C468 P40 normal is represented by the diamond (◆). C463 DE is represented by a triangle (▲), C464 DE is represented by the square (■), and C465 DE is represented by the circle (●). The mean (thick central horizontal bar) and standard deviation (error bars) were calculated for each group. Asterisks indicate statistical significance of $p < 0.001$. (**C**) Each data point represents an individual cell in which NR2A and NR2B greyscale measurements were taken. Quantification of subunit expression within LV1 and RV1 revealed that in both conditions expression of NR2A could be predicted by expression of NR2B. Vertical dashed lines represent the mean NR2B greyscale value for normal (purple) and dark exposure (blue). The horizontal dashed line represents the mean NR2A greyscale value for normal (purple) and dark exposure (blue). The intersection of the same coloured lines represents the average ratio for that condition.

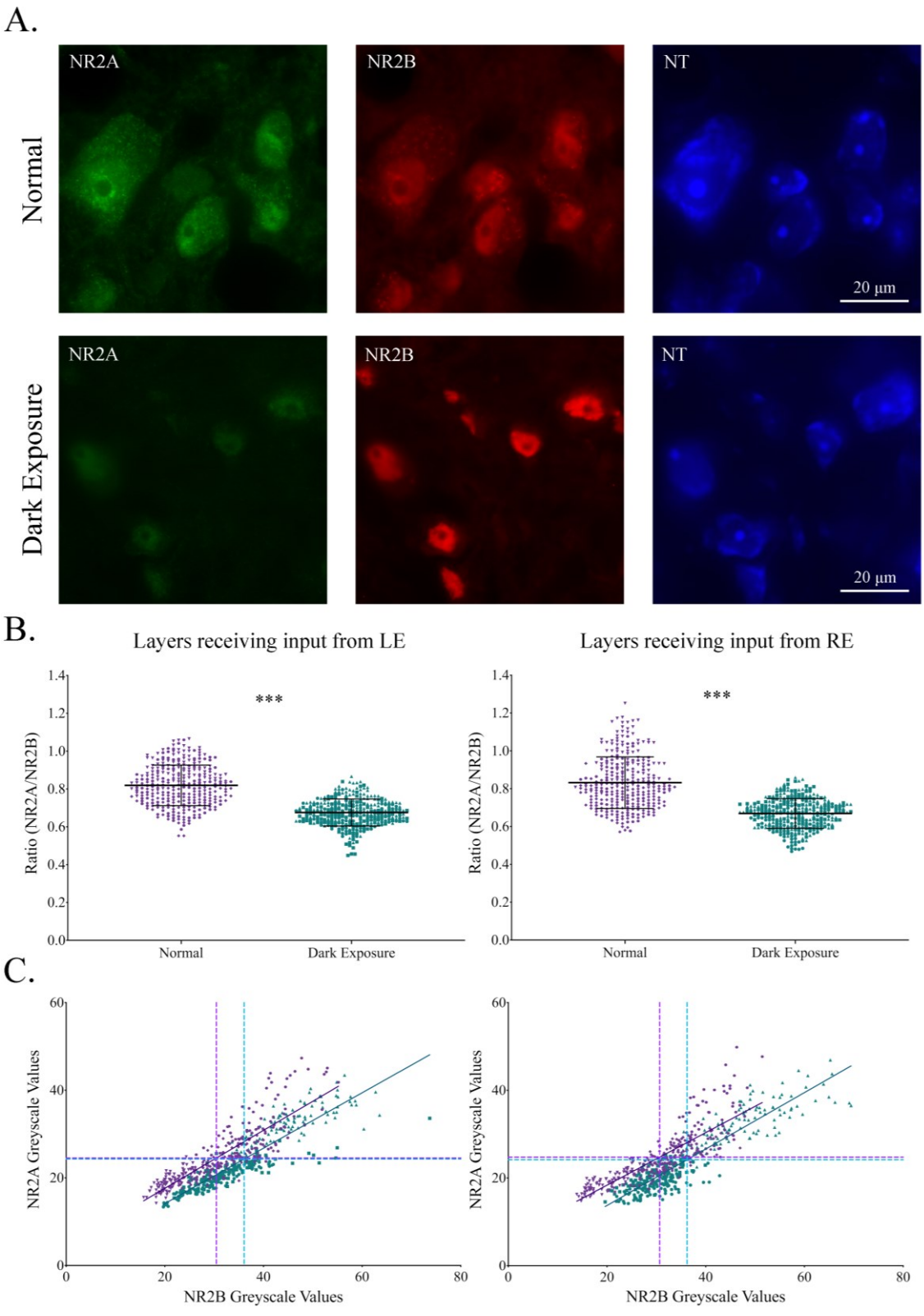
A.
NR2A
NR2B
NT
Normal
20 µm
NR2A
NR2B
NT
Dark Exposure
20 µm
B.
Layers receiving input from LE
Layers receiving input from RE
Ratio (NR2A/NR2B)
***
Normal
Dark Exposure
C.
NR2A Greyscale Values
NR2B Greyscale Values

Figure 8 The effects of a 10-day period of darkness that occurs at the peak of the critical period on the NMDA receptor NR2A/NR2B subunit ratio within the LGN of kittens.

(**A**) Dark exposure-induced changes in the NMDA receptor subunits were revealed by multiplexing tissue with rabbit polyclonal primary antibodies against both NMDAR2B and NMDAR2A. (**B**) Quantification of subunit expression revealed a significant difference in NMDA receptor NR2A/NR2B ratio following dark exposure in layers receiving input from the LE ($p < 0.001$) and RE ($p < 0.001$). Each data point represents the ratio from an individual cell. In **B** and **C**, purple data points indicate the normal animals and teal data points indicate the DE animals. A specific symbol represents each animal. C436 P37 normal is represented by the upside-down triangle (▼), C466 P40 normal is represented by the hexagon (⬢), and C468 P40 normal is represented by the diamond (◆). C463 DE is represented by a triangle (▲), C464 DE is represented by the square (■), and C465 DE is represented by the circle (●). The mean (thick central horizontal bar) and standard deviation (error bars) were calculated for each group. Asterisks indicate statistical significance of $p < 0.001$. (**C**) Each data point represents an individual cell in which NR2A and NR2B greyscale measurements were taken. Quantification of subunit expression within layers receiving input from the left eye (LE) and right eye (RE) revealed that in both conditions expression of NR2A could be predicted by expression of NR2B. Vertical dashed lines represent the mean NR2B greyscale value for normal (purple) and dark exposure (blue). The horizontal dashed line represents the mean NR2A greyscale value for normal (purple) and dark exposure (blue). The intersection of the same coloured lines represents the average ratio for that condition.

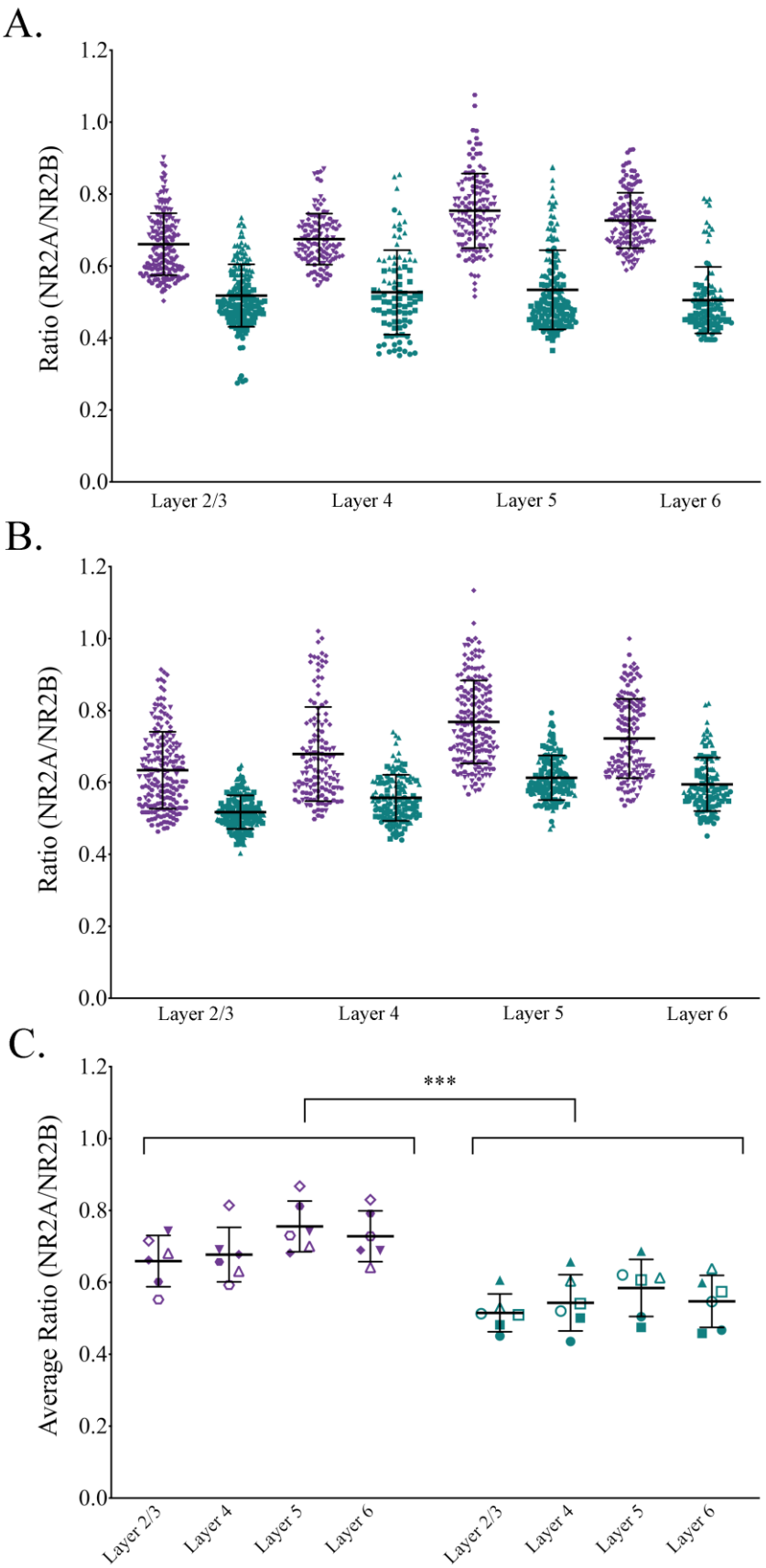
A.
Ratio (NR2A/NR2B)
1.2
1.0
0.8
0.6
0.4
0.2
0.0
Layer 2/3
Layer 4
Layer 5
Layer 6
B.
Ratio (NR2A/NR2B)
1.2
1.0
0.8
0.6
0.4
0.2
0.0
Layer 2/3
Layer 4
Layer 5
Layer 6
C.
Average Ratio (NR2A/NR2B)
***
1.2
1.0
0.8
0.6
0.4
0.2
0.0
Layer 2/3
Layer 4
Layer 5
Layer 6
Layer 2/3
Layer 4
Layer 5
Layer 6

Figure 9 Within V1, the effects of dark exposure on the NMDA receptor NR2A/NR2B subunit ratio is universal and not layer-specific.

(**A**) Raw data of NMDA subunit ratios from the layers within LV1. (**B**) Raw data of NMDA subunit ratios from the layers within RV1. (**C**) Mean of the NMDA receptor subunit ratio for LV1 (filled symbols) and RV1 (open symbol) for each animal from across the layers of V1. Using a factorial ANOVA, a main effect of condition was found ($p < 0.001$), as shown by the brackets. No other effects or interactions were observed, indicating that within V1, darkness alters the receptor subunit composition in a universal, non-layer specific manner. In **A**, **B**, and **C**, purple data points indicate the normal animals and teal data points indicate the DE animals. A specific symbol represents each animal. C436 P37 normal is represented by the upside-down triangle (▼), C466 P40 normal is represented by the hexagon (⬣), and C468 P40 normal is represented by the diamond (◆). C463 DE is represented by a triangle (▲), C464 DE is represented by the square (■), and C465 DE is represented by the circle (●). The mean (thick central horizontal bar) and standard deviation (error bars) were calculated for each layer within each group. Asterisks indicate statistical significance of $p < 0.001$.

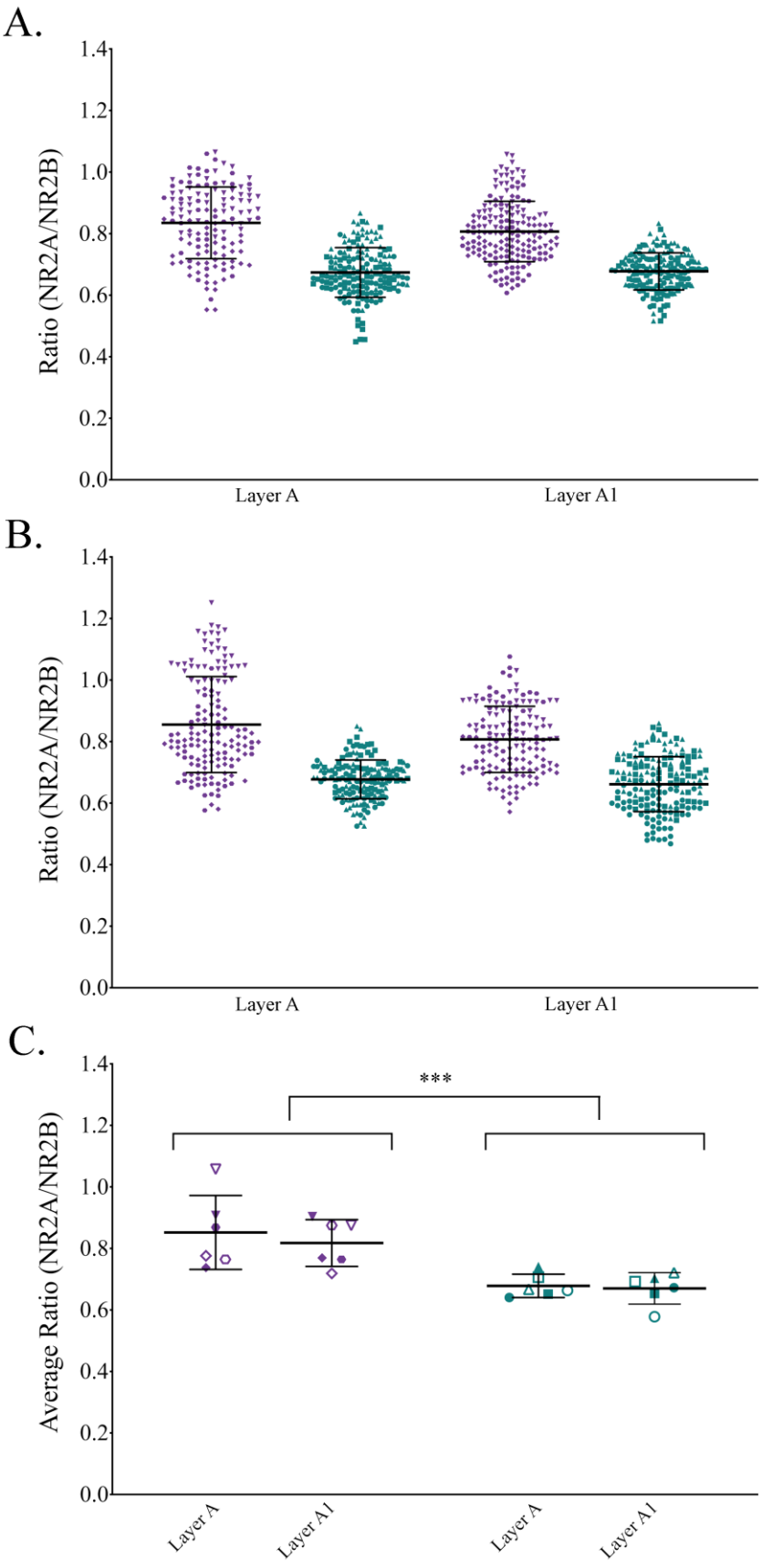
A.
Ratio (NR2A/NR2B)
1.4
1.2
1.0
0.8
0.6
0.4
0.2
0.0
Layer A
Layer A1
B.
Ratio (NR2A/NR2B)
1.4
1.2
1.0
0.8
0.6
0.4
0.2
0.0
Layer A
Layer A1
C.
Average Ratio (NR2A/NR2B)
***
1.4
1.2
1.0
0.8
0.6
0.4
0.2
0.0
Layer A
Layer A1
Layer A
Layer A1

Figure 10 Within the LGN, the effects of dark exposure on the NMDA receptor NR2A/NR2B subunit ratio is universal and not layer-specific.

(**A**) Raw data of NMDA subunit ratios from layers within the LGN receiving input from the left eye. (**B**) Raw data of NMDA subunit ratios from layers within the LGN receiving input from the right eye. (**C**) Means of the NMDA receptor subunit ratio from the LGN layers receiving input from the left eye (filled in symbol) and right eye (open symbol) for each animal. Using a factorial ANOVA, a main effect of condition was found ($p < 0.001$), as shown by the brackets. No other effects or interactions were observed, indicating that within the LGN, darkness alters the receptor subunit composition in a universal, non-layer specific manner. In **A**, **B**, and **C**, purple data points indicate the normal animals and teal data points indicate the DE animals. A specific symbol represents each animal. C436 P37 normal is represented by the upside-down triangle (▼), C466 P40 normal is represented by the hexagon (⬣), and C468 P40 normal is represented by the diamond (◆). C463 DE is represented by a triangle (▲), C464 DE is represented by the square (■), and C465 DE is represented by the circle (●). The mean (thick central horizontal bar) and standard deviation (error bars) were calculated for each layer within each group. Asterisks indicate statistical significance of $p < 0.001$.

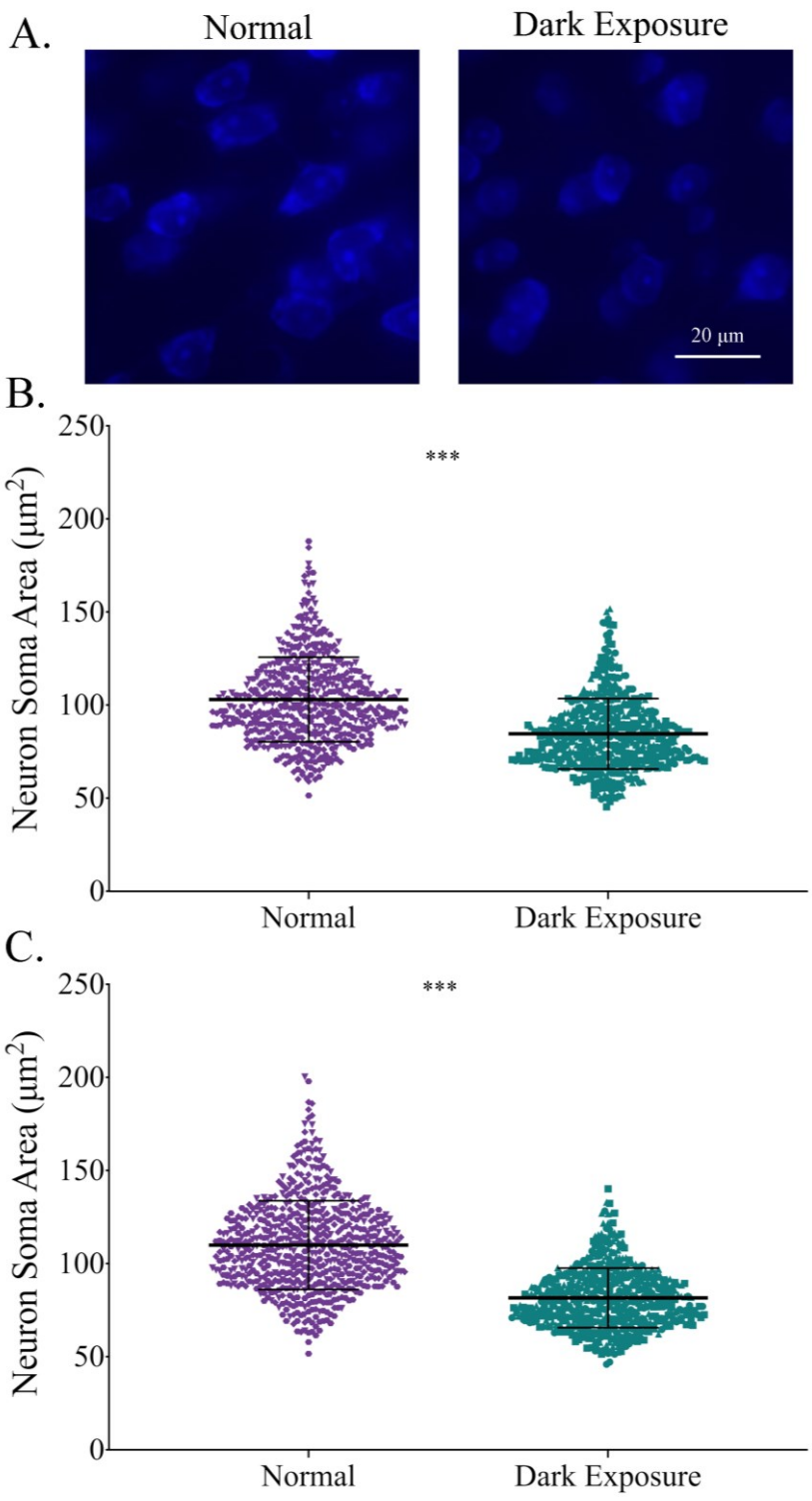
A.
Normal
Dark Exposure
20 µm
B.
Neuron Soma Area (µm²)
250
200
150
100
50
0
***
Normal
Dark Exposure
C.
Neuron Soma Area (µm²)
250
200
150
100
50
0
***
Normal
Dark Exposure

Figure 11 The effects of a 10-day period of darkness on cell size within V1 of young kittens.

(A) The dark exposure-induced changes of neuron soma size were revealed with Nissl stain. (**B**) Quantification of cell size within LV1 revealed that there is a significant difference in soma area between conditions ($p < 0.001$). (**C**) Similarly, quantification of cell size revealed the same difference within RV1, with DE animals having significantly smaller cells compared to normal animals ($p < 0.001$). In **B** and **C**, purple data points indicate the normal animals and teal data points indicate the DE animals. A specific symbol represents each animal. C436 P37 normal is represented by the upside-down triangle (▼), C466 P40 normal is represented by the hexagon (⬣), and C468 P40 normal is represented by the diamond (◆). C463 DE is represented by a triangle (▲), C464 DE is represented by the square (■), and C465 DE is represented by the circle (●). The mean (thick central horizontal bar) and standard deviation (error bars) were calculated for each group. Asterisks indicate statistical significance of $p < 0.001$.

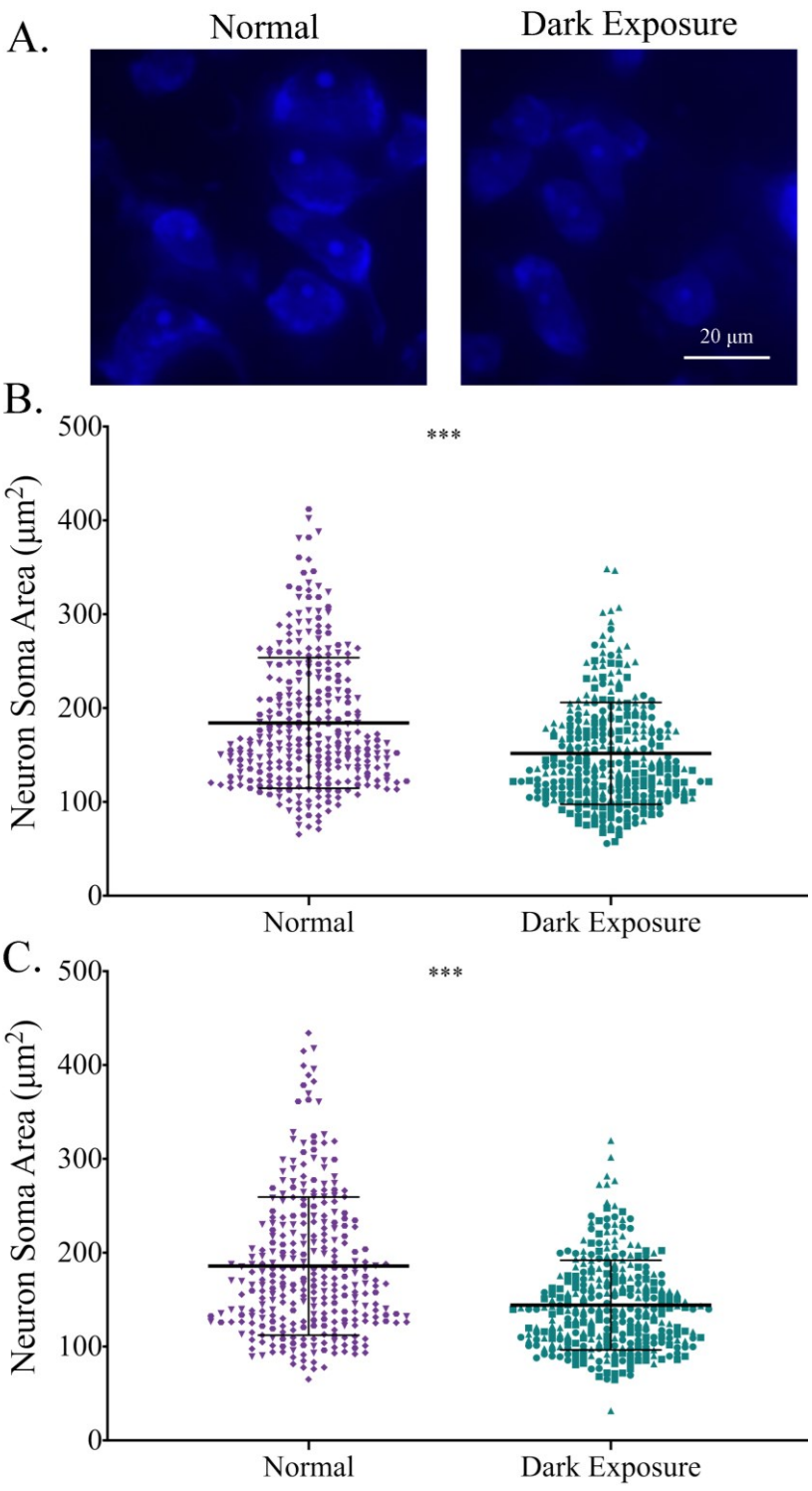
A.
Normal
Dark Exposure
20 µm
B.
Neuron Soma Area (µm²)
500
400
300
200
100
0
***
Normal
Dark Exposure
C.
Neuron Soma Area (µm²)
500
400
300
200
100
0
***
Normal
Dark Exposure

Figure 12 The effects of a 10-day period of darkness on cell size within the LGN of young kittens.

(**A**) The dark exposure-induced changes of neuron soma area were revealed with Nissl stain. (**B**) Quantification of cell size within layers of the LGN receiving input from the left eye revealed that there is a significant difference in soma area between normal and DE animals ($p < 0.001$). (**C**) Similarly, quantification of cell size revealed the same difference within layers of the LGN that receive input from the right eye, with DE animals having significantly smaller cells compared to normal animals ($p < 0.001$). In **B** and **C**, purple data points indicate the normal animals and teal data points indicate the DE animals. A specific symbol represents each animal. C436 P37 normal is represented by the upside-down triangle (▼), C466 P40 normal is represented by the hexagon (⬢), and C468 P40 normal is represented by the diamond (◆). C463 DE is represented by a triangle (▲), C464 DE is represented by the square (■), and C465 DE is represented by the circle (●). The mean (thick central horizontal bar) and standard deviation (error bars) were calculated for each group. Asterisks indicate statistical significance of $p < 0.001$.

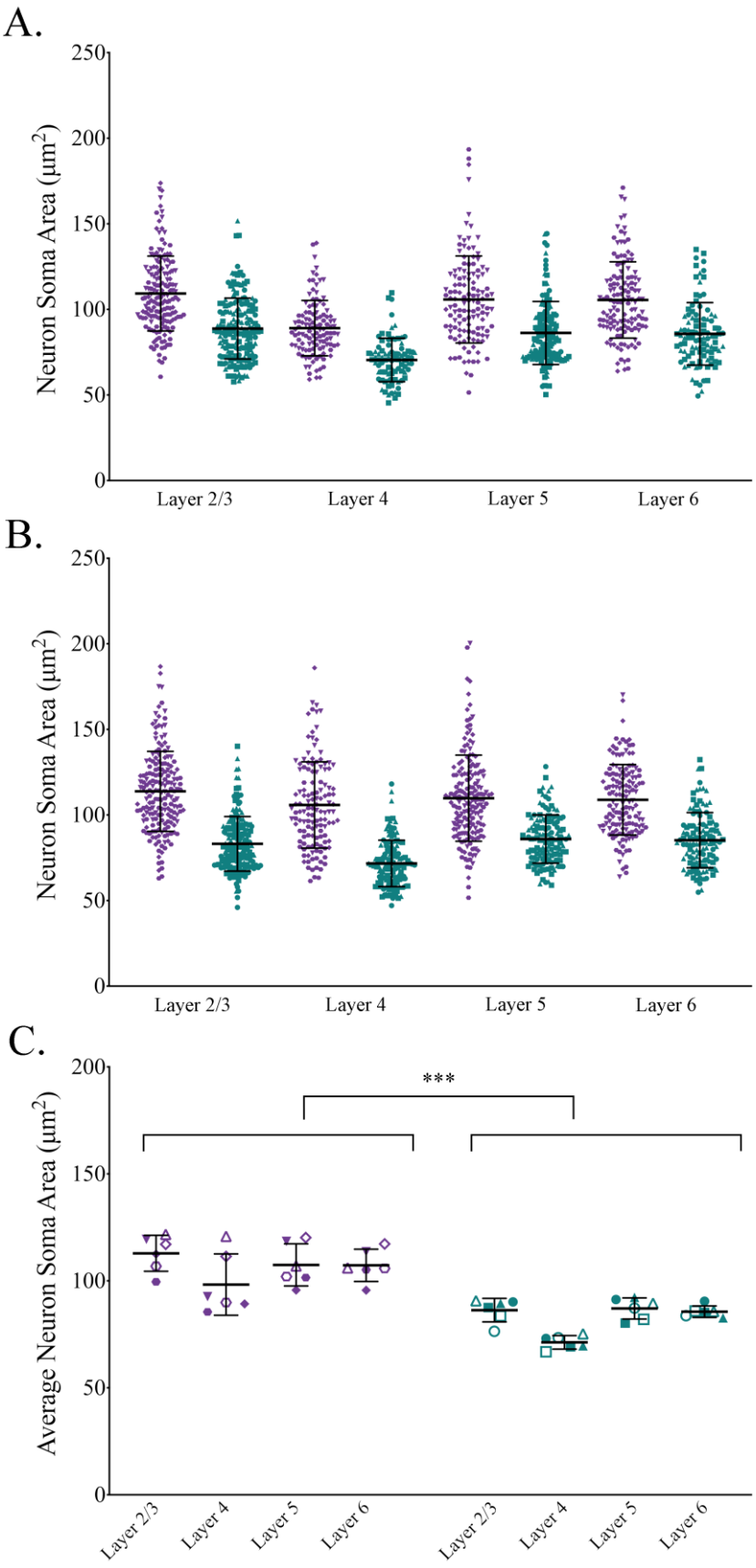
A.
Neuron Soma Area (µm2)
250
200
150
100
50
0
Layer 2/3
Layer 4
Layer 5
Layer 6
B.
Neuron Soma Area (µm2)
250
200
150
100
50
0
Layer 2/3
Layer 4
Layer 5
Layer 6
C.
Average Neuron Soma Area (µm2)
***
200
150
100
50
0
Layer 2/3
Layer 4
Layer 5
Layer 6
Layer 2/3
Layer 4
Layer 5
Layer 6

Figure 13 The effects of a 10-day period of darkness on cell size with V1 is universal and not-layer specific.

(**A**) Raw data of neuron soma area from layers within LV1. (**B**) Raw data of neuron soma area from layers within RV1. (**C**) Means of the neuron soma area for LV1 (filled in symbol) and RV1 (open symbol) for each animal split across the layers of V1. Using a factorial ANOVA, a main effect of condition ($p < 0.001$), as shown by the brackets, and layer ($p < 0.001$) was shown. Post hoc analysis revealed that, regardless of condition, cells within layer 4 were significantly smaller compared to cells in layer 2/3 ($p < 0.001$), layer 5 ($p = 0.002$), and layer 6 ($p = 0.004$). A significant interaction between condition and hemisphere ($p = 0.032$) was also observed. In **A**, **B**, and **C**, purple data points indicate the normal animals and teal data points indicate the DE animals. A specific symbol represents each animal. C436 P37 normal is represented by the upside-down triangle (▼), C466 P40 normal is represented by the hexagon (⬢), and C468 P40 normal is represented by the diamond (◆). C463 DE is represented by a triangle (▲), C464 DE is represented by the square (■), and C465 DE is represented by the circle (●). The mean (thick central horizontal bar) and standard deviation (error bars) were calculated for each layer within each group. Asterisks indicate statistical significance of $p < 0.001$.

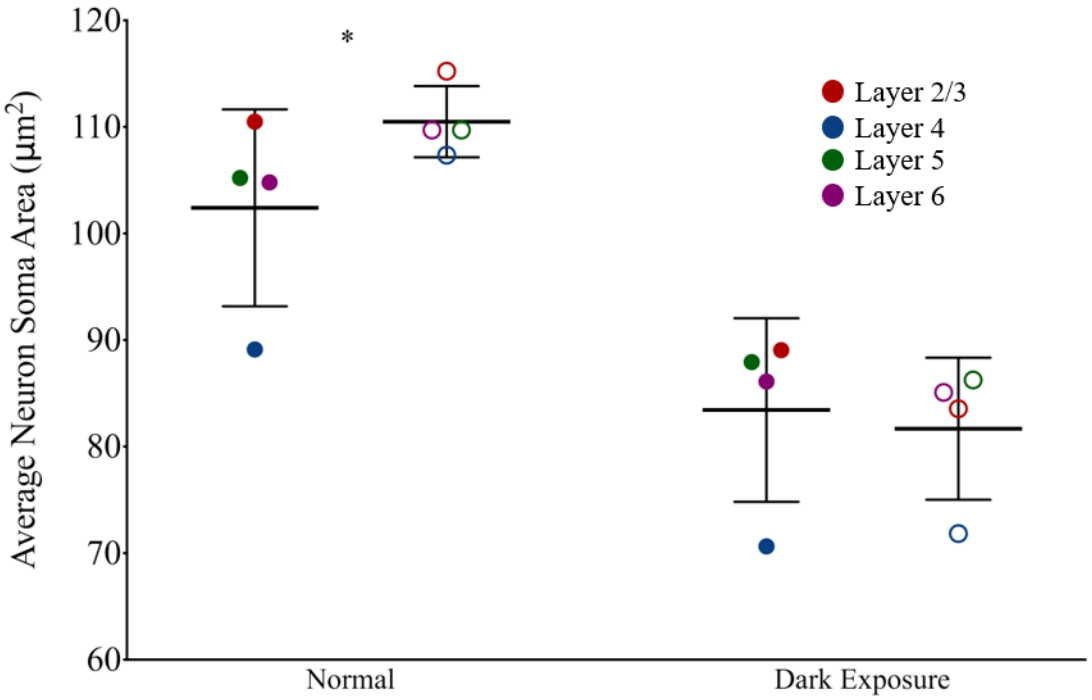

Figure 14 Means for neuron soma area of all the animals for each layer within LV1 and RV1.

LV1 is represented by the filled-in symbols and RV1 is represented by the open symbols. Simple effect analysis revealed that in the normal condition, there was a significant difference in cell size between the two hemispheres, with cells in RV1 being significantly larger compared to cells within LV1 ($p = 0.014$). The mean (thick central horizontal bar) and standard deviation (error bars) were calculated for each layer within each group. Asterisks indicate statistical significance of $p < 0.05$.

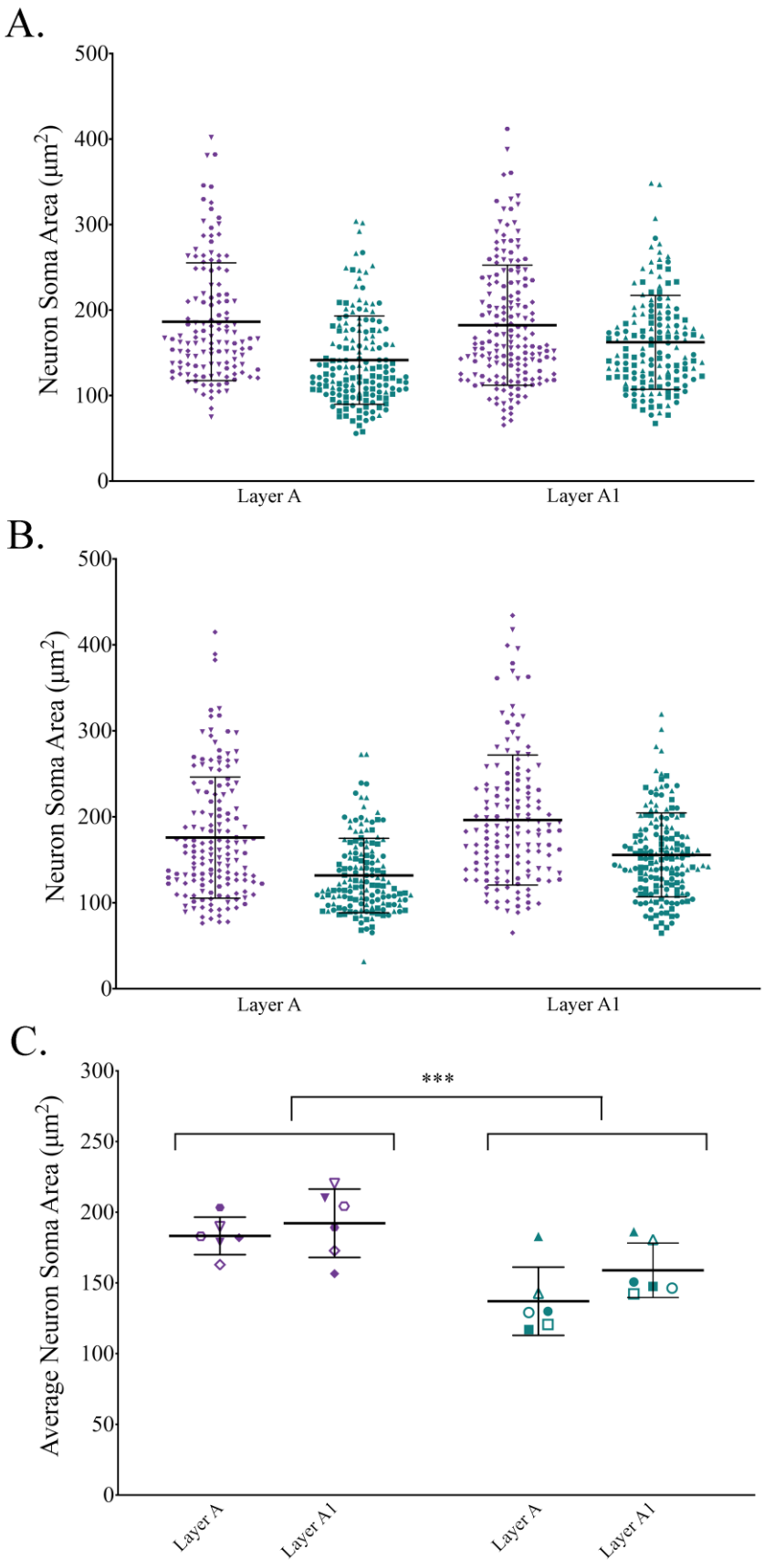
A.
Neuron Soma Area (µm²)
500
400
300
200
100
0
Layer A
Layer A1
B.
Neuron Soma Area (µm²)
500
400
300
200
100
0
Layer A
Layer A1
C.
Average Neuron Soma Area (µm²)
300
250
200
150
100
50
0
***
Layer A
Layer A1
Layer A
Layer A1

Figure 15 The effects of a 10-day period of darkness on cell size with the LGN is universal and not-layer specific.

(**A**) Raw data of neuron soma area from layers within the LGN receiving input from the left eye. (**B**) Raw data of neuron soma area from layers within the LGN receiving input from the right eye. (**C**) Means of the neuron soma area for the LGN layers receiving input from the left eye (filled in symbol) and right eye (open symbol) for each animal split across the layers of the LGN. Using a factorial ANOVA, a main effect of condition was found ($p < 0.001$), as shown by the brackets. No other effects or interactions were observed, indicating that within the LGN, darkness alters cell size in a universal, non-layer specific manner. In **A**, **B**, and **C**, purple data points indicate the normal animals and teal data points indicate the DE animals. A specific symbol represents each animal. C436 P37 normal is represented by the upside-down triangle (▼), C466 P40 normal is represented by the hexagon (⬣), and C468 P40 normal is represented by the diamond (◆). C463 DE is represented by a triangle (▲), C464 DE is represented by the square (■), and C465 DE is represented by the circle (●). The mean (thick central horizontal bar) and standard deviation (error bars) were calculated for each layer within each group. Asterisks indicate statistical significance of $p < 0.001$.

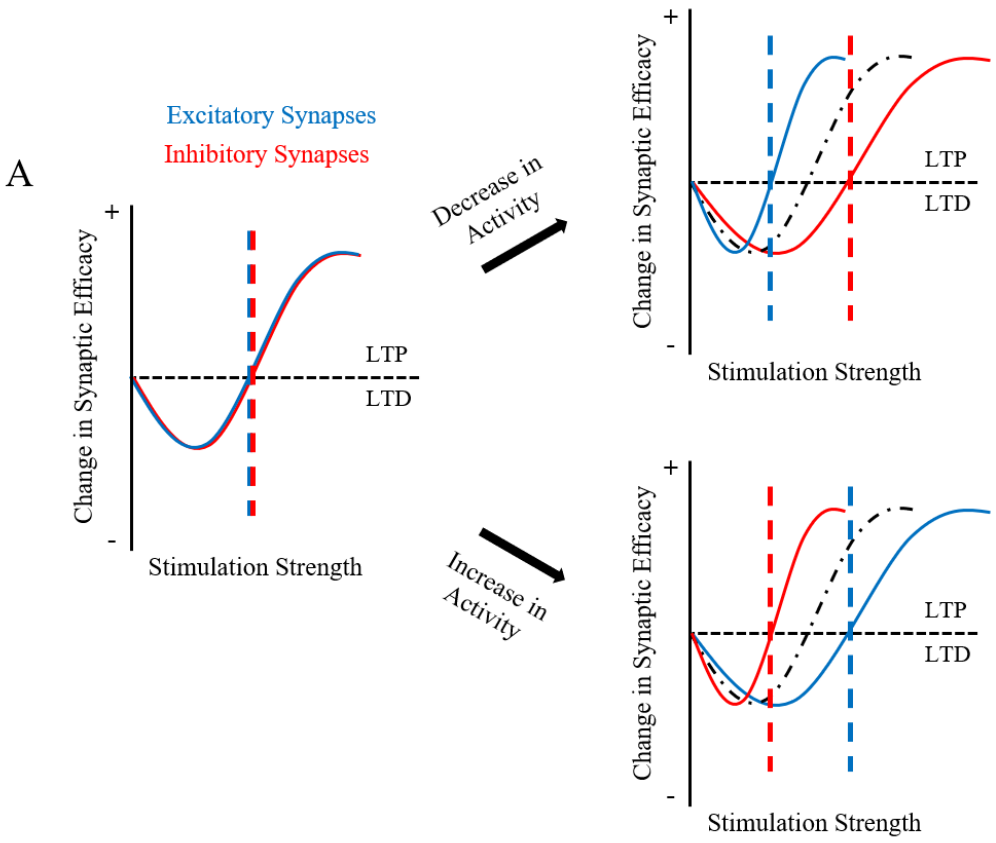
A
Excitatory Synapses
Inhibitory Synapses
Change in Synaptic Efficacy
+
-
LTP
LTD
Stimulation Strength
Decrease in Activity
Increase in Activity
Change in Synaptic Efficacy
+
-
LTP
LTD
Stimulation Strength
Change in Synaptic Efficacy
+
-
LTP
LTD
Stimulation Strength

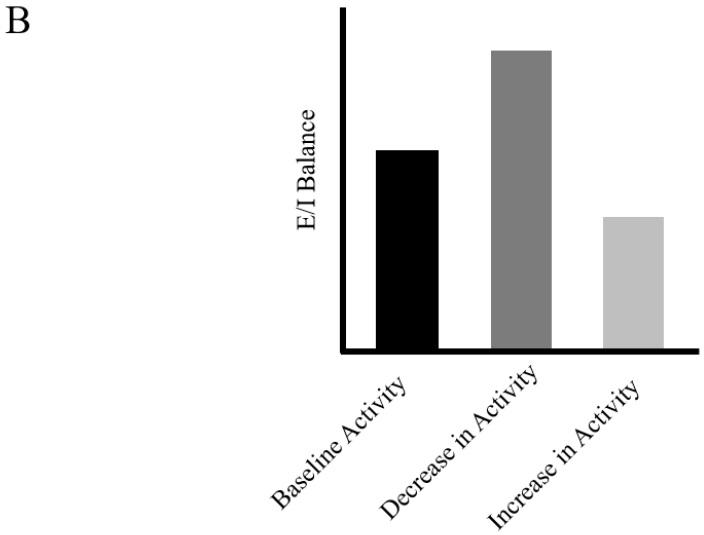
B
E/I Balance
Baseline Activity
Decrease in Activity
Increase in Activity

Figure 16 A possible relationship between the BCM model and the excitatory/inhibitory balance.

(**A**) The sliding threshold model applied to both excitatory synapses (blue) and inhibitory synapses (red). Relative to the baseline threshold (Dot-Dashed line), an increase in activity shifts the threshold lower in excitatory synapses and higher in inhibitory synapses, a decrease in activity causes the thresholds to shift in the reverse direction. Vertical dashed coloured lines indicate the stimulation strength of the threshold. (**B**) The predicted change in excitatory/inhibitory balance when the BCM model is applied to both excitatory synapses and inhibitory synapses. A decrease in activity, such a dark exposure, should cause an increase in excitation and a decrease in inhibition, thus, increasing the excitatory/inhibitory balance. An increase in activity will cause a decrease in excitation and an increase in inhibition, thus, decreasing the excitatory/inhibitory balance (Modified from Keck et al., 2017).